The Role of Synaptopodin in Neuroinflammation and Retinoic Acid-Mediated Synaptic Plasticity in the Mouse Hippocampus

Dissertation

zur Erlangung des Doktorgrades

der Naturwissenschaften

vorgelegt beim Fachbereich Biowissenschaften

der Johann Wolfgang Goethe-Universität

in Frankfurt am Main

von

Andreas Strehl

aus Oberwesel

Frankfurt am Main, 2017

(D 30)

vom Fachbereich Biowissenschaften
der Johann Wolfgang Goethe-Universität als Dissertation angenommen.

Dekan:	Prof. Dr. Sven Klimpel
Gutachter:	Prof. Dr. Manfred Kössl
	Prof. Dr. Andreas Vlachos

Datum der Disputation:

Teile dieser Arbeit wurden veröffentlicht:

Strehl, A., Lenz, M., Itsekson-Hayosh, Z., Becker, D., Chapman, J., Deller, T., Maggio, N., and Vlachos, A. (2014). Systemic inflammation is associated with a reduction in Synaptopodin expression in the mouse hippocampus. Experimental Neurology 261, 230-235.

Für Ida

Table of Contents

1. Zusammenfassung

Das menschliche Gehirn ist eines der komplexesten biologischen Systeme überhaupt. Mehr als 10 Billionen Nervenzellen bilden ein Netzwerk, das ausgehend von der Kontrolle grundlegender Körperfunktionen, diffizile Bewegungen koordiniert, es uns ermöglicht Gedanken, Emotionen und Gefühle zum Ausdruck zu bringen und diese über Jahre und ein gesamtes Leben hinweg zu speichern. Nicht zuletzt, „wir sind wer wir sind, aufgrund dessen, was wir lernen und woran wir uns erinnern“ (Kandel 2006). Insbesondere pathologische Bedingungen beeinflussen dieses fein aufeinander abgestimmte Netzwerk aus Neuronen. Die meisten, wenn nicht alle neurologischen Erkrankungen werden durch entzündliche Prozesse ausgelöst bzw. begleitet (Heppner et al. 2015). Entzündungen im Gehirn haben einen direkten Einfluss auf einen für das Lernen und Gedächtnis elementaren Mechanismus: Synaptische Plastizität. Denn Nervenzellen sind keine starren Strukturen, sondern zu morphologischen und molekularen Anpassungen in der Lage, welche letztlich die Verbindungen (Synapsen) zwischen ihnen verändern. Ziel dieser Arbeit ist es, jene molekularen Strukturen zu identifizieren, welche ausgelöst durch entzündliche Prozesse, die synaptische Plastizität beeinträchtigen. Am besten wurden die Prinzipien der synaptischen Plastizität im Hippocampus untersucht, einer anatomischen Struktur, welche sich im Temporallappen befindet und an der räumlichen Orientierung (O’Keefe & Dostrovsky 1971; O’Keefe & Speakman 1987, Moser et al. 2008), der Verarbeitung von Emotionen sowie allen voran der Konsolidierung deklarativer Erinnerungen beteiligt ist (Kandel et al. 2000; Anderson et al. 2007). Für die Koordinierung synaptischer Plastizität bedarf es komplexer Wechselwirkungen tausender Moleküle und Proteine, von denen vor allem jene interessant sind, die an strategisch wichtigen Positionen innerhalb der Nervenzelle lokalisiert sind. Das aktin-modulierende Protein Synaptopodin (SP) ist eines dieser Moleküle. Es wird im zentralen Nervensystem ausschließlich von Neuronen exprimiert und ist innerhalb der Dornfortsätze erregender Synapsen zu finden (Deller et al. 2003; Vlachos et al. 2012), d.h. unmittelbar an der Schnittstelle

zwischen zwei Neuronen, und ist direkt an der Regulation synaptischer Plastizität beteiligt (Deller et al. 2003; Vlachos et al. 2009; Vlachos et al. 2013).

Die hier präsentierte Arbeit konzentriert sich im ersten Abschnitt auf die Beeinflussung der Funktion synaptischer Plastizität durch entzündliche Prozesse, welche durch ein Lipopolysaccharid (LPS) des Bakteriums *E.coli* induziert wurden – ein klassisches Modell um inflammatorische Prozesse auszulösen (Qin et al. 2007; Erickson et al. 2011; Catorce & Gevorkian 2016). Sämtliche Experimente wurden hierzu an akuten bzw. perfundierten Maushirnschnitten sowie *in vitro*, mittels organotypischer entorhino-hippocampaler Schnittkulturen (OTCs), durchgeführt. Zunächst befasst sich die Arbeit mit der Frage, ob eine systemische, d.h. in der Körperperipherie ausgelöste Inflammation, einen Einfluss auf die Funktion des Gehirns hat. Hierzu wurde Mäusen LPS (1 mg/kg) intraperitoneal injiziert und der Einfluss auf synaptische Plastizität 24 Stunden darauf untersucht. Hierzu wurde sich des klassischen Modells der Langzeitpotenzierung (englisch: ‚long term potentiation', LTP) exzitatorischer Synapsen des Hippocampus bedient (Bliss & Lømo 1973). Unter Kontrollbedingungen führte eine hochfrequente Stimulation (100 Hz, 1 Sekunde) erwartungsgemäß zu einer Verstärkung der synaptischen Stärke, gemessen als Summenpotential in der CA1-Region des Hippocampus. Interessanterweise konnte gezeigt werden, dass in akuten Hirnschnitten von LPS-injizierten Mäusen diese Fähigkeit der Langzeitpotenzierung erheblich geschwächt wird.

Tatsächlich zeigte eine Genexpressionsanalyse mittels quantitativer RT-PCR einen deutlichen Anstieg der mRNA des proinflammatorischen Proteins Tumornekrosefaktor alpha (TNFα) im Hippocampus dieser Mäuse. Bemerkenswerterweise wurde gleichzeitig die Genexpression von SP herunterreguliert. Weitere Analysen mittels Immunhistochemie konnten zeigen, dass SP auch auf Proteinebene durch eine LPS-Behandlung herunterreguliert wird. Dies drückte sich durch eine reduzierte Größe von SP-Aggregaten in der LPS-Gruppe aus. Zusammengefasst deuten diese Ergebnisse darauf hin, dass SP eines jener Proteine sein könnte, durch welche inflammatorische Prozesse synaptische Plastizität und somit neuronale Funktionalität beeinflussen. Um

mehr über die zugrundeliegenden zellulären und molekularen Mechanismen zu erfahren, wurde im Folgeschritt mittels OTCs der Maus, ein LPS *in vitro* Modell etabliert, mit dem Ziel einen direkten Effekt von LPS auf neuronales Gewebe zu studieren. Der Fokus lag insbesondere auf möglichen Schlüsselmolekülen der entzündlichen Reaktionskaskade, welche einen direkten Einfluss auf die Funktionsweise der Synapse nehmen. Es wurde bereits in anderem Zusammenhang gezeigt, dass das proinflammatorische Protein TNFα in der Lage ist die synaptische Plastizität zu modifizieren (Butler et al. 2004; Cunningham et al. 1996; Becker et al. 2013; Pribiag & Stellwagen 2013; Steinmetz & Turrigiano 2010; Stellwagen & Malenka 2006). Zunächst konnte gezeigt werden, dass auch eine Behandlung organotypischer Schnittkulturen mit LPS (1 µg/ml; 3 Tage) dazu führt, dass TNFα hochreguliert wird und SP-mRNA sowie SP-Aggregate herunterreguliert werden. Die Reproduktion des Ausgangsbefundes war entscheidend und zeigt, dass das *in vitro* Modell geeignet ist, um den Einfluss LPS-induzierter, inflammatorischer Prozesse im Hippocampus zu studieren. Die Rolle von TNFα wurde mit Hilfe zweier Knockout-Mauslinien studiert: TNF KO (Gen-Knockout des Proteins TNFα) und TNFR1/2 KO (Gen-Knockout der TNFα Rezeptoren 1 und 2). Interessanterweise stellte sich heraus, dass im Gegensatz zu Kulturen von wildtypischen Wurfgeschwistern, nach einer LPS-Behandlung, die Reduktion der SP-Aggregate in Kulturen beider Knockoutlinien nicht zu beobachten war und verdeutlichte, dass TNFα im Rahmen einer entzündlichen Reaktion einen direkten Einfluss auf die Regulation von SP hat.

Um die durch LPS ausgelöste Reaktionskaskade in neuronalem Gewebe besser zu verstehen, stellte sich die Frage, welche Zellen in organotypischen Schnittkulturen für die Produktion von TNFα verantwortlich sind. Mittels der transgenen Reportermauslinie tg(TNF-eGFP), welche GFP unter der Kontrolle des TNFα-Promotors exprimiert, war es möglich TNFα-synthetisierende Zellen zu identifizieren. Wie zu erwarten führte eine Behandlung mit LPS (1 µg/ml, 3 Tage) zu einem signifikanten Anstieg der GFP-Fluoreszenz im Vergleich mit Kontrollkulturen. Für die Synthese von proinflammatorischen Signalmolekülen kommen in erster Linie Gliazellen in Betracht; allen voran Astrozyten und

Mikroglia (Hanisch 2002; Ekdahl et al. 2009; Monji et al. 2013). Um diese Vermutung zu überprüfen, wurden immunhistochemische Färbungen mit dem Astrozyten-Marker GFAP (englisch: ‚glial fibrillary acidic protein') sowie dem Mikroglia-Marker Iba1 (englisch: ‚ionized calcium-binding adapter molecule 1') durchgeführt. Kolokalisationsanalysen bestätigten diese Vermutung und verdeutlichten, dass nahezu alle GFP-positiven Zellen mit dem Marker Iba1 kolokalisierten und somit Mikrogliazellen die wesentliche Quelle des TNFα in OTCs darstellen.

Zusammenfassend konnte mit dieser Arbeit zum ersten Mal gezeigt werden, dass eine akute systemische Inflammation in LPS-injizierten Mäusen, sowie eine direkte Inflammation, ausgelöst durch eine LPS-Behandlung von organotypischen entorhino-hippocampalen Schnittkulturen, zu einer Reduktion von SP führt, welche in Verbindung mit einer Beeinträchtigung synaptischer Funktion steht, wie durch LTP-Experimente belegt werden konnte. Ferner wird die zentrale Rolle von SP für die Ausprägung synaptischer Plastizität deutlich, wobei die genauen Regulationsmechanismen hierzu unbekannt sind.

Interessanterweise weist Retinsäure (englisch: ‚retinoic acid', RA), ein Derivat des Vitamin A und insbesondere der über RA gesteuerte RA-Rezeptor alpha (RARα) interessante Gemeinsamkeiten mit SP bezüglich der Regulation synaptischer Stärke auf. Dies betrifft in erster Linie die Lokalisation sowie die Regulation der Akkumulation von AMPA-Rezeptoren in der postsynaptischen Membran exzitatorischer Synapsen (Maden 2002; Aoto et al. 2008; Arendt et al. 2015a). Diese erfolgt bei RA direkt über die Steuerung lokaler Proteinsynthese mittels RARα. Letzterer bindet die mRNA der AMPA-Rezeptor Untereinheit GluA1 und blockiert dadurch dessen Translation, welche erst in Anwesenheit von RA enthemmt wird (Aoto et al. 2008; Poon & Chen 2008; Arendt et al. 2015b). Da SP sowohl mit der Regulation von AMPA Rezeptoren in Dornfortsätzen als auch mit lokaler Proteinsynthese assoziiert wird (Pierce et al. 2000; Vlachos et al. 2009), war es naheliegend die Rolle von SP in der RA-vermittelten Regulation synaptischer Plastizität genauer zu studieren. Tatsächlich zeigte sich, dass RA sowohl *in vitro* in OTCs (1 µM, 3 Tage), als auch *in vivo* in Mäusen (1 mg/kg intraperitoneal, 3 Tage) zu einer Vergrößerung

der SP-Aggregate in der Molekularschicht des Gyrus Dentatus führt. Gleichzeitig führte die RA-Behandlung zu einer Verstärkung der Synapsen von Körnerzellen, wie mittels Patch-Clamp-Technik belegt werden konnte. Bei der Patch-Clamp-Technik werden spontan ausgelöste (d.h. aktivitätsunabhängige) exzitatorische postsynaptische Miniaturströme (englisch: ‚miniature excitatory postsynaptic currents', mEPSCs) abgeleitet, welche einen Rückschluss auf die synaptische Stärke individueller Neurone erlauben. Während die mEPSC Amplitude eine Aussage über die synaptische Stärke zulässt, können über die mEPSC Frequenz Rückschlüsse über die Konnektivität einer Nervenzelle bzw. präsynaptische Mechanismen gezogen werden. Interessanterweise wird dieser Effekt in Abwesenheit von SP, d.h. in Schnittkulturen von SP-defizienten Mäusen, nicht beobachtet (Deller et al. 2003). Dies deutet auf ein direktes Zusammenspiel zwischen RA- und SP-abhängiger synaptischer Plastizität hin, möglicherweise durch Regulation auf Ebene der lokalen Proteintranslation. Tatsächlich verhindert die Blockade der Proteinsynthese mittels Anisomycin (10 µM) während der RA-Behandlung sowohl einen Anstieg der mEPSC Amplitude als auch eine Vergrößerung der SP-Aggregate. Es stellte sich daher die Frage, insofern eine Regulation der (lokalen) Proteinsynthese eine Rolle bei der SP-anhängigen synaptischen Verstärkung spielt, ob RARα mit der mRNA von SP interagiert. Um diesen Zusammenhang zu analysieren wurde eine RNA-Immunpräzipitation (RIP) mit OTCs durchgeführt und diese sowohl mittels Standard- als auch quantitativer RT-PCR analysiert. Interessanterweise zeigte sich eine potentielle Interaktion zwischen RARα-Protein und SP-mRNA. Zudem ergab ein Vergleich der SP-mRNA-Sequenz mit den bereits publizierten RARα/RNA-Bindemotiven (Poon & Chen 2008) mehrere mögliche Interaktionsstellen zwischen RARα und SP-mRNA, welche zumeist in der 3'untranslatierten Region (UTR) lokalisiert sind. Aufgrund dieses Befundes war es nahelegend davon auszugehen, dass die SP-3'UTR hauptsächlich an der Vermittlung der RA-induzierten und SP-abhängigen synaptischen Plastizität beteiligt ist. Um dieser Hypothese auf den Grund zu gehen, wurde die Mauslinie tg(Thy1-GFP/SP) x SP KO verwendet (Vlachos et al. 2013), welche ausschließlich eine transgene mRNA aus SP und GFP exprimiert, welcher die

SP-3'UTR fehlt. Tatsächlich ist die Fähigkeit der synaptischen Verstärkung in Körnerzellen dieser Mauslinie nach einer RA-Behandlung blockiert. Überraschenderweise zeigen RIP-Experimente, dass trotz Fehlen der SP-3'UTR eine Interaktion zwischen RARα und SP-mRNA stattzufinden scheint. Dies legt nahe, dass andere Sequenzabschnitte, womöglich in der 5'UTR, RARα binden, jedoch nicht funktional sind im Sinne einer Regulation der Proteinexpression. Auch eine posttranslationale Modifikation von RARα, e.g. durch Phosphorylierung, kann als mögliche Ursache genannt werden. Diese Hypothesen decken sich mit einer Studie von Poon & Chen, in der gezeigt werden konnte, dass das alleinige Vorhandensein einer RARα-Bindestelle nicht notwendigerweise ausreichend ist, um die Proteinsynthese zu blockieren (Poon & Chen 2008). Des Weiteren galt es zu klären, ob der Mechanismus der RA-vermittelten synaptischen Verstärkung homöostatischer (Aoto et al. 2008; Arendt et al. 2015b) oder assoziativer Natur ist. Hierzu wurden OTCs drei Tage mit TTX (2 µM) behandelt, ein klassisches Modell, welches basierend auf einer völligen Aktivitätsblockade der Neurone, eine kompensatorische Verstärkung exzitatorischer Synapsen bewirkt (Turrigiano et al. 1998; Wierenga et al. 2006). Interessanterweise zeigte sich, dass eine Blockade des RARα während der TTX-Behandlung die synaptische Verstärkung in OTCs verhindert. Dies deutet darauf hin, dass es sich bei der RA-induzierten und SP-abhängigen synaptischen Verstärkung, um einen homöostatischen Mechanismus handelt. Darüber hinaus belegt dieser Befund das Vorhandensein endogener, also in OTCs synthetisierter RA. Ferner konnte ein NMDA-abhängiger, assoziativer Mechanismus ausgeschlossen werden, denn die Blockade von NMDA-Rezeptoren mittels APV (50 µM) hatte keinen Einfluss auf die synaptische Verstärkung durch RA.

Neben der Relevanz der Regulation synaptischer Plastizität unter physiologischen Bedingungen, wird RA auch als mögliche Indikation im Falle einer Neuroinflammation bzw. Neurodegeneration diskutiert (Nozaki et al. 2006; Goncalves et al. 2013; siehe auch Shearer et al. 2012). Tatsächlich verhindert eine simultane Behandlung von LPS (1 µg/ml) und RA (1 µM) eine Reduktion der SP-mRNA. Interessanterweise handelt es sich hierbei also um eine

Regulation auf der transkriptionellen Ebene und deutet an, dass RA als Möglichkeit in Betracht gezogen werden kann, um eine gestörte synaptische Funktion, ausgelöst oder verstärkt durch eine Neuroinflammation, zu kompensieren.

Zusammenfassend konnte mit dieser Arbeit gezeigt werden, dass SP eine elementare Rolle bei der Regulation synaptischer Plastizität unter pathophysiologischen Bedingungen, die durch eine Neuroinflammation ausgelöst werden, spielt, sowie auch unter physiologischen Bedingungen durch eine Regulation synaptischer Plastizität, welche durch den RA/RARα-Signalweg vermittelt wird.

Ich bin zuversichtlich, dass zukünftige Arbeiten, die sich mit dem Einfluss inflammatorischer Prozesse auf die Expression von SP und SP-abhängige synaptische Plastizität befassen, mögliche Perspektiven aufzeigen werden, um neue therapeutische Strategien gegen inflammations-assoziierte Neuropathologien wie der Alzheimer Erkrankung, Multipler Sklerose, Epilepsie oder Schlaganfall zu entwickeln.

2. Abstract

The human brain is one of the most complex biological systems. More than 100 billion neurons build networks that control basic body functions and highly coordinated movements, enable us to express emotions, feelings and thoughts and to store memories over years and even throughout life time. Ultimately, “We are who we are because of what we learn and what we remember” (Kandel 2006). Under pathological conditions, the brain function is challenged. Most if not all neurological diseases have in common that they are either triggered and/or accompanied by inflammatory processes of brain tissue, referred to as *neuroinflammation*. Such inflammatory processes directly affect an elementary neural mechanism relevant for learning and memory: *synaptic plasticity*. Indeed, neurons are highly dynamic structures and able to respond to specific stimuli with morphological, functional and molecular adaptations that modify the strength and number of neuronal contact sides (synapses). Hence, the main motivation of this thesis was to identify the neural targets through which inflammation affects brain function and *synaptic plasticity* in particular. The principles of synaptic plasticity have been studied intensively in the *hippocampus*, an anatomical structure localized within the temporal lobes that is essential for the consolidation of memories and spatial navigation. Synaptic plasticity is coordinated by complex interactions of thousands of molecules and proteins. Among those proteins, *synaptopodin* (SP) is localized at a strategic position within excitatory synapses and has been shown to be fundamentally involved in the regulation of synaptic plasticity.

To induce neuroinflammation and to study its effects on SP as well as synaptic plasticity, the classic model of lipopolysaccharide (LPS) was applied. This thesis discloses that inflammatory processes impair the ability of neurons to express hippocampal synaptic plasticity *in vivo*, which is accompanied by a downregulation of SP-mRNA and protein level in the mouse hippocampus, indicating that SP is one of the cellular targets through which inflammatory signaling pathways affect synaptic plasticity and hence neural function. To learn more about the cellular and molecular mechanisms, an *in vitro* LPS model was

established using entorhino-hippocampal organotypic slice cultures (OTCs). While confirming the major effect of LPS on SP, this thesis furthermore shows that neuroinflammation crucially involves the cytokine TNFα to transduce its effects on SP, and that microglial cells are the main source of TNFα production under inflammatory conditions.

In an attempt to learn more about the mechanisms that are affected under conditions of neuroinflammation effects of *retinoic acid* (RA), a vitamin A derivate were tested. This is mainly because SP as well as RA have been shown to modulate synaptic plasticity through the accumulation of glutamate receptors at the postsynaptic site: SP via the association with the actin-cytoskeleton as well as intracellular calcium stores, and RA directly via the modulation of local protein synthesis within dendrites. Indeed, in slice cultures exposed to RA, hippocampal SP-cluster size is upregulated, both *in vitro* and *in vivo*. Intriguingly, a lack of SP prevents RA-induced synaptic strengthening of hippocampal dentate granule cells in OTCs. This suggests a direct contribution of SP in RA-dependent synaptic plasticity. Interestingly, co-immunoprecipitation of SP-mRNA together with the RA-receptor alpha (RARα) further implies that RA directly controls synaptic plasticity via regulation of SP-protein expression. It is therefore interesting to speculate that RA may increase SP expression or prevent its reduction and thus alterations in synaptic plasticity under conditions of neuroinflammation. Taken together, this thesis identifies SP as an important neuronal target of TNFα-mediated alterations in synaptic plasticity. Moreover, the work on RA indicates that SP affects the ability of neurons to express synaptic plasticity by modulating/mediating local protein synthesis. Since neuroinflammatory processes are an elementary concomitant feature and/or cause of neurological diseases, I am confident that future work on the effects of inflammatory processes on brain function may provide the perspective in devising new therapeutic strategies for the treatment of neuropathologies such as Alzheimer’s disease, multiple sclerosis, epilepsy or stroke, by targeting SP expression and SP-mediated synaptic plasticity.

3. Introduction

What makes the mammalian and especially the human brain the most complex and fascinating organ across species? How do trillions of brain cells coordinate each other allowing us to learn and to remember? A basic understanding about the function of the brain is given by its structure. This key principle of structure- function-relationship is conserved across all systems in biology; from plants to mammalians and from molecules to complex tissues. The anatomy of the brain has been studied for thousands of years. Among the ancient Greeks, Alcmaeon (500 B.C.) discovered that the brain controls body functions (Zemelka 2017). In the renaissance, Andreas Vesalius dissected and illustrated the human brain in great anatomical detail (Cambiaghi 2017). Major breakthroughs in optical technics – that is the invention of the microscope by Huygens at the end of the 17th century – and the understanding of electricity, lead to a remarkable increase in the insights into the brain structure and function (Van Helden & Van Gent 1999). In the middle of the 18th century Luigi Galvani discovered the electrical component of neurotransmission (Kazamel & Warren 2017) and histologists including Camillo Golgi and Ramón y Cajal who stained and studied brain cells in detail in the 19th century (Yuste 2015) depicted first neuronal cells with their three main compartments: The dendritic tree, receiving incoming signals which are integrated at the cell body (soma), and forwarded across an axon to downstream neuronal and other targets.

3.1 Neurotransmission

The signal transmission from one neuron to another is achieved electrochemically. That is, within individual neurons the signal is propagated electrically, while at the synapse, in between two neurons, the signal is transmitted chemically. Under resting conditions, the neuron is kept at a constant potential, the resting membrane potential (RMP) of about -60 to -75 mV, depending on the ion concentration across the plasma membrane (Table 1) as well as the permeability of these ions to cross the membrane, which in turn is dependent on the presence of ion channels.

	C_{OUT}[mmol]	C_{IN} in [mmol]	Nernst potential [mV]
Na^+	440	50	+55
K^+	20	400	-75
Cl^-	550	52	-60

Table 1. Ion concentration across the plasma membrane of a giant squid axon (Kandel et al. 2000)**.**

This relation is summarized by the Goldman-Hodgkin-Katz equation which describes the passive properties of a plasma membrane (Equation 1):

$$U_{\mathrm{M}} = \frac{RT}{F} \cdot \ln \frac{P_{\mathrm{Na}} \cdot [\mathrm{Na}^+]_a + P_{\mathrm{K}} \cdot [\mathrm{K}^+]_a + P_{\mathrm{Cl}} \cdot [\mathrm{Cl}^-]_i}{P_{\mathrm{Na}} \cdot [\mathrm{Na}^+]_i + P_{\mathrm{K}} \cdot [\mathrm{K}^+]_i + P_{\mathrm{Cl}} \cdot [\mathrm{Cl}^-]_a}$$

Equation 1. Goldman-Hodgkin-Katz equation. The electric potential across a plasma membrane (U_M) is mainly defined by the ion concentration within (i) and outside (a) the cell, as well as the permeability (P) of these ions across the membrane. The potential is further dependent on the temperature (T) in Kelvin and two constants: R = gas constant and F = Faraday constant.

Depolarization of the plasma membrane, mainly driven by the influx of sodium through voltage-gated sodium channels (Na_V), increases the membrane potential. Once a certain threshold is reached (around -40 mV), voltage-gated sodium channels open immediately and trigger an action potential (AP). In the first phase of the AP, fast opening Na_V drive the membrane potential toward the equilibrium potential of sodium, around +40 mV. However, before reaching this potential, the Na_V closes slowly and voltage-gated potassium channels (K_V) open. In phase 2, the AP decays, mainly driven by the efflux of potassium. A delayed closing of K_V leads to a temporary hyperpolarization (phase 3) of the AP, due to the driving force of potassium toward its equilibrium around -90 mV. Finally, during the repolarization the membrane potential recovers (phase 4). The AP is transduced unidirectionally along the axon which ends in the presynaptic terminal. At the synapse, the signal is transduced chemically across a few nanometers wide synaptic cleft to the post-synaptic side of a neighboring

neuron. Briefly, an AP activates voltage-gated calcium channels (Ca_V) within the presynaptic terminal. Calcium influx fulfills two main functions: First, by binding to a Calcium/calmodulin dependent protein kinase (CaMK), it mobilizes neurotransmitter-containing synaptic vesicles which are bound to the cytoskeleton. Vesicle fusion with the pre-synaptic plasma membrane is achieved via t-SNARE (including SNAP-25 and synthaxin) and v-SNARE proteins. Second, calcium binds to synaptotagmin leading to the opening of a channel pore through which neurotransmitters are released into the synaptic cleft. Depending on the type of neurotransmitter (excitatory/inhibitory) released into the synaptic cleft, the postsynaptic membrane will be depolarized or hyperpolarized.

In the central nervous system (CNS), the most abundant excitatory neurotransmitter is the amino acid glutamate, while inhibition of mature neurons is driven mainly by gamma-aminobutyric acid (GABA). Most excitatory synapses appear at thorny protrusions emanating from dendrites, known as dendritic *spines* (Newpher & Ehlers 2008; Sheng & Hoogenraad 2007). Most inhibitory postsynaptic sites do not show such a characteristic morphology and are localized at the dendritic shaft (Gao & Penzes 2015). On the one hand, neurotransmitters activate receptor channels (e.g. Ca^{2+}/Na^{+}/K^{+}-gating AMPA-/ NMDA receptors or Cl^{-}-gating GABA receptors) which depolarize/ hyperpolarize the plasma membrane and/or activate downstream signaling cascades, as is the case for Ca^{2+} (activation of CaMK) finally regulates gene expression]. On the other hand neurotransmitters can activate metabotropic G-protein coupled receptors that activate second messengers via phosphorylation reactions.

3.2 The hippocampus and learning and memory

Synaptic and neuronal network functions have been studied in great detail in a region of the brain known as the *hippocampus*. In humans, the hippocampus is located in the medial temporal lobes of the brain. Similar to other brain regions, the functional significance of the hippocampus has been demonstrated in clinical studies on patients with hippocampal lesions. The

probably most prominent case was published in the mid 1950s which describes the patient Henry G. Molaison, known as H.M., who underwent surgical bilateral temporal-lobectomy to alleviate epilepsy localized in this particular brain region. After removal of large parts of both temporal lobes, including the hippocampal region, H.M. could still very well remember most memories that he gained until the day of surgery. He could also retrieve new experiences for a short time, but he was unable to transfer those experiences into long-term memory (anterograde amnesia). Interestingly perceptual learning and other types of simple reflexive learning were not affected by the lesion, although he was unable to remember the person who taught him, the places where he acquired the skills, or any other explicit information associated with the learning procedure (Scoville & Milner 1957; Anderson et al. 2007). Studies on humans and animals demonstrated that the most important function of the hippocampus is indeed the encoding and retrieval of long-term memory, which concerns exclusively explicit (or declarative) memories (i.e. facts and events), but not long-term, non-mnemonic or short-term memories. Studies in rodents disclosed that the entorhinal-hippocampal formation is crucially involved in spatial navigation (O'Keefe & Dostrovsky 1971; O'Keefe & Speakman 1987). The hippocampus contains various pyramidal neurons known as place cells which show activity only when the animal is located at a specific position in an environment, providing important information required for spatial orientation (O'Keefe & Dostrovsky 1971; Moser et al. 2008). Grid cells localized in the EC contribute to a spatiotemporal neural representation of the environment (Hafting et al. 2005).

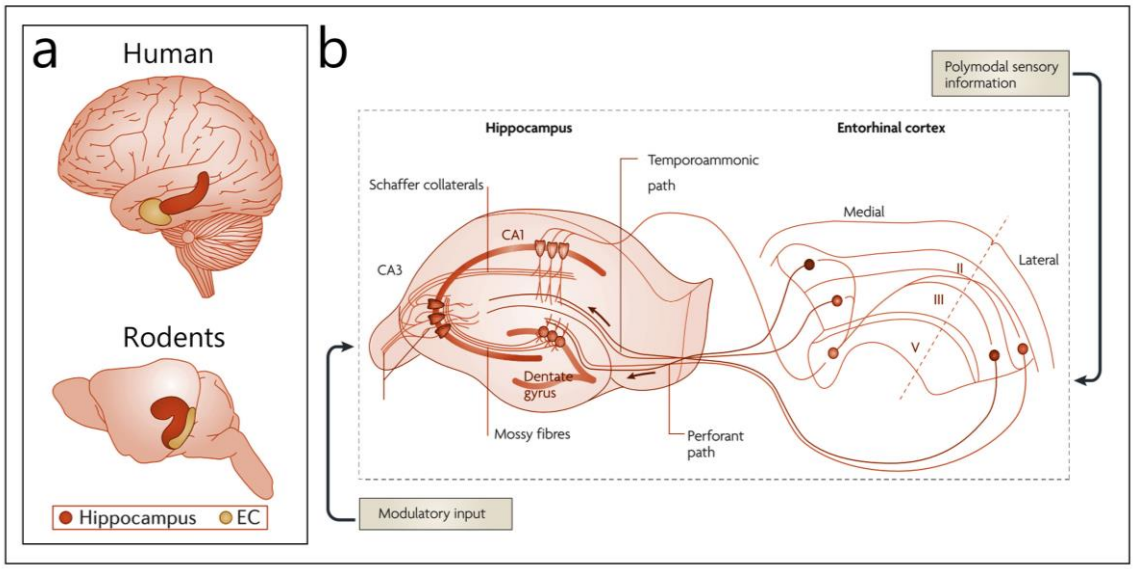

Figure 1. Anatomical localization and organization of the hippocampus. (a) Localization of the hippocampus (red) and entorhinal cortex (EC, yellow) in the human and rodent brain. **(b)** Neural network of the hippocampus and laminar organization of the EC depicting the trisynaptic loop of the perforant path, mossy fibers and Schaffer collaterals. Illustartion in (a) adapted from Strange et al. (2014) and (b) Neves et al. (2008).

3.3 Anatomy of the hippocampal formation

Anatomically the hippocampal formation consists of three main sections: the dentate gyrus (DG), the hippocampus proper (known as the cornu ammonis CA region), which is subdivided into CA1, CA2 and CA3 as well as the entorhinal cortex (EC) (Amaral & Witter 1989, Andersen et al. 2007). Barring proportional and organizational differences, the hippocampal architecture is highly conserved across mammalian species (rodents, primates, humans). The basic structure of the hippocampus can be described as a tri-synaptic network composed of excitatory neurons: Sensory input from the neocortex reaches the hippocampus through the EC and is forwarded mainly via fibers of the perforant path to granule cells of the DG – only a subdivision of fibers directly targets the Ammon's horn (temporoammonic path). Granule cell axons (also called mossy fibers) forward signals to CA3 pyramidal neurons which in turn send Schaffer collateral axons to the apical dendrites of CA1 pyramidal neurons. From here, output goes back, via the subiculum to the EC (Figure 1). Indeed, most hippocampal input arises from within the boundaries of the hippocampus, the

DG, and the EC. This comprises connections from the same hemisphere (associative connections) and commissural connections from the contralateral hippocampal formation. A variety of inhibitory neurons within the hippocampus modulates and controls the hippocampal neural circuit. Recent studies highlight the three-dimensional organization of the hippocampus and correlate it with a functional dissociation along the dorso-ventral axis, which is part of a vivid debate (Strange et al. 2014). As mentioned above, the hippocampal complex comprises two main regions which are structurally and functionally distinct. The *dentate gyrus* is divided into three layers: A widely cell-free molecular layer bordering the hippocampal fissure which contains the apical dendritic trees of the dentate granule cells (Figure 2). The molecular layer can be further subdivided into an inner, middle and outer molecular layer (IML, MML and OML). The IML is connected mainly to commissural/associational afferents (Deller et al. 1996), while the MML and the OML, adjacent to the hippocampal fissure, receive perforant path fibers projected from stellate cells located in EC layer II. Fibers of the lateral perforant path (ascending from the lateral EC) target dendrites close to the hippocampal fissure within the OML, while medial perforant path fibers (originating from the medial EC) get in contact with dendrites within the middle third of the molecular layer. The granule cell layer comprises densely packed somata of the principle cells of the dentate gyrus, the dentate granule cells, which are characterized by an elliptic cell body and a cone-shaped spiny dendritic tree. Different interneurons, such as large pyramidal basket cells, populate the dentate gyrus. Most of these inhibitory neurons are immunoreactive to GABA. Below the granule cell layer and adjacent to the hilar region lies the polymorphic layer. While the main efferent projection, the mossy fiber pathway, connects to CA3 pyramidal neurons, granule cells are further connected to excitatory hilar mossy cells of the polymorphic layer (Frotscher et al. 1991). While the majority of the extrinsic input to the dentate gyrus originates from the EC, a subpopulation of axons targeting the molecular layer comes from the pre- and parasubiculum (Köhler 1985). Only little input arrives from subcortical structures. Cholinergic and GABAergic fibers for example can be traced back to the septal nuclei of the

forebrain (Mosko et al. 1973; Nyakas et al. 1987), while noradrenergic fibers are projected from the pontine nucleus locus coeruleus (Pickel et al. 1974; Loughlin et al. 1986), diffuse distributed dopaminergic fibers originate in the ventral tegmental area, and serotonergic axons from the raphe nuclei project from the brain stem and terminate mainly in the polymorphic layer of dentate gyrus (Conrad et al. 1974; Vertes et al. 1999). The principle cell of the *hippocampus*

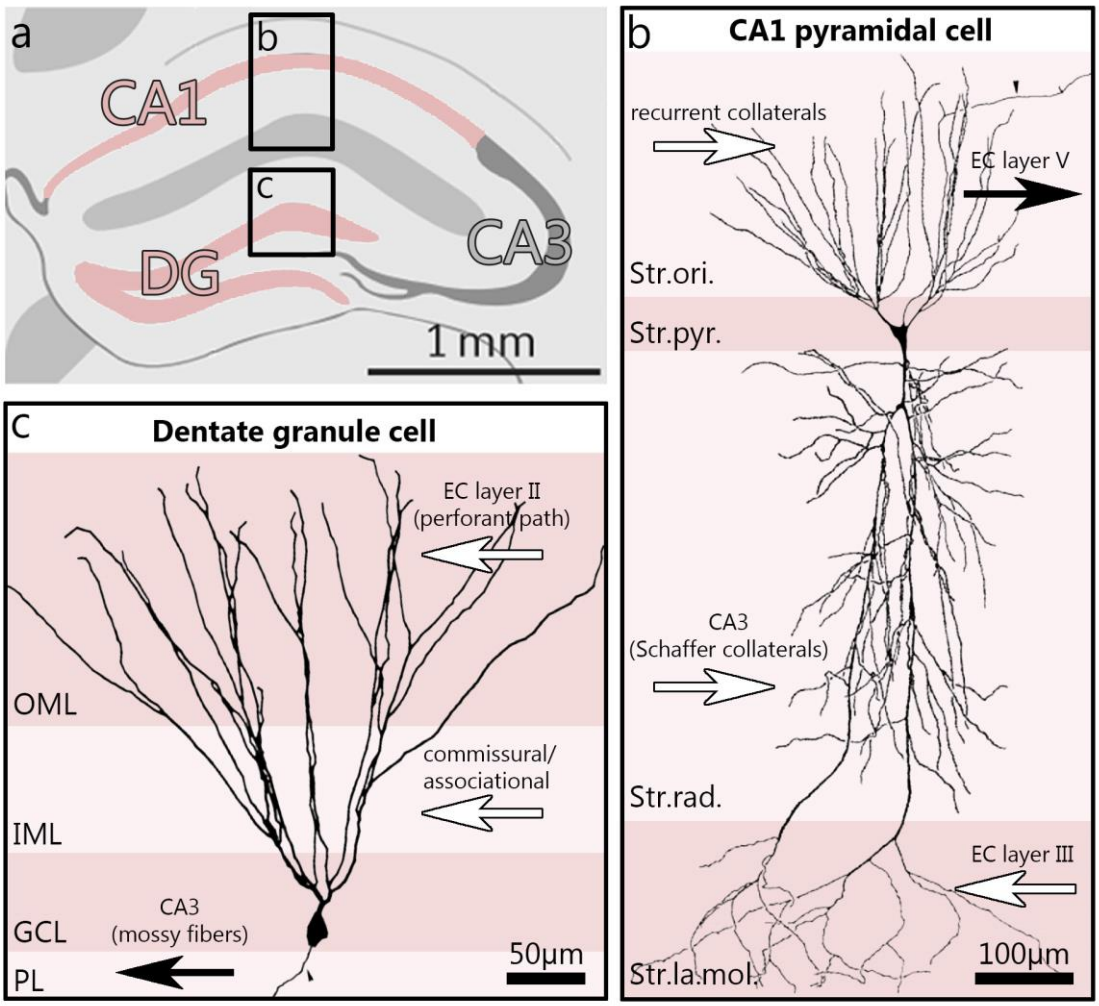

Figure 2. Schematic of the hippocampus and localization as well as network integration of dentate granule as well as CA1 pyramidal cells. (a) Drawing of a mouse hippocampal Nissl cross-section. This thesis focuses on the dentate gyrus (DG) and CA1 area which are highlighted in red. (b) Camera lucida drawing of a CA1 pyramidal neuron and (c) a computer-generated reconstruction of a horseradish peroxidase-filled granule cell from the suprapyramidal blade. (b+c) Afferent fibers are indicated by white arrows; efferent fibers are indicated by black arrows. OML = Outer molecular laye, IML = inner molecular layer, GCL = granule cell layer, PL = polymorphic cell layer, Str.ori. = Stratum oriens, Str.pyr. = Stratum pyramidale, Str.rad. = Stratum radiatum, Str.la.mol. = Stratum lacunosum moleculare, EC = entorhinal cortex. Illustration shown in (a) adapted from Strange et al. (2014) and (b+c) adapted from Andersen et al. (2007).

proper is the pyramidal cell. The laminated structure of the hippocampal complex continues in the areas of CA1 to CA3. Cell bodies of pyramidal neurons are located within the pyramidal cell layer and give rise to one or two apical and one basal dendritic tree. The basal dendrites branch into the layer of stratum oriens, while the apical dendrites occupy the layers of stratum radiatum and stratum lacunosum moleculare. CA3 pyramidal cells receive their main excitatory input via mossy fibers arising from granule cells of the dentate gyrus, while it has also been demonstrated that perforant path fibers arising from EC layer II project into the CA3 region (Witter 1993). Schaffer collateral axons of CA3 neurons in turn form synapses onto CA1 dendrites within the stratum radiatum. While the cytoarchitecture of CA3 pyramidal neurons is noticeably heterogenic, CA1 neurons are characterized by a relatively homogeneous dendritic organization e.g. total dendritic length and configuration are relatively similar across different locations within the CA1 region (Pyapali et al. 1998). Extrinsic input towards CA1 neurons arises from the EC layer III which ends at the distal tips of CA1 neurons within the stratum lacunosum moleculare or on interneurons that contact CA1 synapses of that region. Afferents from different brain regions terminate in the stratum lacunosum moleculare as well. The hippocampus is also widely connected to various types of interneurons which are localized across all layers of CA1. Most interneurons, such as pyramidal basket cells, axo-axonic cells (also named chandelier cells) and bistratified cells are localized closely to the pyramidal cell layer, while a far smaller population of interneurons is found in the stratum radiatum and stratum lacunosum moleculare. Although the hippocampus receives relatively little extrinsic input from other brain regions, they are crucial to understanding its function. Most cortical input comes from the peri- (area 35 and 36) and postrhinal cortices targeting CA1 dendrites within the stratum lacunosum moleculare which borders the subiculum. Several subcortical afferents target the hippocampus arising from the basal forebrain, thalamic regions, as well as serotonergic, noradrenergic, and dopaminergic afferents from the brain stem.

3.4 Associative synaptic plasticity

The question how consolidation of memory is achieved at the cellular and molecular level has been studied for decades. The key mechanism how information is incorporated into long-term memory is known as synaptic plasticity. Indeed, neurons are very dynamic, and synaptic connections can be modulated depending on their activation. In the late 1940s Donald Hebb postulated: “When an axon of cell A is near enough to excite a cell B and repeatedly or persistently takes part in firing it, some growth process or metabolic change takes place in one or both cells such that A's efficiency, as one of the cells firing B, is increased” (Hebb 1949). Hence, Hebbian plasticity outlines a positive feedback loop. Based on that assumption, Bliss & Lømo (1973) experimentally proved that a high frequency (100 Hz) stimulation of synaptic connections leads to long-lasting changes of synaptic strength, known as long-term potentiation (LTP) and its counterpart long-term depression (LTD) which outlines a weakening of synapses in response to low frequency (1 Hz) stimulation. Indeed, LTP is considered to be the cellular basis of various types of memory (Bliss & Collingridge 1993; Bi & Poo 2001; Sjöström et al. 2008; Collingridge et al. 2010; Cooper & Bear 2012). LTP crucially depends on two glutamate-gated receptor-channels, both localized in the post-synaptic membrane: The *N*-Methyl-D-aspartate-receptor (NMDAR) and α-amino-3-hydroxy-5-methyl-4-isoxazole propionic acid receptor (AMPAR). LTP is formed either when multiple afferents from one pathway converge in the vicinity of a synapse (=cooperative LTP) or when two separate stimuli, e.g. a weak stimulus followed by a strong stimulus meet synchronically at the same synapse (=associative LTP). To produce LTP, NMDARs act as coincidence detectors, since they are only functional when two criteria are met: Firstly, glutamate released during presynaptic activity must be present and secondly, the postsynaptic membrane needs to be depolarized sufficiently and synchronically to expel an Mg^{2+}-ion that blocks the channel pore. Hence, the pre- and post-synaptic site must be active at the same time. The depolarization of the presynaptic site is mainly achieved by AMPARs through Na^{2+}-influx/ K^{+}-efflux.

Therefore, AMPARs define the strength of a synapse. NMDARs are permeable to Ca^{2+}. As a second messenger Ca^{2+} activates signaling cascades that regulate the amount of AMPARs incorporated into the postsynaptic membrane and thereby contributes to the formation of short-term synaptic modifications (e.g. via the protein kinase A (PKA) -mediated phosphorylation of AMPARs) as well as long-term changes (via the PKC-mediated activation of gene expression) (Kandel et al. 2000). Furthermore, depending on pre/posttranslational modifications and their subunit composition, AMPARs can also be permeable to Ca^{2+}. Four AMPAR subunits (GluA1-4) have been identified, which are assembled as two homodimers to form the channel pore. The most common subunits in the brain are GluA1 and 2. A posttranscriptional modification (RNA-editing) leads to an exchange of a negatively charged glutamine at position 607 (i.e. within the pore loop) with a positively charged arginine (Sommer et al. 1991; Burnashev et al. 1992). This single amino acid modification renders GluA2-containing AMPARs impermeable to Ca^{2+}. Hence, only GluA2-lacking AMPARs are able to conduct Ca^{2+} (reviewed in detail by Lee 2012).

3.5 Homeostatic synaptic plasticity

The concept of associative, i.e., Hebbian plasticity as a self-enhancing, positive feedback mechanism calls for a regulatory and balancing mechanism to prevent the neural circuit from runaway-excitation. *Homeostatic synaptic plasticity* is such a mechanism that acts as a negative feedback loop. While Hebbian plasticity affects synaptic contacts locally in an input specific manner within seconds, homeostatic synaptic plasticity is a rather slow adaptive mechanism modulating thousands of synaptic connections over longer periods of time (minutes and hours; Vitureira & Goda 2013; Turrigiano 2012). Homeostatic plasticity has been shown to modulate both inhibitory as well as excitatory synapses to keep the network in balance (Hartman et al. 2006; Maffei et al. 2006; Vlachos et al. 2012). Changes of network activity lead to a global adaptation of synaptic efficacy, known as *synaptic scaling* which is achieved by

modulating the amount of AMPARs at the post-synaptic site. This ensures that differences in synaptic weights, which are the principle of information storage and processing mechanisms, are preserved. Especially, under pathological conditions, which lead to a loss of connectivity (e.g. Alzheimer's disease, stroke etc.), homeostatic synaptic plasticity aims in keeping the network in balance. Experimentally synaptic scaling can be assessed by electrophysiological recordings of miniature excitatory postsynaptic currents (mEPSCs, also referred to as 'minis') which represent single post-synaptic inward currents that are elicited by spontaneous, i.e., action potential-independent vesicle fusions at the pre-synaptic terminal. In general, the amplitude of mEPSC events represents the strength of synapses, while changes in mEPSC frequency most likely indicate overall changes in the number of synaptic connections of the recorded neuron and/or pre-synaptic adaptations, e.g. modifications of vesicle-release probability. Synaptic scaling can be induced by pharmacological inhibition of network activity (e.g. by blocking Na_V with tetrodotoxin, TTX), which leads to a compensatory increase of AMPARs at the post-synaptic membrane, which can be detected as an increase in mEPSC amplitude.

As mentioned above, homeostatic synaptic plasticity is generally considered a slow mechanism, affecting a number of synaptic contacts. However, recent studies also discuss rapid compensatory processes acting locally (Turrigiano 2008; Pozo & Goda 2010; Zenke et al. 2017).

3.6 Neuroinflammation

Most if not all neurodegenerative diseases like Alzheimer's disease (AD), Parkinson's disease (PD), multiple sclerosis (MS) or amyotrophic lateral sclerosis (ALS) are accompanied by inflammatory processes (Heppner et al. 2015). In addition, the course of acute neurological pathologies like trauma or stroke are accompanied by inflammation of brain tissue (reviewed in detail by Ceulemans et al. 2010). In order to optimize treatment strategies and to finally cure such diseases, it is elementary to understand the causes and mechanisms of inflammatory processes. Several pro-inflammatory molecules (originating

from the periphery and/or the CNS) contribute to the induction and maintenance of neuroinflammation. Among them, TNFα appears to be of particular importance in initiating and sustaining the inflammatory response. The proinflammatory cytokine TNFα was first described in 1975 as a molecule with necrotic effects on tumors *in vitro* (Carswell et al. 1975). TNFα is expressed as a 26 kDa precursor transmembrane protein (sometimes referred to as pro-TNFα). Proteolytic cleavage by the metalloprotease TNFα-converting enzyme (TACE) liberates a soluble trimeric 17 kDa isoform (sTNF). Both isoforms, membrane-bound and soluble, are biologically active. TNFα signaling comprises various important functions within the CNS (Mccoy & Tansey 2008), including activation of microglia (Merrill 1991), regulation of glutamatergic neurotransmission (Pickering et al. 2005), and control of synaptic strength (Beattie et al. 2002). While basal release of TNFα appears to be substantial for synaptic functioning, excess TNFα production has opposing effects. This becomes clinically relevant since elevated TNFα levels have been documented in several neurodegenerative disorders, including AD (Álvarez et al. 2007), PD (Nagatsu et al. 2000), and HIV-associated dementia (Wesselingh et al. 1993), rendering TNFα as a potential therapeutic target for such diseases. TNFα signaling is mediated via two transmembrane receptors, TNFR1 (also known was p55/p60) and TNFR2 (also known as p75/p80), which have opposing effects on cell fate upon activation. While TNFR1s are capable of inducing apoptosis by recruiting various caspases, TNFR2s contribute to pathways promoting cell survival (summarized in Figure 4). For a detailed insight into the principles of TNFα-mediated signaling cascades, the interested reader is referred to an in-depth review by Sedger & McDermott 2014.

Several cell types of the CNS are involved in mediating the inflammatory response. Among neurons, astrocytes, and endothelial cells, microglia play a central role in neuroinflammatory processes as well as cellular and molecular mechanisms involved in neurodegenerative diseases (Hanisch 2002; Ekdahl et al. 2009; Monji et al. 2013). Under physiological conditions, microglial cells are elementary for the maintenance of homeostasis within the brain (Perry & Teeling 2013). The plasma membrane of microglia is equipped with specific

receptive surface molecules that enable microglia to continuously monitor the environment. Moreover, microglia are able to secrete soluble factors which (in turn) influence astrocytes and neurons (Kettenmann et al. 2011). Furthermore, microglia facilitate clearance of cellular metabolites and aggregated proteins (Lee et al. 2010).

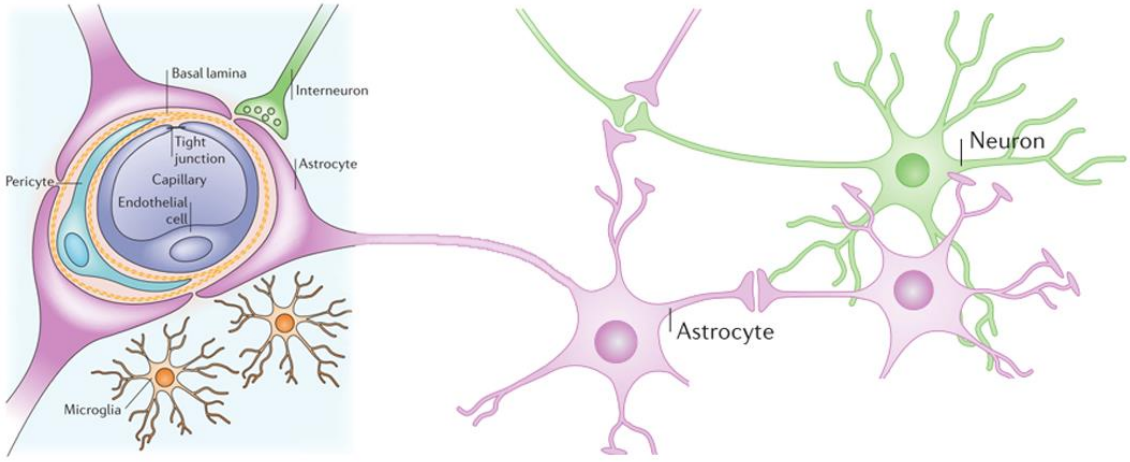

Figure 3. Cellular elements of the blood–brain barrier (BBB). Endothelial cells are connected via tight junctions and form the inner layer of the BBB. Astrocytic perivascular endfeet form a second layer and build the connection to the neural network. The space between astrocytes and endothelial cells is filled with basal lamina. Pericytes embedded in the basal lamina are also directly involved in sustaining the BBB and brain function. Microglia are especially important under pathological conditions to maintain brain function and are the main contributors to the inflammatory response. Illustration adapted from Abbott et al. (2006).

Under pathological conditions, e.g. severe inflammation or tissue damage, microglia show several similarities to peripheral macrophages, regarding the response to pathogenic stimuli (reviewed in detail by González et al. 2014). Like macrophages, microglia can respond to pro- or anti-inflammatory signals upon activation. In the presence of anti-inflammatory cytokines IL-4 or IL-10 for example, microglia acquire an M2-like phenotype which is characterized by branched processes, thin cell bodies, and expression of certain marker molecules (Nimmerjahn et al. 2005; Ransohoff & Perry 2009). Upon activation by LPS or IFN-y, however, microglia switch to an M1-like phenotypes which is characterized by an amoeboid shape, release of high amounts of pro-inflammatory cytokines, increased mobility, and strong phagocytic activity (Bedi et al. 2013; Burguillos et al. 2011; Ransohoff & Perry 2009). Both, M1- and M2-like phenotype are necessary for an efficient and controlled immune response.

During the initial phase after brain injury or infection, microglia with M1-like featurs create a microbicide environment and display phagocytic activity to eliminate cellular debris. In the subsequent M2-like phase, microglia attenuate the inflammatory response by the release of anti-inflammatory cytokines and facilitate tissue repair via the production of neurotrophic factors (Shechter et al. 2013). However, the second phase can also be detrimental, when microglia are continuously activated in an uncontrolled manner (Takeuchi & Akira 2010). In that case, microglia trigger chronic inflammation which is accompanied by permanent release of neurotoxic factors and pro-inflammatory mediators like TNFα, IL-6, IL-1a/b, nitric oxide or proteolytic enzymes, and glutamate, which ultimately leads to neuronal damage and loss (Burguillos et al. 2011; Barger & Basile 2001; Block et al. 2007; Kettenmann et al. 2011).

Neuroinflammation can either originate from within the brain tissue or it can be triggered by pro-inflammatory substances coming from the periphery. However, the CNS is seen as a rather immune privileged region of the body, mainly because of its isolation from external passage by the blood brain barrier (BBB) which is a highly dynamic biological membrane interface separating peripheral circulation from the CNS. The BBB represents a physical barrier of cerebral microvessels, which is mainly formed by an endothelial cell layer that is interconnected by tight-junctions, and is surrounded by basal lamina and astrocytic perivascular endfeet (Begley & Brightman 2003; Wolburg & Lippoldt 2002; reviewed in detail by Abbott et al. 2006) (Figure 3). Of note, several pathologies, among them inflammatory processes, lead to a permeabilization of the BBB, allowing the passage of pro-inflammatory substances from the periphery into the CNS. The bacterial lipopolysaccharide (LPS) is a strong inflammatory stimulus and a classic model to study effects of inflammatory processes under experimental conditions (for details on LPS-mediated inflammation see Box 1 below). LPS-induced inflammation directly affects tight junctions of endothelial cells, mainly via the production of free radicals and interleukins (Gaillard et al. 2003).

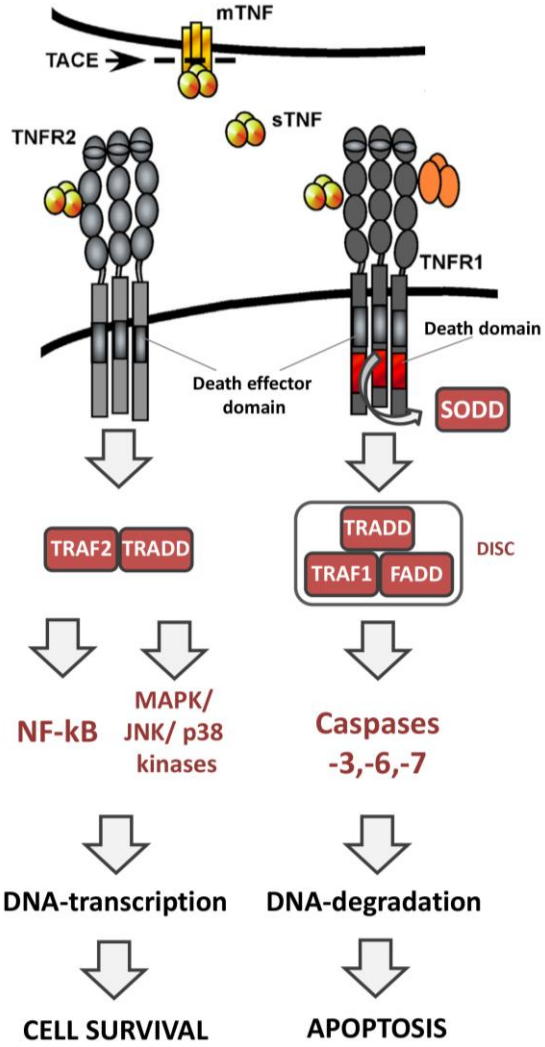

Figure 4. Overview of TNFα-receptor TNFR1/2 signaling cascades. TNFα signaling is mediated via two receptors: TNFR1 and TNFR2. After release of the silencer of death domain (SODD), TNFR1 signaling activates a signaling pathway which finally leads to programmed cell death. In contrast, activation of TNFR2 has opposite effects, leading to the activation of gene-expression promoting cell survival. Abbreviations: DISC = Death inducing signaling complex, FADD = Fas-associated death domain, JNK = c-Jun-terminal kinase, MAPK = mitogen-activated protein kinase, NF-κB = nuclear factor kappa-light-chain-enhancer of activated B cells, TACE = TNFα-converting enzyme, TRADD = TNFR-associated death domain, TRAF = TNFR-associated factor. Schematic adapted from Sedger & McDermott (2014).

Box 1 | **Mechanism of LPS/TLR4-signal transduction pathway**

Lipopolysaccharides (LPS) are glycolipids localized within the outer cell membrane of Gram negative bacteria (Seltman & Holst 2002). The LPS molecule consists of a lipid domain (lipid A) that anchors the molecule to the bacterial cell membrane. Attached to lipid A is a sugar containing an inner- and outer core domain bound to a polysaccharide domain (O antigen) (Raetz 1990). Both core and the O antigen vary greatly among species and even within strains (Lerouge & Vanderleyden 2002). As a potent endotoxin, LPS exposed to mammalian cells triggers a strong inflammatory reaction. Initially, LPS interacts with the LPS binding protein (LBP) which recruits a complex that facilitates the activation of the toll-like receptor 4 (TLR4). Downstream, either a MyD88-dependent or a MyD88-indepent (TRIF-dependent) cascade is triggered. Activation of the MyD88-dependent pathway leads to the expression of pro-inflammatory cytokines like TNFα and interleukins. The TRIF-dependent path triggers the expression of type 1 interferons. (Kagan 2008; Kenny et al. 2008; reviewed in detail by Lu et al. 2008 and Rhee 2014).

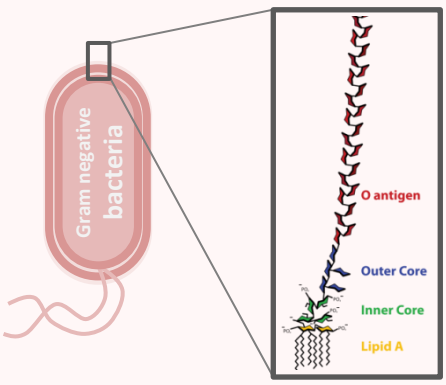

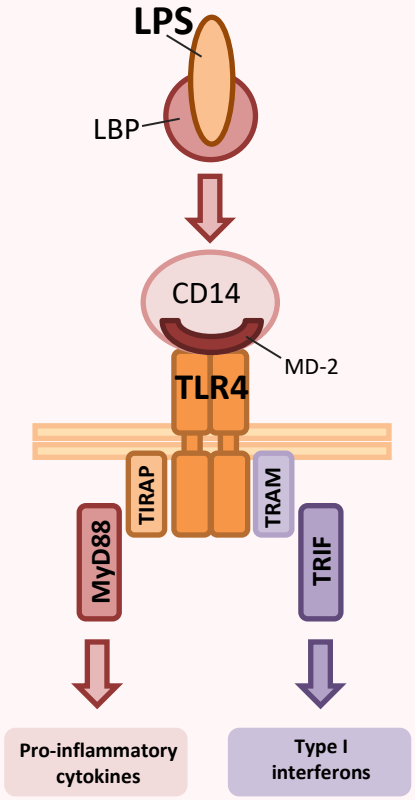

3.7 Synaptopodin

Synaptic plasticity is regulated by various types of proteins at distinct sites within a neuron. Proteins localized in close proximity to or within the synapse are most efficient in modulating synaptic structure and function. The actin-binding proline-rich protein synaptopodin (SP) is located at such a strategic position within the spine neck of cortical and hippocampal neurons (Mundel et al. 1997) (Figure 5). SP is involved in regulating both associative and homeostatic forms of synaptic plasticity (Deller et al. 2003; Vlachos et al. 2009; Vlachos et al. 2013). The name “synaptopodin” describes the fact that this molecule is found in dendritic spines, i.e. in proximity to synapses as well as in renal podocytes (Mundel et al. 1997; Deller et al. 2000). Later, it was shown that SP is also localized in other neuronal compartments, like the axon initial segment (Bas Orth et al. 2007). About 95% of dendritic SP localize to variable positions within spines. Only a minority of about 5% of SP is found in the dendritic shaft, except for the stratum lacunosum moleculare of the CA1 region, where approximately 20% of SP is localized outside of spines and within the dendritic shaft (Bas Orth et al. 2005). Spine analysis revealed that approximately 30% of all spines in the hippocampus contain SP (Vlachos et al. 2009), which is distributed in a lamina- and region-specific fashion (Deller et al. 2000; Bas Orth et al. 2005). SP is closely associated with the spine apparatus (SA), a structure which is found in a subset of dendritic spines. Since its first description in 1959 by E. G. Gray, the role of the SA in regulating synaptic function has been vividly investigated and

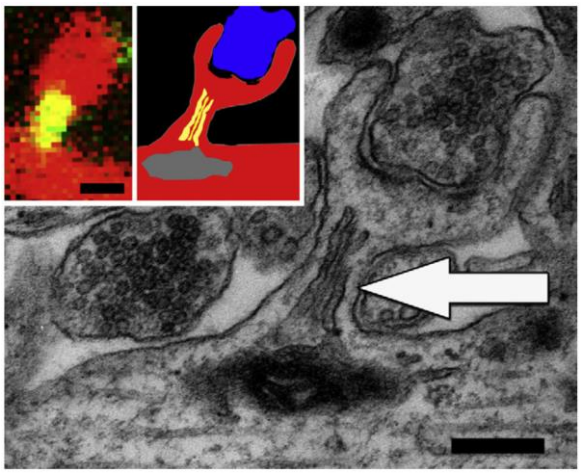

Figure 5. Dendritic synaptopodin (SP) is mainly localized to spines and a marker of the spine apparatus (SA). The SA is a stacked membranous structure composed of smooth endoplasmic reticulum. Electron micrograph of SA (arrow) localized within a spine neck of a dentate granule cell (DGC). Alexa568-filled DGC in red immunostained for SP (green; appears yellow due to colocalization with the red signal; left) and the corresponding schematic based on the electron micrograph. Scale bars: 500 nm. Figure original from Vlachos (2012).

discussed (Gray, 1959). As a derivate of the smooth endoplasmic reticulum (sER), which forms stacks that are organized by electron dense material, the SA has been proposed to serve as Ca^{2+}-reservoir that regulates Ca^{2+} homeostasis during synaptic activity (Fifková et al. 1983; Vlachos et al. 2009; Segal et al. 2010). Furthermore, the SA has been considered to play a role in local protein synthesis (Pierce et al. 2000). SP seems to be crucial for the formation of the SA, since mice lacking SP do not form SAs (Deller et al. 2003; Korkotian et al. 2014) and show deficits in Hebbian plasticity (LTP) *in vitro* (Deller et al. 2003) and *in vivo* (Jedlicka et al. 2009), as well as defects in spatial learning (Deller et al. 2003; reviewed in Jedlicka et al. 2008). This indicates a direct correlation between SP and the SA in regulating associative forms of synaptic plasticity. Within spines, SP has been shown to be localized most preferentially at the proximal base of the spine head (Vlachos et al. 2009). Spine head sizes are significantly larger in SP(+) compared to SP(-) spines, indicating a role for SP in regulating spine morphology (Vlachos et al. 2009). This observation is linked to the association of SP to the actin cytoskeleton via an actin/actinin binding domain (Asanuma et al. 2005), which has been shown to be important for controlling the incorporation of the AMPAR subunit GluA1 into the post-synaptic membrane (Vlachos et al. 2009). Furthermore, the SP-dependent increase of GluA1 within dendritic spines has been shown to require both activation of NMDARs (controlling calcium from extracellular space) as well as activation of ryanodine receptors (RyR; controlling calcium entry of internal stores) (Vlachos et al. 2009). Altogether, these findings reveal a fundamental role of SP in synaptic plasticity. It is interesting to note that some of the findings that link SP to GluA1-dependent synaptic plasticity resemble what has been reported in the context of retinoic acid (RA)-mediated synaptic plasticity.

3.8 Retinoic acid (RA)

Biochemically RA represents a metabolite of vitamin A. Precursors of RA are mainly ingested as ester (primarily retinyl palmitate) which are oxidized in two steps to retinol by the retinol dehydrogenase (ROLD) and, finally, to RA via

retinal dehydrogenase (RALD) (Figure 6a). RA is best studied for its role in neural development. Recently evidence has been provided that RA is an important signaling molecule and regulator of both, associative and homeostatic synaptic plasticity (Maden 2002; Aoto et al. 2008; Arendt et al. 2015a/b). RA binds to retinoic acid receptors RAR(α,β,γ) and RXR(α,β,γ) which are expressed in various tissues and brain regions to mainly regulate DNA-transcription in the nucleus as well as mRNA-translation in the soma (Krezel et al. 1999). Especially RARα has been studied intensively for its involvement in regulating synaptic function within the hippocampus (Maghsoodi et al. 2008; Aoto et al. 2008; Arendt et al. 2015a/b). RARα consists of six modular domains (A-F). In the N-terminus, the domains A to D are involved in transcriptional regulation, while domain E represents the ligand-binding domain, and the F-domain at the C-terminus functions as the mRNA binding motif (Sarti et al. 2012; Figure 6b). Poon and colleagues (2008) showed that this motif binds to a specific sequence element within the 5'UTR of GluA1 mRNA, thereby repressing its translation. Reduced synaptic activity leads to a drop in intracellular calcium levels, which triggers RA synthesis in a calcineurin (CaN) dependent manner (Arendt et al. 2015b). Once RA binds to the RA-recognition site RARα is released from the transcript, GluA1 protein is expressed and incorporated at post-synaptic sites, leading to an increase in synaptic strength (Aoto et al. 2008; Poon & Chen 2008). Thus, RA holds a fundamental function by modulating synaptic plasticity via regulation of local protein synthesis within dendrites. Intriguingly it enables a neuron to locally react to activity changes, aiming to adapt to perturbations of network activity. Further, the fact that RARα targets the mRNA of GluA1 poses the fascinating question whether RA also affects expression of other transcripts that are known to be involved in synaptic plasticity.

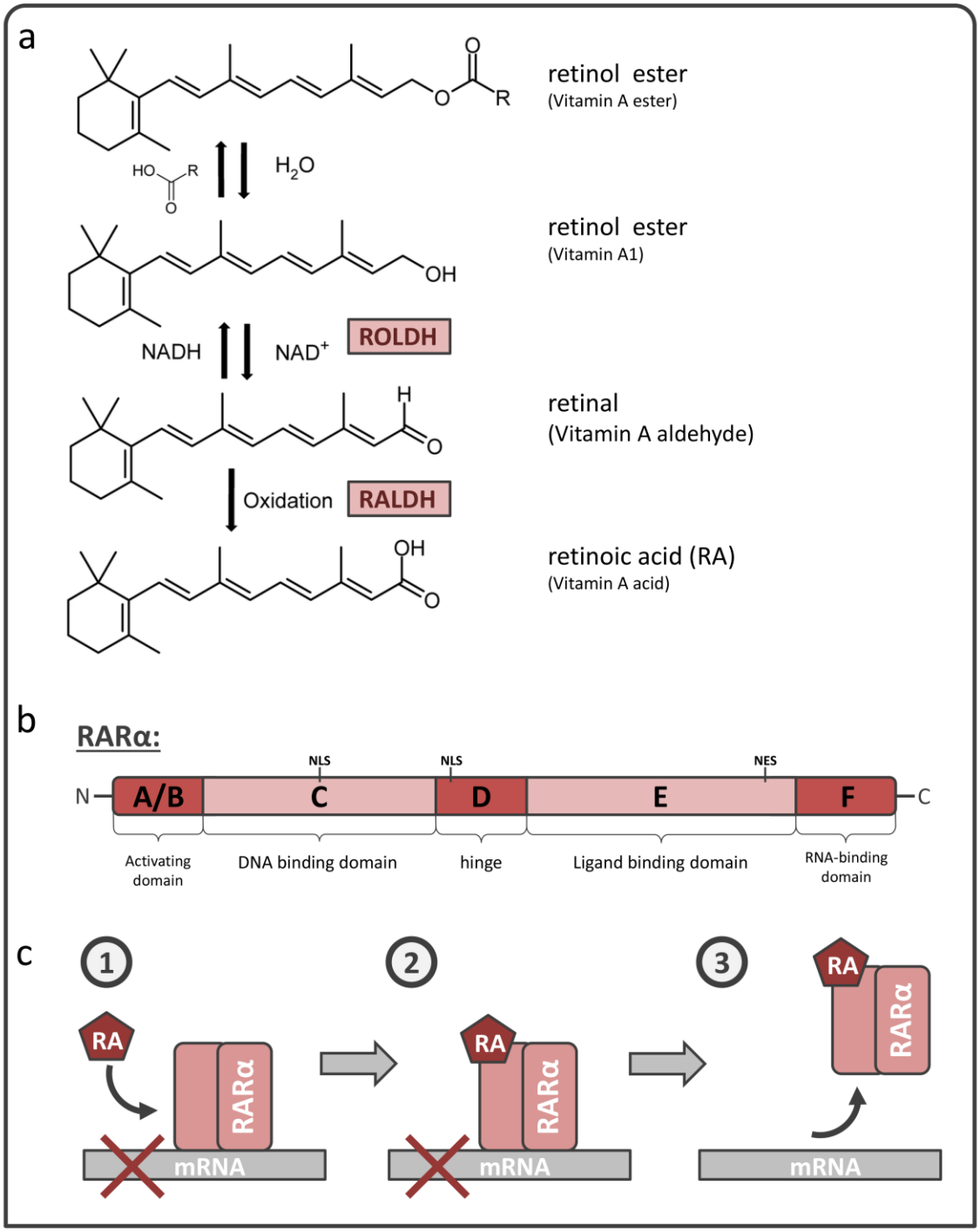

Figure 6. Main components and principle of RA/RARα signaling. (a) Synthesis of retinoic acid (RA) via oxidation of retinol ester. The main steps are catalyzed via two enzymes: retinol dehydrogenase (ROLDH) and retinal dehydrogenase (RALDH). **(b)** Functional domains of the amino acid sequence of RARα. NLS = Nucleus localization sequence, NES = Nuclear export signal (Sarti et al. 2012). **(c)** Principle of RA/RARα signaling. (1) RARα blocks protein translation by binding to a target mRNA. (2) Once RA binds to RARα, the RA/RARα complex disassembles from the mRNA and (3) translation can be initiated (Poon & Chen 2008).

3.9 Focus and aims of the thesis

3.9.1 The role of SP in LPS-mediated neuroinflammation

The first part of this thesis focuses on the cellular and molecular mechanisms through which inflammation affects synaptic plasticity. While it is well-established that pro-inflammatory cytokines affect plasticity, the neuronal targets through which these factors mediate their effects on synapses remain unknown. SP is an interesting target molecule in this context, since it has been shown to affect both homeostatic as well as Hebbian forms of synaptic plasticity, and due to the fact that changes in SP expression correlate with the ability of neurons to express synaptic plasticity. Most importantly, however, within the central nervous system SP is expressed exclusively by neurons.
Hence, the following major questions were addressed in this thesis:

1) Is SP expression and thus synaptopodin-dependent synaptic plasticity affected by inflammation?

2) Are the effects of inflammation on SP mediated by TNFα?

3) What is the source of TNFα in LPS-mediated neuroinflammation?

To address these questions systemic inflammation was induced in mice by intraperitoneal (i.p.) injection of LPS and SP-mRNA as well as protein levels were analyzed in the hippocampus. LTP was probed in acute hippocampal slices to correlate changes in SP expression with the ability of neurons to express synaptic plasticity during neuroinflammation. To learn more about the cellular and molecular mechanisms of inflammation-associated alterations in SP-dependent synaptic plasticity an *in vitro* LPS-model was established using organotypic entorhino-hippocampal slice cultures (OTCs). TNFα was studied using OTCs prepared from TNFα- and TNFR1/2-deficient mice. To assess the source of TNFα, OTCs prepared from the unpublished transgenic reporter

mouse line tg(TNF-eGFP) expressing GFP under the control of the TNFα promotor were used.

3.9.2 The role of SP in RA/RARα-dependent synaptic plasticity

The obvious similarities between RA/RARα and SP: (1) Localization to the synapse, (2) calcium-dependency and (3) regulation of AMPAR accumulation within spines, raise the question whether SP is involved in RA/RARα signaling. Therefore, the major questions addressed in the second part of the thesis are:

1) Does RA affect SP expression and SP-dependent synaptic plasticity?

2) Is the presence of SP required for RA/RARα-dependent synaptic plasticity?

3) What is the role of protein synthesis in RA-mediated SP-dependent synaptic plasticity?

4) Does RARα interact with SP-mRNA?

5) Is it possible to counteract inflammation-induced alterations in SP-dependent synaptic plasticity with RA treatment?

To test for changes in SP expression, brain slices from RA-injected mice and RA-treated OTCs were analyzed using immunohistochemistry. Effects on synaptic plasticity upon RA treatment were assessed in OTCs by whole-cell patch-clamp recordings of dentate granule cells. RA-dependent changes in the SP-transcript level and the hippocampal protein level were assessed using quantitative RT-PCR as well as western blot respectively. In addition, OTCs prepared from SP-deficient mice were used to clarify whether a lack of SP prevents RA-mediated synaptic strengthening. Experiments were repeated in presence of anisomycin, an inhibitor of mRNA translation, to study the role of *de*

novo protein synthesis. Finally, RNA-immunoprecipitation was performed to investigate a potential interaction between SP-mRNA and RARα protein.

4. Materials and Methods

4.1 Ethics statement

All experimental procedures were performed in agreement with the German animal welfare legislation (animal welfare act; TierSchG; §4 par 3; approved by the local animal welfare officer of the Goethe-University Frankfurt, Faculty of Medicine) or the Institutional Animal Care and Use Committee of The Chaim Sheba Medical Center (Tel HaShomer, Israel), which adheres to the Israeli law on the use of laboratory animals as well as NIH guidelines.

4.2 Animal care

Mice used for preparation of organotypic slice cultures were housed at the animal facility "Zentrale Forschungseinrichtung" (ZFE) of the Goethe-University, Faculty of Medicine. Mice used for *in vivo* experiments were housed in the animal facility of Chaim Sheba Medical Center (Tel HaShomer, Israel). For a detailed list of animals see Table 2 All animals were kept in a twelve hour dark/light cycle with standard lab animal diet *ad libitum*.

Animal	Description	Source	Housing
Balb/c	wildtype inbred strain	Harlan	Tel HaShomer, Israel
C57BL/6	wildtype inbred strain	Janvier Labs	Frankfurt, Germany
C57BL/6	wildtype inbred strain	Harlan	Tel HaShomer, Israel
SP KO	SP knockout, C57BL/6 background	AG Deller[1]	Frankfurt, Germany
Tg(Thy1-GFP/ SP) x SP KO	SP knockout background expressing only transgenic SP-EGFP protein.	AG Deller[2]	Frankfurt, Germany
TNF KO	TNFα knockout line	Jackson Laboratory	Frankfurt, Germany
TNFR1/2-KO	TNFα receptor 1 and 2 knockout line	Jackson Laboratory	Frankfurt, Germany
Tg(TNF-eGFP)	Expression of GFP under control of the TNFα promoter	AG Itamar Goren	Frankfurt, Germany
Tg(Iba1-eGFP)	Expression of GFP under control of the Iba1 promoter	Jackson Laboratory	Frankfurt, Germany

Table 2. List of animals used for experimental procedures. [1]Deller et al. 2003; [2]Vlachos et al. 2013

4.3 Preparation of organotypic slice cultures

All entorhino-hippocampal organotypic slice cultures (OTCs) were prepared from pups 4-6 days postnatally. Pups were decapitated rapidly and brains were removed. Brains were mounted on a probe table with Histoacryl® tissue glue (Braun, Spain), centered in the buffer tub of the vibratome containing preparation medium (Table 3) and cut horizontally in 300 µm thin slices using a vibratome (VT1200S, Leica) at a speed of 0.14 mm/s and an amplitude of 1.5 mm. Temperature of preparation medium was kept in a range of 5-8°C using a bath thermostat (K/W CC-K6, Huber). Horizontal brain slices were transferred into a 30 mm-Petri dish containing pre-cooled preparation medium and ventral hippocampi were dissected as indicated in Figure 7. Five to six hippocampi were prepared per brain and pooled on a Millicell® cell culture insert (Merck, Ireland) soaked in preparation medium (Table 3). Filter membranes were transferred into a six-well plate containing 1 mL incubation medium Table 4 and cultured in an incubator at 35°C (95% O_2/ 5% CO_2). Incubation medium was replaced every two days with fresh medium.

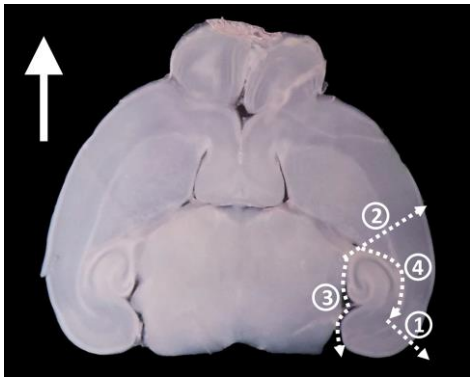

Figure 7. Horizontal mouse brain slice. Numbers and white dashed arrows indicate order of incisions. Upper left white arrow indicates direction of blade movement.

Reagent	Volume	Supplier
MEM	470.5 mL	Gibco
Glutamax	5 mL	Gibco
Glucose	5 mL	Sigma
HEPES	12.5 mL	Invitrogen/ Gibco
Penicilin/ Streptamycin	5 mL	Sigma PO781
NaOH	2 mL	AppliChem
Total	500 mL	

Table 3. Composition of the preparation medium. pH was adjusted to 7.3 with NaOH or HCl.

Reagent	Volume	
MEM	42 mL	Gibco
BME	25 mL	Gibco
NHS	25 mL	Gibco
Glutamax	1 mL	Gibco
Glucose	1.5 mL	Sigma
HEPES	2.5 mL	Invitrogen/ Gibco
Penicilin/ Streptamycin	1 mL	Sigma PO781
Bicarbonate (7.5%)	2 mL	Gibco
Total	100 mL	

Table 4. Composition of the incubation medium. pH was adjusted to 7.3 with NaOH or HCl.

4.4 Pharmacology

For *in vivo* experiments, mice were injected intraperitoneally (i.p.) with lipopolysaccharide (LPS) from *Escherichia coli* O111:B4 (1 mg/ kg; Sigma). Organotypic slice cultures were treated by adding LPS (1 µg/ml; Sigma), retinoic acid (RA, 1 µM; Tocris), BMS614 (2 µM, Tocris), anisomycin (10 µM; Sigma-Aldrich), N-methyl-D-aspartate (NMDA, 50 µM; Sigma), and/or APV (50 µM; BioTrend) to the incubation medium for three days. Incubation medium was replaced every two days by new incubation medium containing the appropriate treatment. For short-term experiments, cultures were treated with RA for 4 hours. 1-Naphthyl acetyl spermine trihydrochloride (NASPM, 100 µM; Sigma) was added to the bath solution prior to electrophysiological recording.

4.5 RNA isolation and reverse transcription reaction

4.5.1 RNA extraction of whole brain tissue

Prior to decapitation, adult 2-month-old male mice were anesthetized with CO_2. Hippocampi were dissected and immediately deep-frozen with liquid nitrogen. Tissue was homogenized in ice-cold TRIzol®. To extract RNA, phenol-chloroform phase separation was performed and the RNA was precipitated using isopropyl alcohol (Figure 8). RNA quality was determined using optical density (OD) measurement (Nanodrop1000; Thermo Scientific) as well as gel

electrophoresis [1% (w/v) agarose]. Samples with $OD_{260/280}$ ≤ 1.8 and $OD_{260/230}$ ≤ 2.0 were not analyzed (Fleige & Pfaffl 2006; $OD_{260/280}$ = 1.90 ± 0.07; $OD_{260/230}$ nm: 2.10 ± 0.37). mRNA from one animal (i.e. two hippocampi) were excluded based on these criteria. To remove potential genomic contaminations, RNA was further treated with DNase1 (Invitrogen, DNAse1 Amplification Grade) and reverse transcribed according to manufacturer's instructions using the High-Capacity cDNA Reverse Transcription Kit (Applied Biosystems). cDNA was stored at 4°C until further use.

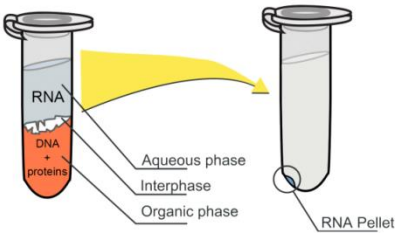

Figure 8. Principle of RNA extraction using phenol-chloroform phase separation.

4.5.2 RNA extraction of organotypic slice cultures

OTCs were transferred into β-mercaptoethanol containing RLT-buffer (QUIAGEN) and immediately frozen in liquid nitrogen. RNA was isolated according to the manufacturer's instructions (QIAGEN, RNeasy Plus Micro Kit). RNA quality was assessed by OD measurement (Nanodrop1000; Thermo Scientific). Purified RNA was treated with DNase1 (Ambion, DNA-free™ DNA Removal Kit) and reverse transcribed (Applied Biosystems, High-Capacity cDNA Reverse Transcription Kit). cDNA was stored at 4°C until further use.

4.6 Standard RT-PCR

Templates were amplified with a Taq PCR Mastermix kit (QIAGEN; for primer sequence details see Table 6) according to manufacturer's instructions (Table 5, Table 7, and Table 8) with the Mastercycler® pro (Eppendorf). PCR samples were stored at -20°C.

Reagent	Volume
Mastermix	12.50µl
Primer pair [10 µM]	1.00µl
Yellow Sub^{TM}	2.50µl
H_2O	7.00µl
cDNA/gDNA	2.00µl
Total	25.00µl

Table 5. Composition of the reaction used for standard RT-PCR.

Primer	Sequence (5'-3')	Supplier
SP KO	GCG GTG GGC TGA CTG TGG TGA CT CAG GCG CAG GCA GAG GGT GAA CG CCA GCT GGC GAA AGG GGG ATG TG	Eurofins
TNF KO	AGT GCC TCT TCT GCC AGT TC TAG CCA GGA GGG AGA ACA GA CGT TGG CTA CCC GTG ATA TT	Eurofins
TNFR1/2-KO	GGA TTG TCA CGG TGC CGT TGA AG TGA CAA GGA CAC GGT GTG TGG C TGC TGA TGG GGA TAC ATC CAT C CCG GTG GAT GTG GAA TGT GTG	Eurofins
GFP	CGC ACC ATC TTC TTC AAG GAC GAC AAC TTC AGC AGG ACC ATG TGA TCG	Eurofins

Table 6. Sequences of primers used for genotyping of transgenic mice.

Primer	Sequence (5'-3')	Supplier
SP-5'UTR	GAA GAG GCC GAT TGA CAG AG CCT GGC TTT GAT GGA GAT GT	Eurofins
SP-CDS	GCT CAT TGA CAT GCA GCC TA GCC TTC TCT CCA AAC TGT CG	Eurofins
SP-3'UTR	AGA CCT CAG TCC TGC TTC CA GCC AGC CTG TTC TCT CAA TC	Eurofins

Table 7. Sequences of primers used for the SP-mRNA sequence analysis of the Tg(Thy1-GFP/ SP) x SP KO mouse line.

	1 cycle	30 cycles			1 cycle	∞
Primer	*Initiation*	*Denaturation*	*Annealing*	*Amplification*	*Termination*	*Storage*
Iba1	94°C, 5min	95°C, 25 sec	56°C, 45 sec	72°C, 45 sec	72°C, 10 min	4°C
SP	94°C, 5min	94°C, 1 min	65°C, 1 min	72°C, 1.5 min	72°C, 10 min	4°C
TNFα	94°C, 3min	94°C, 30 sec	62°C, 1 min	72°C, 1 min	72°C, 2 min	4°C
TNFR1/2	94°C, 3min	94°C, 30 sec	55°C, 1 min	72°C, 1 min	72°C, 2 min	4°C
GFP	94°C, 3min	94°C, 30 sec	60°C, 30 sec	72°C, 45 sec	72°C, 5 min	4°C
SP-5'UTR	94°C, 5min	94°C, 1 min	65°C, 1 min	72°C, 1.5 min	72°C, 10 min	4°C
SP-CDS	94°C, 5min	94°C, 1 min	65°C, 1 min	72°C, 1.5 min	72°C, 10 min	4°C
SP-3'UTR	94°C, 5min	94°C, 1 min	65°C, 1 min	72°C, 1.5 min	72°C, 10 min	4°C

Table 8. Standard RT-PCR protocol for the individual primer pairs.

4.7 Real time quantitative RT-PCR (qPCR)

cDNA was diluted to a final concentration of 1-2 ng/ µl with aqua dest. The qPCR reaction (see Table 9 for details) was transferred into a 96 well plate and templates were amplified with TaqMan® assays (Applied Biosystems; for assay sequence details see Table 10) using a standard protocol with the StepOnePlus™ Real-Time PCR system (Applied Biosystems, USA; for details see Table 11). Efficiency of target assays (E_T) and reference assays (E_R) of qPCR assays was determined with the StepOnePlus software (Applied Biosystems, USA) using a dilution series of five samples. The house keeping gene GAPDH (Glyceraldehyde 3-phosphate dehydrogenase) was used as internal reference. Data were analyzed according to the model published by Pfaffl (2001; Equation 2). Relative values were normalized to untreated or vehicle-treated controls.

$$X_{rel} = \frac{E_T^{(\bar{T}-T)}}{E_R^{(\bar{R}-R)}}$$

Equation 2. Calculation of gene expression using the model of Pfaffl. X_{rel} = relative gene expression of a target gene, E_T = target assay efficiency, E_R = reference assay efficiency, T = CT-value of target gene, R = CT-value of reference gene.

Reagent	Volume
TaqMan® Mastermix	7.50µl
TaqMan® Assay	0.75µl
ddH20	4.75µl
cDNA	2.00µl
Total	15.00µl

Table 9. qPCR reaction: composition of reagents.

Assay	sequence (5'-3') or assay ID
SP-fwd	GTCTCCTCGAGCCAAGCA
SP-rev	CACACCTGGGCCTCGAT
SP-probe	TCTCCACCCGGAATGC
TNFα	Mm00443258_m1
GAPDH	4352932E

Table 10. Sequences and IDs of qPCR Assays (Applied Biosystems).

1 cycle	1 cycle	40 cycles		∞
50°C, 2 min	95°C	95°C, 15 s	60°C, 1 min	4°C

Table 11. qPCR protocol.

4.8 Immunohistochemistry and imaging

OTCs were transferred into fixative 1, containing 4% (w/v) PFA (Sigma Aldrich) and 4% (w/v) sucrose (Sigma Aldrich) for 1 hour at room temperature (RT), washed in PBS (AppliChem), and transferred into fixative 2 containing 2% PFA and 30% sucrose overnight at 4°C. Next, OTCs were transferred into PBS and re-sliced into 30 µm thin slices using a cryostat (3050CM S, Leica). For whole brain slices, agarose-embedded brains of PFA-perfused mice were resliced (thickness = 30 µm) using a vibratome (VT1000S, Leica). For immunostainings cultures were washed in PBS and incubated for 1 hour at RT in blocking solution containing PBS (89.5%, v/v), Triton X-100 (0.5%, v/v; VWR Prolabo, Darmstadt, Germany), and normal goat or horse serum (10%, v/v). OTCs were incubated overnight at 4°C in antibody solution containing primary

antibodies (Table 12), PBS (89.90%, v/v), TritonX100 (0.1%, v/v) and normal goat or horse serum (10%, v/v). Cultures were washed three times in PBS and incubated for 4 hours at RT in antibody-solution containing secondary antibodies diluted 1:1000 (Table 13). For post-hoc-immunostainings, OTCs were incubated in antibody-solution containing Alexa-conjugated streptavidin (Life Technologies; 1:500) for 2 hours at RT prior to incubation with primary antibody solution. For nuclear staining, cultures were incubated in PBS containing TO-PRO®-3 iodide (Invitrogen, 1:5000) for 15 minutes at RT. OTCs were immobilized on glass slides (Engelbrecht, Edermünde, Germany) with DAKO fluorescent mounting medium (Agilent, USA) and stored at 4°C until imaging using confocal microscopy.

Primary antibody	Host	Dilution	Supplier
Synaptopodin (SE-19)	rabbit	1:1000	Sigma
Iba1	rabbit	1:1000	Wako
GFAP	mouse	1:1000	Sigma
RARα (C-20): sc-551	rabbit	1:250	Santa Cruz

Table 12. List of primary antibodies used for immunohistochemistry.

Host	Antigen	Fluorophore	Dilution	Supplier
Donkey	mouse	Alexa Fluor 568®	1:1000	Molecular Probes
Donkey	mouse	Alexa Fluor 633®	1:1000	Invitrogen
Donkey	rabbit	Alexa Fluor 647®	1:1000	Molecular Probes
Donkey	rabbit	Alexa Fluor 488®	1:1000	Molecular Probes
Donkey	rabbit	Alexa Fluor 568®	1:1000	Invitrogen
Donkey	goat	Alexa Fluor 633®	1:1000	Molecular Probes

Table 13. List of secondary antibodies used for immunohistochemistry.

4.9 Confocal microscopy and analysis of confocal images

Fixed and re-sliced tissue from OTCs or whole brain slices were imaged using a laser scanning confocal microscope (Nikon Eclipse 80i), equipped with a 488 nm, a 561 nm and a 633nm excitation laser, and a 4x (numerical aperture

(NA) 0.2, Nikon), 10x (NA 0.3, Nikon), 20x (NA 0.75, Nikon), 40x oil immersion (NA 1.3, Nikon), and 60x oil immersion objective (NA 1.4, Nikon).

4.9.1 Imaging and analysis of SP-clusters

For imaging of SP-clusters, the hippocampal area of interest was selected using the 60x objective. Next, regions of interest (ROI) were selected within the dentate gyrus (outer molecular layer, OML and inner molecular layer, IML) and CA1 region (stratum oriens, str.oriens.; stratum radiatum, str. rad. and stratum lacunosum moleculare, str. la-mol.). Images of three ROIs per layer were taken using a zoom factor 7 in a depth of 5 µm below the surface of the tissue. Image resolution was set to 512 x 512 pixels and pixel dwell time to 3.12 ms. Laser intensity and gain were adjusted before imaging and values were kept constant during the imaging procedure. Images were saved as tif-files and batch analyzed in ImageJ software package (Schindelin et al. 2012, available at http://imagej.nih.gov/ij/) using an appropriate makro with the following code lines:

```
run("Options...", "iterations = 1 count = 1 black edm = Overwrite")
run("Despeckle", "stack");
run("Subtract Background...", "rolling = 10 stack");
run("8-bit");
//run("Threshold...");
setThreshold(30, 255);
run("Convert to Mask", "  black");
run("Watershed", "stack");
run("Analyze Particles...", "size = 1-infinity circularity = 0.10 - 20 show = Outlines display clear summarize stack")
```

Intensity threshold as well as values defining the range of particle size and circularity were kept constant during the experiments. Values of mean cluster area and cluster size were transferred to an excel sheet and normalized to the control group. Statistics were performed using GraphPad Prism 6 (GraphPad Software, Inc.).

4.9.2 Imaging and analysis of GFP-fluorescence distribution:

GFP-fluorescence distribution of OTCs gained from tg(TNF-eGFP) mice was obtained using the 20x objective at a resolution of 1024 x 1024 pixels (pixel dwell time: 3.12 ms) of the hippocampal CA1 region. Gain and laser intensity were adjusted before imaging and kept constant during the imaging procedure. Images were saved as ids-files and analyzed using the ImageJ software package. In ImageJ, channels of each image were split and saved separately as 8-bit jpeg-files to be analyzed using the *'versatile wand tool'* plugin for ImageJ (for settings, see Table 14).

Parameter	Setting
Value tolerance	0
Color	-100 (gray only)
Gradient tolerance	0
Connectedness	0
Eyedropper	disabled
Include holes	disabled

Table 14. Settings of the Image J 'versatile wand tool' plugin used for GFP-expression analysis.

The 'versatile wand tool' plugin creates a mask comprising all pixels above a preselected signal intensity threshold. The gained area of GFP-expression was transferred to an excel data sheet and values were normalized to the control group. Statistics were performed using GraphPad Prism 6 (GraphPad Software, Inc.).

4.9.3 Co-localization analysis

Images of the hippocampal CA1 region were captured using the 20x objective at a resolution of 1024 x 1024 pixels (pixel dwell time: 3.12 ms). Gain and laser intensity were adjusted before imaging and kept constant during the imaging procedure. Images were saved as ids-files and analyzed using the ImageJ software package. Co-localization of GFP- vs. Iba1-/ GFAP-signal was assessed using the *'coloc2'* plugin for ImageJ. For comparison, Pearson's coefficients (also referred to as PCC or Pearson's r) were used. PCC measures

the pixel-by-pixel covariance of signal intensities of two images (see Equation 3). Compared to other co-localization calculations, like Manders and Costes, Pearson's calculation is not sensitive to differences in mean signal intensity or range, or a zero offset between both (e.g. black regions, where pixel intensities are zero) that could result in a false positive co-localization. Therefore, the calculation of Pearson r subtracts the mean intensity from each pixel (see Equation 3; the interested reader is referred to a comprehensive review about co-localization analysis published by Dunn et al. 2011).

$$r = \frac{\sum_{i=1}^{n}(x_i - \bar{x})(y_i - \bar{y})}{\sqrt{\sum_{i=1}^{n}(x_i - \bar{x})^2}\sqrt{\sum_{i=1}^{n}(y_i - \bar{y})^2}}$$

Equation 3. Calculation of Pearson's coefficient. n indicates the size of the image, i.e. number of pixels that are compared between channel 1 and 2; x_i and y_i represent the individual channel intensities of each pixel of channel 1 (x_1,x_2…x_n) vs. channel 2 (y_1,y_2…y_n). $\bar{x}$ and $\bar{y}$ represent their mean intensities.

4.10 Western blot

OTCs were removed carefully from the filter membrane using a scalpel and transferred into an RNase-free sterile 1.5 mL tube containing 500 µl homogenization buffer (Table 15). Next, buffered slices were homogenized using an electric hand-operated pestle system (Fisherbrand™, Fisher scientific) and centrifuged at 4°C, 25,000 RPM for 30 minutes. Protein concentration was assessed using the Quant-iT™ -assay (Invitrogen) according to the manufactures instructions. Samples were diluted 1:1 in probe buffer containing 95% (v/v) Lämmli probe buffer (BioRad) and 5% (v/v) β-mercaptoethanol (AppliChem). 33µl of protein containing solution was pipetted into the pockets of a gel for electrophoresis (Table 19). The voltage was set to 120 V during collection phase and 160 V during separation phase. For western blotting, Protran® NC membrane (Sigma Aldrich) was humidified with pure water and pre-incubated for 10 minutes in transfer buffer (Table 16). A filter membrane (soaked in transfer buffer) was placed on the bottom (cathode) of the Trans-Blot Semi-Dry device (BioRad). The NC-membrane was placed on top, followed by

the gel and a second filter membrane. Finally, the electrophoresis device was closed with the anode on top. Western blot was performed by applying 15 Volts for 75 minutes (max. 5.5 mA/ cm²). NC-membranes were carefully removed, washed twice in TBS, and incubated in blocking solution (containing 5% nonfat dry milk in TBS, Table 17) for 1 hour. NC-membranes were washed three times with TBS and incubated in antibody-1-solution (Table 12) overnight at 4°C. NC-membranes were washed three times in TBS/T (Table 18) and incubated in antibody-2-solution (Table 21) at RT for 60 minutes. NC-membranes were washed again three times in TBS/T and transferred into PBS for quantification using the Odyssey imaging device (Li-Cor).

Reagent	Volume (100 mL)
Tris (pH 7.5; 20 mM)	0.242 g
NaCl (500 mM)	2.92g
CHAPS (0.5%)	0.5g
EDTA (5 mM)	0.186g

Table 15. Composition of homogenization buffer. Protease inhibitor (Roche complete mini) was added: 1 Tablet per 10 mL.

Reagent	Amount
Tris (25 mM)	3.03 g
Glycine (192mM)	14.4 g
Methanol	200 mL
ddH_2O	800 mL

Table 16. Composition of transfer buffer.

Reagent	Amount
Tris (20 mM)	2.42 g
NaCl (150 mM)	8.77 g
ddH_2O (pH 7.6)	1000 mL

Table 17. Composition of 10 x TBS buffer.

Reagent	Volume
10x TBS	100 mL
Tween-20	1 mL
ddH_2O (pH 7.6)	1000 mL

Table 18. Composition of TBS/T.

Reagent	Volume (Collection gel: 4%, 10 mL)	Volume (Separation gel: 8%, 10 mL)
ddH_2O	6.1 mL	4.1 mL
Separation buffer	2.5 mL	2.5 mL
Acrylamid solution	1.3 mL	3.3 mL
SDS (10%)	0.1 mL	0.1 mL
Temed	50 µl	25 µl
APS (10%)	100 µl	50 µl

Table 19. Composition of 4% collection gel and 8% separation gel.

Primary antibody	Host	Dilution	Supplier
Synaptopodin	rabbit	1:1000	SYSY
GAPDH	mouse	1:10000	Calbiochem

Table 20. Primary antibodies used for western blot.

Host	Antigen	Fluorophore	Dilution	Supplier
goat	rabbit	IR800	1:10000	Li-Cor Odyssey
donkey	mouse	IR680	1:10000	Li-Cor Odyssey

Table 21. Secondary antibodies used for western blot.

4.11 RNA-immunoprecipitation (RIP)

To investigate a potential interaction between the protein retinoic acid receptor alpha (RARAα) and the mRNA of synaptopodin (SP), a RNA-immunoprecipitation reaction was performed using the Magna RIP™ kit (Millipore, Cat.#17-701). The procedure is summarized in Figure 10.

4.11.1 Lysate preparation (step 1)

OTCs were homogenized in ice-cold PBS. The cell suspension was centrifuged at 1500 RPM for 4 minutes at 4°C, the pellet was re-suspended in lysis buffer (Table 22) and incubated on ice for 5 minutes. Samples were stored at -80°C.

Reagent	Amount
RIP Lysis buffer	100µl
Protease inhibitor	0.5µl
RNase inhibitor	0.25µl

Table 22. Composition of the lysis buffer.

4.11.2 Preparation of magnetic beads (step 2)

Magnetic beads (50 µl) were washed in 500 µl wash buffer. Tubes were placed on a magnetic separator (Millipore, Cat.#20-400) and the supernatant discarded after bead aggregation (Figure 9). Washing was repeated once and 100 µl wash buffer, together with 5 µg of antibody (Table 23), were added. Tubes were incubated on a shaker for 30 minutes at RT. Beads were washed again twice. Finally, 500 µl wash buffer were added and tubes were placed on ice.

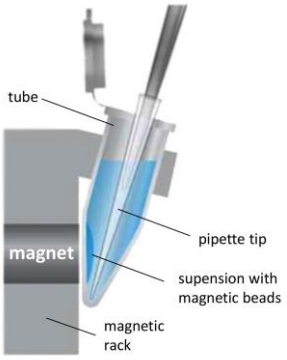

Figure 9. To remove supernatant, tubes are placed in a magnetic separator. Schematic adapted from Magna RIP™ Kit user manual.

Antibody	Host	Supplier
IgG	rabbit	Millipore
Anti-SNRNP70	rabbit	Millipore
RARα (C-20): sc-551	rabbit	Santa Cruz

Table 23. List of antibodies used for the RIP reaction.

4.11.3 RNA-Immunoprecipitation (step 3)

Tubes from step 2 were placed on a magnetic separator to remove supernatant and 900 µl of RIP buffer was added. The lysate from step 1 was centrifuged at 14,000 RPM for 10 minutes at 4°C and 100 µl supernatant was added to each beads-antibody complex in RIP buffer (Table 24). Additionally, 10 µl of lysate supernatant were removed, labeled as ‘input’, and stored at -80°C to serve as positive control. For RNA-immunoprecipitation, tubes were incubated with rotations overnight at 4°C.

Reagent	Amount
RIP wash buffer	860µl
EDTA (0.5 M)	35µl
RNase inhibitor	5µl

Table 24. RIP buffer

4.11.4 RNA-purification (step 4)

Immunoprecipitates from step 3 were re-suspended in 150 µl proteinase K buffer (Table 25). The input sample from step 3 was treated similarly. All tubes were incubated at 55°C for 30 minutes with shaking to digest the protein. Supernatant was removed using the magnetic separator and transferred into a new tube and diluted in 250 µl wash buffer. 400 µl phenol:chloroform:isoamyl alcohol (125:24:1, Sigma-Aldrich) were added to each tube and vortexed for 15 seconds. Tubes were centrifuged at 14,000 RPM for 10 minutes at RT. 350 µl from the upper, aqueous phase were removed carefully and placed in a new tube. 400 µl of chloroform were added, the tube vortexed and centrifuged again for phase separation. 300 µl of the aqueous phase were transferred into a new tube. 50 µl of salt solution I, 15 µl of salt solution II, 5 µl of precipitate enhancer and 850 µl of absolute ethanol (AppliChem) were added. After 30 minutes centrifugation (14,000 RPM, 4°C), the supernatant was discarded. The pellet was air dried and re-suspended in 20 µl RNase-free water. The RNA solution was stored at -80°C. RNA integrity was assed using Nanodrop 1000.

Reagent	Amount
RIP wash buffer	117µl
SDS (10%)	15µl
Proteinase K	18µl

Table 25. Proteinase K buffer

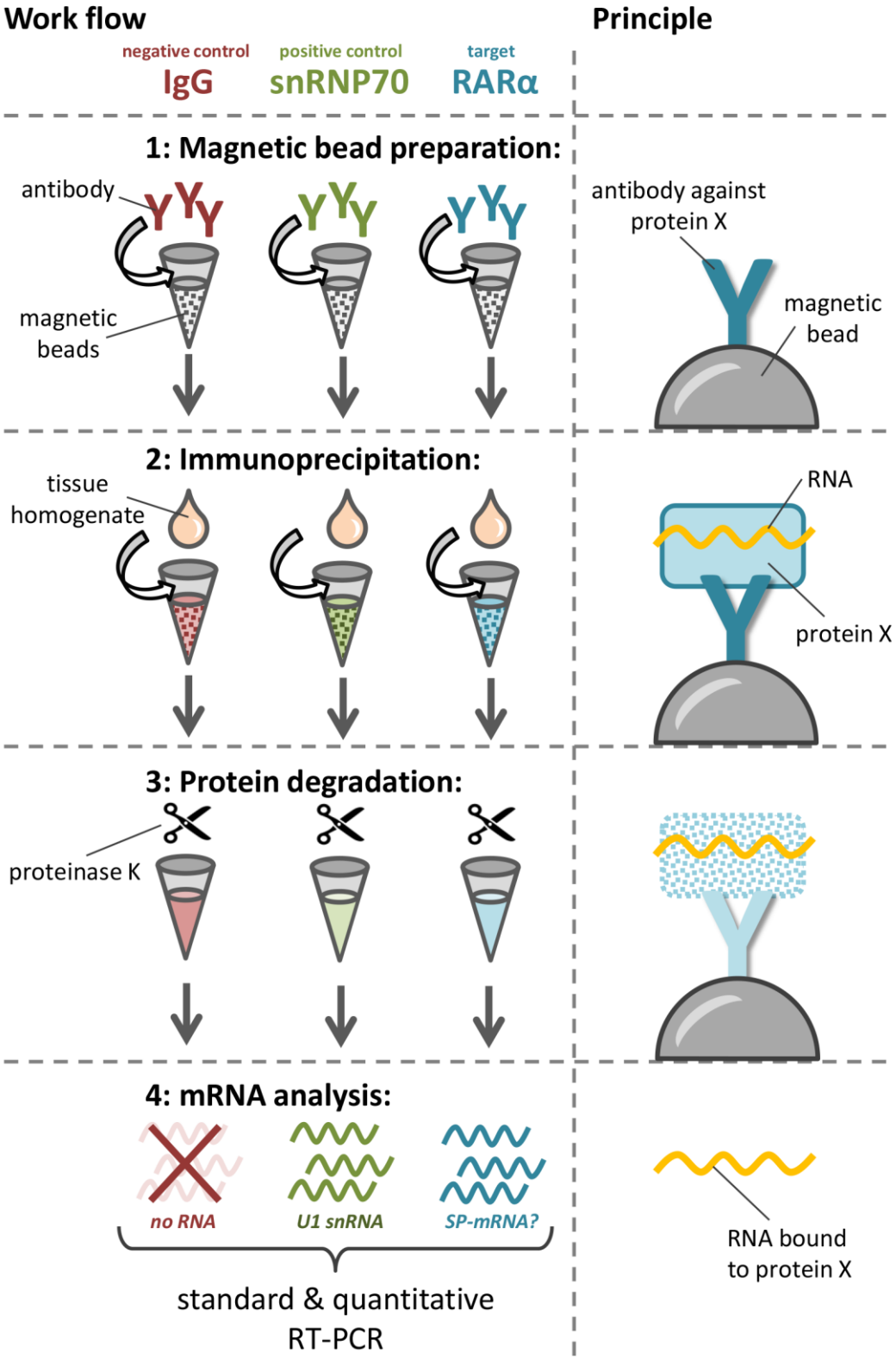

Figure 10. Workflow and principle of RNA-immunoprecipitation using antibody-coated magnetic beads. Step 1: Magnetic beads were coated with antibodies against an unspecific IgG epitope (negative control), the ribosomal protein snRNP70 (positive control) and retinoic acid receptor alpha (RARα). Step 2: Tissue of organotypic slice cultures (OTCs) was homogenized and incubated in the solution containing antibody coated magnetic beads. Step 3: To isolate RNAs bound to the proteins of interest a protein digestion was performed using protease K. Step 4: RNA was reverse transcribed and analyzed using standard and quantitative RT-PCR.

4.12 Sequence analysis of SP-mRNA

The murine (*Mus musculus*) mRNA sequence of SP (NM_001109975.1) was acquired from the NCBI database in FASTA format and screened for the 25 nucleotide combinations of RARα binding motifs 1 and 2 (see Table 26) as published by Poon and Chen (2008) using a standard string search algorithm (Microsoft Software Package).

4.13 Propidium iodide staining

Upon treatment with LPS (1 µg/ml; 3 d) or NMDA (50 µM; 4 h) propidium iodide (PI) was directly transferred to the OTC culturing medium to a final concentration of 5 µg/ml. Cultures were placed back into the incubator for 2 h, washed with PBS (0.1 M, pH 7.4) and fixed in 4% (w/v) PFA, 4% (w/v) sucrose containing PBS for 1 h, followed by fixation overnight in 2% (w/v) PFA, 30% (w/v) sucrose containing PBS at 4°C. Cell nuclei were stained with TO-PRO (1:5000; Invitrogen) in PBS for 10 min to assess the total amount of cells and to visualize cytoarchitecture. Cultures were mounted on microscope slides using Dako anti-fading mounting medium (Agilent). Confocal images of hippocampal region CA1 were acquired using a Nikon Eclipse C1si laser-scanning microscope equipped with a 60x oil-immersion objective lens (NA 1.4; Nikon) and saved as ids-files. Images were analyzed using the ImageJ software package (Schindelin et al. 2012, available at http://imagej.nih.gov/ij/). The dentate gyrus and hippocampal CA1 and CA3 areas were selected as regions of interest (ROI) using the mask tool of ImageJ and the mean fluorescence intensities of the ROIs were determined. Slices stained with PI after fixation (referred to as ‘post-fixation’ in text and figures) served as a positive control and as a reference in these experiments.

4.14 Whole-cell patch-clamp recordings

Whole-cell voltage-clamp recordings from dentate granule cells (GCs) and CA1 pyramidal neurons of OTCs were performed at 35°C as described

previously (Vlachos, Müller-Dahlhaus, et al. 2012; Vlachos et al. 2012). Up to five cells per culture were recorded. The bath solution contained (in mM) 126 NaCl, 2.5 KCl, 26 $NaHCO_3$, 1.25 NaH_2PO_4, 2 $CaCl_2$, 2 $MgCl_2$, and 10 glucose. Patch pipettes were pulled with DMZ Universal Electrode Puller (Zeitz-instruments) to a tip resistance of 4-6 MΩ. For mEPSCs (miniature excitatory postsynaptic currents) recording pipettes were filled with internal solution containing (in mM), 126 K-gluconate, 10 HEPES, 4 KCl, 4 ATP-Mg, 0.3 GTP-Na_2, 10 PO-Creatine, and 10 Biocytin (pH = 7.25 with KOH, 290 mOsm with sucrose). To visualize neural morphology, Alexa 488 or Alexa 568 was added to the internal solution, each with a final concentration of 10 µM. During recording the membrane potential was clamped to -70 mV. For mEPSC recordings, 10 µM APV (BioTrend) and 0.5 µM TTX (BioTrend) were added to the bath solution. Series resistance (R_S) and capacitance (C) were documented in 2 minute intervals. Recordings were discarded if R_S changed significantly and/ or reached values ≥ 30 MΩ.

4.15 Long-term potentiation (LTP) in acute brain slices

Extracellular recordings of field excitatory postsynaptic potentials (fEPSPs) in acute slices prepared from dorsal hippocampi were performed as previously described (Maggio et al. 2013). Briefly, mice were anesthetized with ketamine/ xylazine (100 mg/kg and 10 mg/kg, respectively) and rapidly decapitated (12 animals per group). Brains were dissected and cut into 400 µm thin slices using a vibroslicer. Slices were incubated for 1.5 h in a humidified, carbogenated (5% CO_2 and 95% O_2) gas atmosphere at 33 ± 1°C and perfused with artificial cerebrospinal fluid (ACSF) containing (in mM), 124 NaCl, 2 KCl, 26 $NaHCO_3$, 1.24 KH_2PO_4, 2.5 $CaCl_2$, 2 $MgSO_4$, and 10 glucose (pH 7.4) in a standard interface chamber. Recordings were performed using a 4 MΩ glass pipette containing 0.75 M NaCl placed in the stratum radiatum of CA1. Stimulation of Schaffer collaterals was evoked using a pulse stimulator and delivered through a bipolar nichrome electrode. Before starting the experiment, an input-output curve was recorded on each slice. Prior to tetanic stimulation, baseline values

were recorded at a frequency of 0.033 Hz. Finally, LTP was induced by high-frequency stimulation (HFS) composed of 100 pulses at twice the test intensity, delivered at a frequency of 100 Hz (1 second). Responses were digitized at 5 kHz and stored on a hard drive. Data were analyzed off-line using Spike 2 software (Cambridge Electronic Design). Changes of fEPSP slope following tetanic stimulation were determined with respect to baseline.

4.16 Quantification and statistics

For direct comparison of two data sets, the non-parametric Mann-Whitney test was applied in most cases, since normal distribution of these data could not be assured. In case of multiple comparisons between groups the non-parametric Kruskal-Wallis test was performed followed by Dunn's multiple comparison test to specify intergroup differences. Electrophysiological extracellular recordings were statistically compared using an unpaired, two-tailed t-test. Outliers were identified by means of Grubbs test (also referred to as extreme studentized deviate, ESD test) and were excluded from analysis. p values smaller than 0.05 were considered a significant difference between means. In the text and figures, values represent mean ± standard error of the mean (SEM). * $p < 0.05$, ** $p < 0.01$, *** $p < 0.001$. Not significant differences are indicated by 'NS'.

5. Results

5.1 Neuroinflammation *in vivo* – the role of Synaptopodin

To study the effects of inflammatory processes on brain function, adult male Balb/c mice (two-month-old) were intraperitoneally (i.p.) injected with LPS (1 mg/kg). Experiments were conducted 24 h after injection. All results were compared to vehicle-treated (PBS), gender-, age-, and time-matched controls.

5.1.1 SP-mRNA levels are reduced upon LPS treatment

First, it had to be verified that systemic (i.p.) LPS (1 mg/kg) leads to the induction of inflammation in the central nervous system. Therefore, hippocampal mRNA levels of the pro-inflammatory cytokine TNFα were assessed using quantitative RT-PCR. The housekeeping gene GAPDH was used as a reference in this set of experiments. Indeed, a ~40-fold (42 ± 12 fold; $p < 0.01$) increase in TNFα-mRNA levels was detected. Next, SP-transcript expression was analyzed and a significant decrease in SP-mRNA to about 50% (53 ± 4%; $p < 0.01$) compared to the vehicle-injected group was detected 24 hours after LPS-injection (Figure 11). These data indicate that LPS-induced systemic inflammation leads to inflammation in the hippocampus that is accompanied by a reduction in SP-mRNA levels.

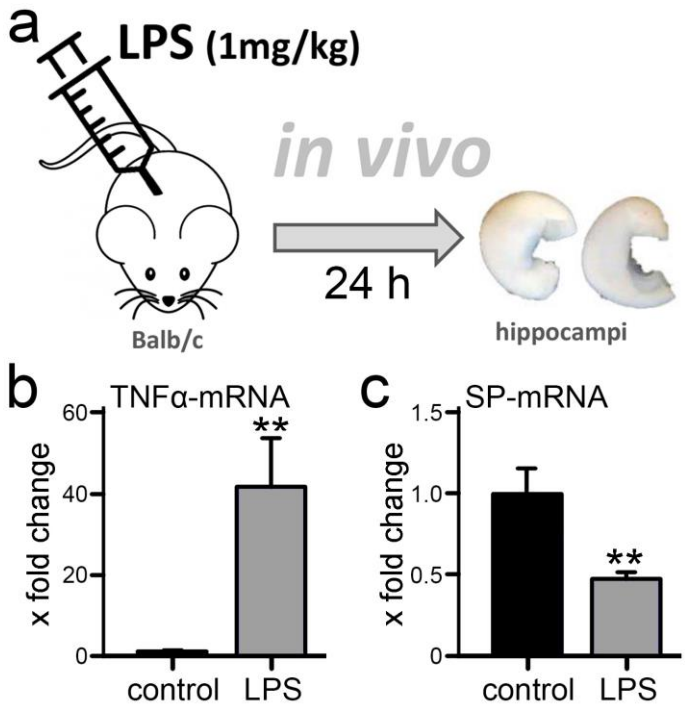

Figure 11. LPS-induced systemic inflammation leads to a reduction of hippocampal SP-mRNA levels. (a) Schematic of experimental workflow. 24 hours upon injection of LPS (1 mg/kg) hippocampi were dissected for gene expression analysis via quantitative RT-PCR. **(b+c)** Relative quantification of TNFα- and SP-mRNA expression normalized to GAPDH (Control, n = 7; LPS, n = 6; Mann-Whitney test; Values represent mean ± SEM; **p < 0.01).

5.1.2 SP-cluster sizes are reduced following LPS-injection

Slices of the dorsal hippocampus were immunostained for SP and SP-cluster sizes and numbers were analyzed within the stratum lacunosum-moleculare (str. la-mol.), stratum radiatum (str. rad.), and stratum oriens (str. oriens) of the hippocampal area CA1. Indeed, 24 hours after LPS-injection, mean SP-cluster sizes were significantly reduced in the stratum radiatum (-22 ± 6%; $p < 0.05$) and stratum lacunosum moleculare (-32 ± 7%; $p < 0.01$). A trend toward reduced SP-cluster sizes was observed in the stratum oriens that was, however, not significant. SP-cluster numbers were not significantly altered (normalized values; Str. ori., control: 1.0 ± 0.14 vs. LPS: 1.06 ± 0.29, $p = 0.78$; Str. rad., control: 1.0 ± 0.11 vs. LPS: 0.82 ± 0.21, $p = 0.16$; Str. la-mol., control: 1.0 ± 0.17 vs. LPS: 0.76 ± 0.17; $p = 0.19$; Figure 12). These results show that

SP-protein is down-regulated 24 h upon LPS-injection in a lamina-specific fashion.

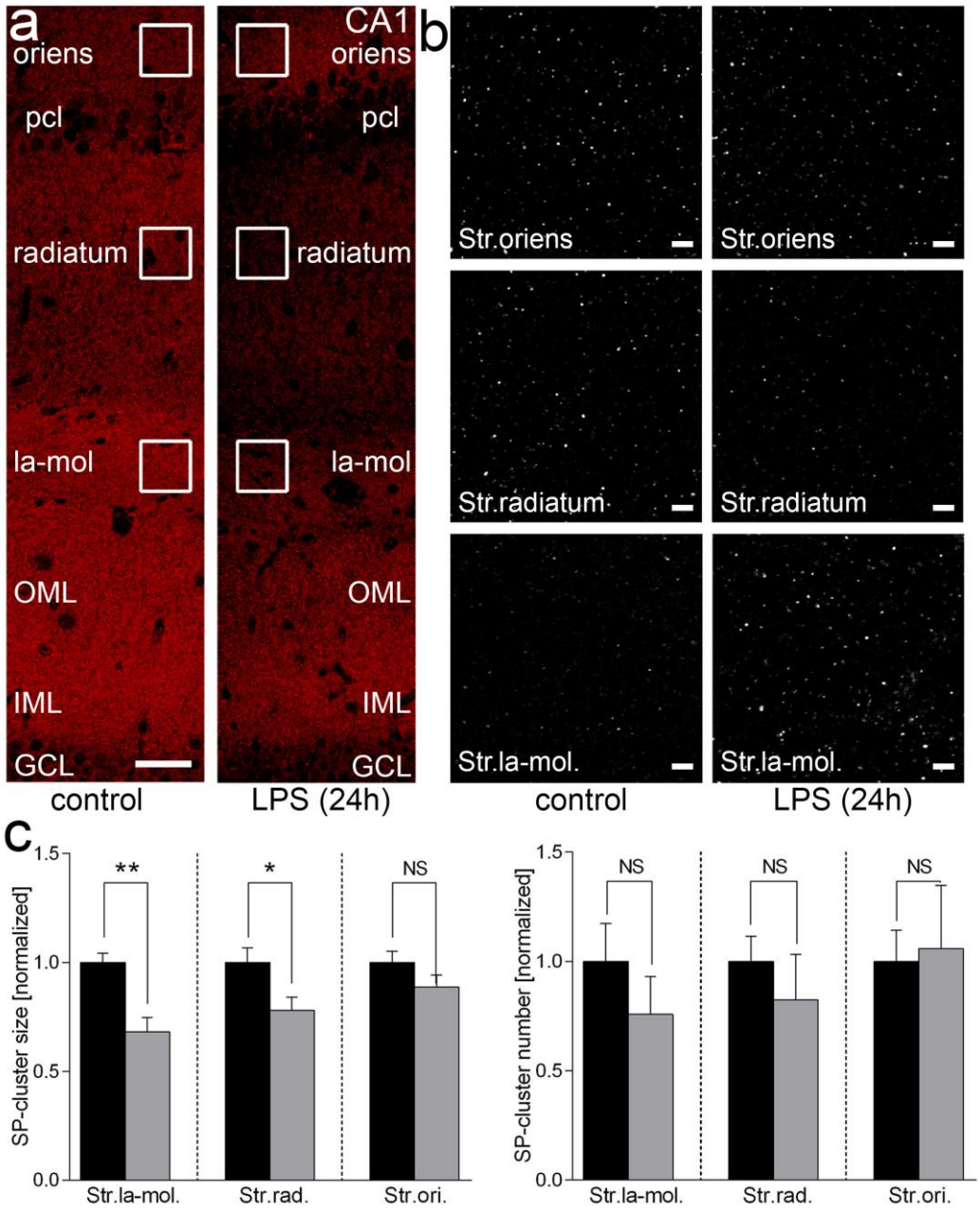

Figure 12. SP-cluster sizes are reduced following LPS-injection. (a) SP-clusters were analyzed within the hippocampal area CA1 in selected regions at high magnification (indicated by white squares) within the lamina of Str.oriens (Str.ori), Str.radiatum (Str.rad) and Stratum lacunosum moleculare (Str.la-mol.). Pyramidal cell layer, pcl; Outer molecular layer, OML; Inner molecular layer, IML; Granule cell layer, GCL; Scale bar: 30 µm. **(b)** Higher magnification of selected regions showing SP-cluster in white. Scale bar: 2 µm. **(c)** SP-cluster sizes were significantly reduced in Str.la-mol. and Str.rad., but not in Str.ori. upon 24 hours of LPS treatment compared to vehicle-treated controls. SP-cluster numbers were not significantly changed following 24 hours LPS-injection (n=8 hippocampi per group; 4 animals each; Values represent mean ± SEM; Mann-Whitney test; *$p < 0.05$; **$p < 0.01$; not significant difference indicated by 'NS'). Figure adapted from Strehl et al. (2014).

5.1.3 LPS-induced systemic inflammation impairs LTP

To correlate LPS-mediated changes in SP with the ability of neurons to express synaptic plasticity, LTP (tetanus-induced: 1 s; 100 Hz) was induced at Schaffer collateral CA1 synapses in acute dorsal hippocampal slices from LPS- and vehicle-injected mice. The acute slices anatomically matched the preparations that were used for the abovementioned immunohistochemical analysis.

LPS-injected animals showed a markedly reduced LTP ($control_{87min}$: 1.81 ± 0.06 vs. LPS_{87min}: 1.44 ± 0.05; $p < 0.001$), while the input/output properties and pre-synaptic parameters of CA1 Schaffer collateral synapses were not affected. This observation is in line with findings obtained from SP-deficient mice showing defects in LTP without changes in baseline synaptic transmission (Deller et al. 2003; Jedlicka et al. 2009; Vlachos et al. 2013; Figure 13). Together these findings disclosed that systemic inflammation affects synaptic plasticity, which is reflected by a reduction in SP expression.

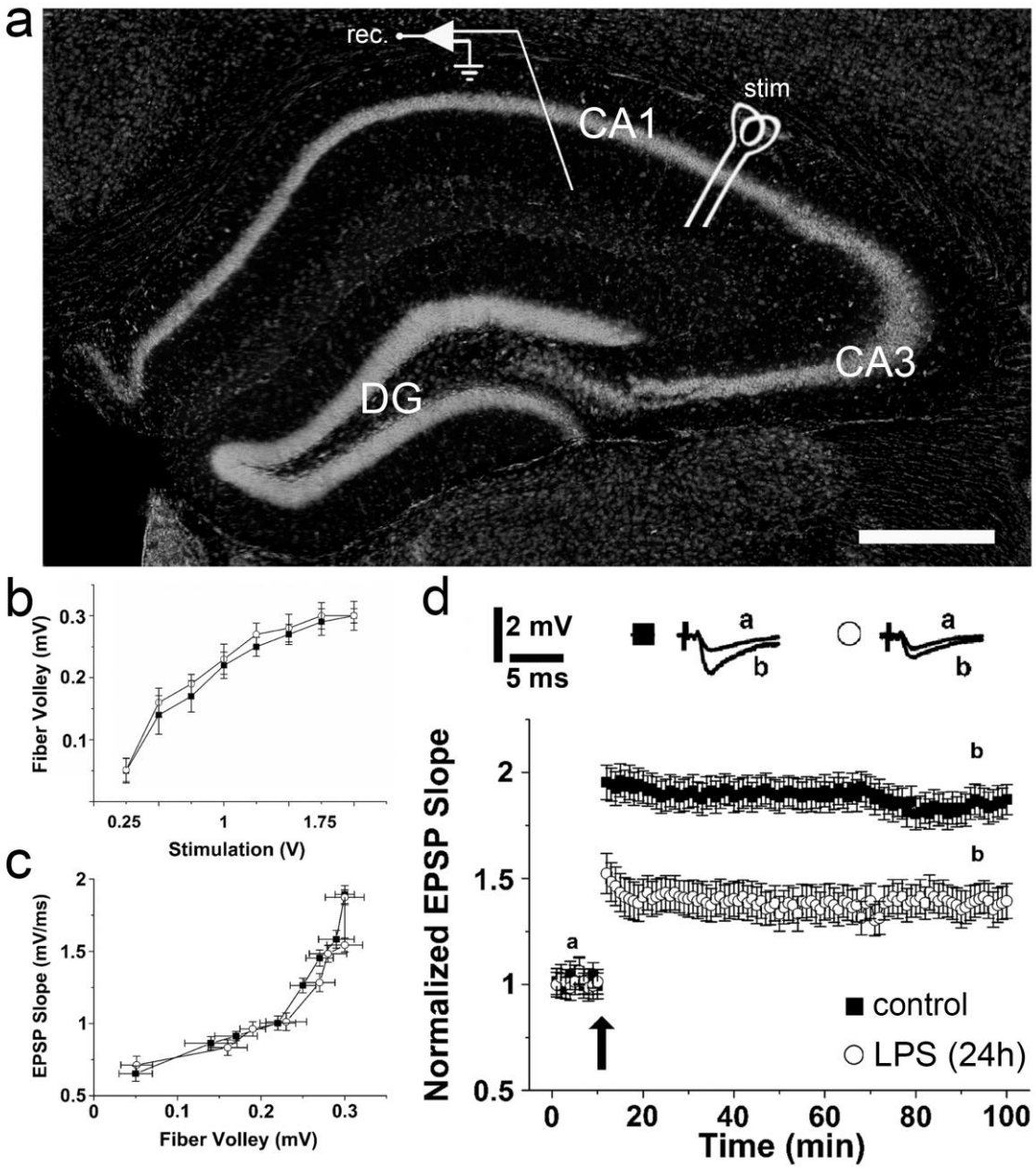

Figure 13. LPS-induced systemic inflammation leads to impaired LTP. To examine the effects of LPS-induced systemic inflammation on synaptic plasticity, long-term potentiation (LTP) was probed at Schaffer collateral-CA1 synapses in acute hippocampal slices treated with LPS (1 µg/ml) using a single 100 Hz tetanus protocol (1 s) and compared to vehicle-treated controls. **(a)** TO-PRO® nuclear stain showing cytoarchitecture; Scale bar: 300 µm. **(b)** Fiber volley and **(c)** EPSPs as a function of stimulation intensity were not significantly altered between the groups. **(d)** Interestingly, LTP was significantly reduced following 24 hours LPS-injections as compared to the vehicle-treated control group. (n=12 animals per group; 'a' denotes the time point from which the illustrated baseline recordings were taken; t = 87 min indicated by 'b'; t-test; $b_{control}$ vs. b_{LPS}; $p < 0.001$). Figure adapted from Strehl et al. (2014).

5.2 Neuroinflammation *in vitro* – the role of TNFα

5.2.1 LPS triggers inflammation in hippocampal slice cultures

Intraperitoneal injection of LPS induces inflammation in the brain by various means. One plausible way is the direct passage of LPS through the blood brain barrier (BBB). This idea is supported by the finding that inflammation leads to a permeabilization of the BBB (Erickson & Banks 2011). Furthermore, microglia express the receptor TLR4 which LPS has been shown to bind to and act through (Poltorak et al. 1998; reviewed in detail by Trotta et al. 2014). To test whether LPS acts directly on brain tissue and in order to learn more about the mechanism through which LPS affects SP and synaptic plasticity, entorhino-hippocampal slice culture preparations obtained from C57BL/6 mice were used. To determine the minimal concentration of LPS that is needed to trigger inflammation *in vitro*, LPS was applied at distinct concentrations between 1 ng/mL

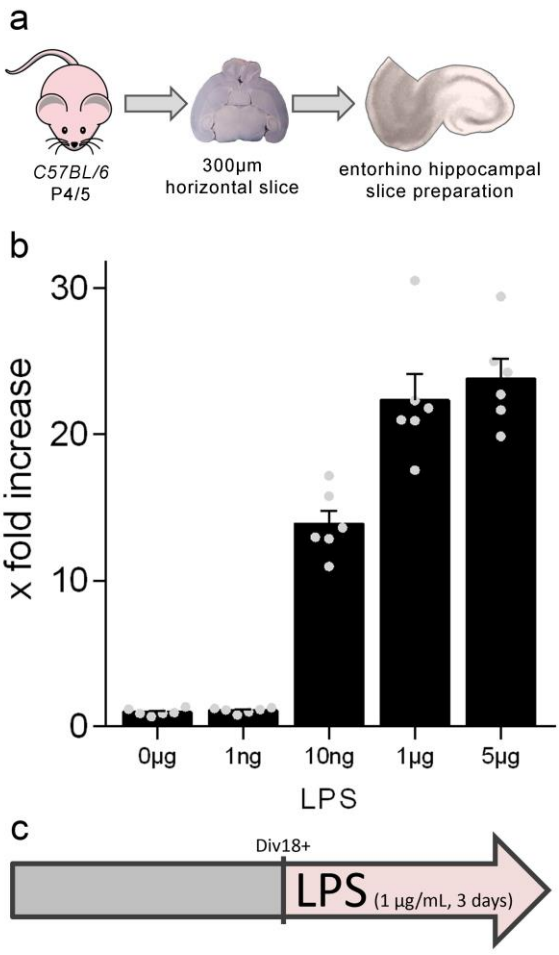

Figure 14. A concentration of 1 µg/mL LPS is sufficient to induce inflammatory processes in entorhinal hippocampal slice cultures. (a) Workflow of organotypic slice culture preparation. **(b)** Analysis of TNFα-mRNA expression following LPS treatment (0 ng, 1 ng, 10 ng, 1 µg and 5 µg per ml) for three days using quantitative RT-PCR (n = 6 per group; Values represent mean ± SEM). **(c)** Based on the LPS-titration row (b) 1 µg/ml LPS was concidered sufficient to induce a neuroinflammatory response and hence used as standard treatment for the following experiments.

up to 5 µg/ml LPS for 3 days to the incubation medium of three-weeks-old cultures. TNFα-mRNA levels were analyzed using quantitative RT-PCR. GAPDH served as a reference gene for these experiments and data were normalized to age- and time-matched vehicle-treated controls. Indeed, TNFα-mRNA levels were increased following three days LPS treatment in a dose-dependent manner. While TNFα-mRNA expression did not significantly change following 1 ng/mL LPS treatment, it increased about 14 fold (14 ± 0.07 fold; $p < 0.01$) at 10 ng/mL and reached a plateau at 1 µg/ml LPS (22 ± 0.9 fold; $p < 0.01$; Figure 14). All further experiments, a concentration of 1 µg/ml LPS applied for 3 days to the incubation medium was used as standard protocol.

5.2.2 SP-mRNA levels and cluster sizes are reduced following LPS treatment *in vitro*

In a different round of experiments, slice cultures were treated with LPS (1 µg/ml; 3 days) and SP-mRNA levels were quantified. While TNFα-mRNA showed an ~8 fold increase (7.9 ± 0.89 fold; $p < 0.001$), the expression of SP-mRNA was significantly reduced (65 ± 5%; $p < 0.01$) in the LPS-treated group as compared to age- and time-matched vehicle-only-treated control cultures (Figure 15b). These results confirm the *in vivo* findings (see above; Strehl et al. 2014) and reveal that LPS acts directly on brain tissue and leads to a downregulation of SP-mRNA.

To assess whether the effect of LPS-induced inflammation on SP-protein can also be observed *in vitro*, LPS-treated and vehicle-treated control cultures were immunostained for SP, and SP-cluster sizes and numbers were analyzed (Figure 15c-e). Interestingly, similar to the *in vivo* situation, SP-cluster sizes were also reduced in the hippocampal CA1-region in a laminar-specific fashion. While SP-cluster sizes did not change significantly in the stratum oriens, SP-cluster sizes were significantly reduced in the stratum radiatum (-25 ± 9%; $p < 0.05$) and stratum lacunosum moleculare (-30 ± 9%; $p < 0.05$). SP-cluster sizes did not change significantly in the stratum oriens (-2 ± 8%; $p > 0.99$). Furthermore, SP-cluster numbers were decreased in all layers, however a

significant reduction was only reached in the stratum lacunosum moleculare (str.la-mol.: -47 ± 11%, $p < 0.01$; str. rad.: -40 ± 19%, $p > 0.09$; str. oriens: 42 ± 12%, $p > 0.21$; Figure 15c-e). Together these results reveal that LPS affects the expression of both, SP-mRNA and -protein levels *in vitro*. This makes the organotypic slice culture system a suitable tool to study the inflammatory signaling pathways that affect SP and neuronal plasticity.

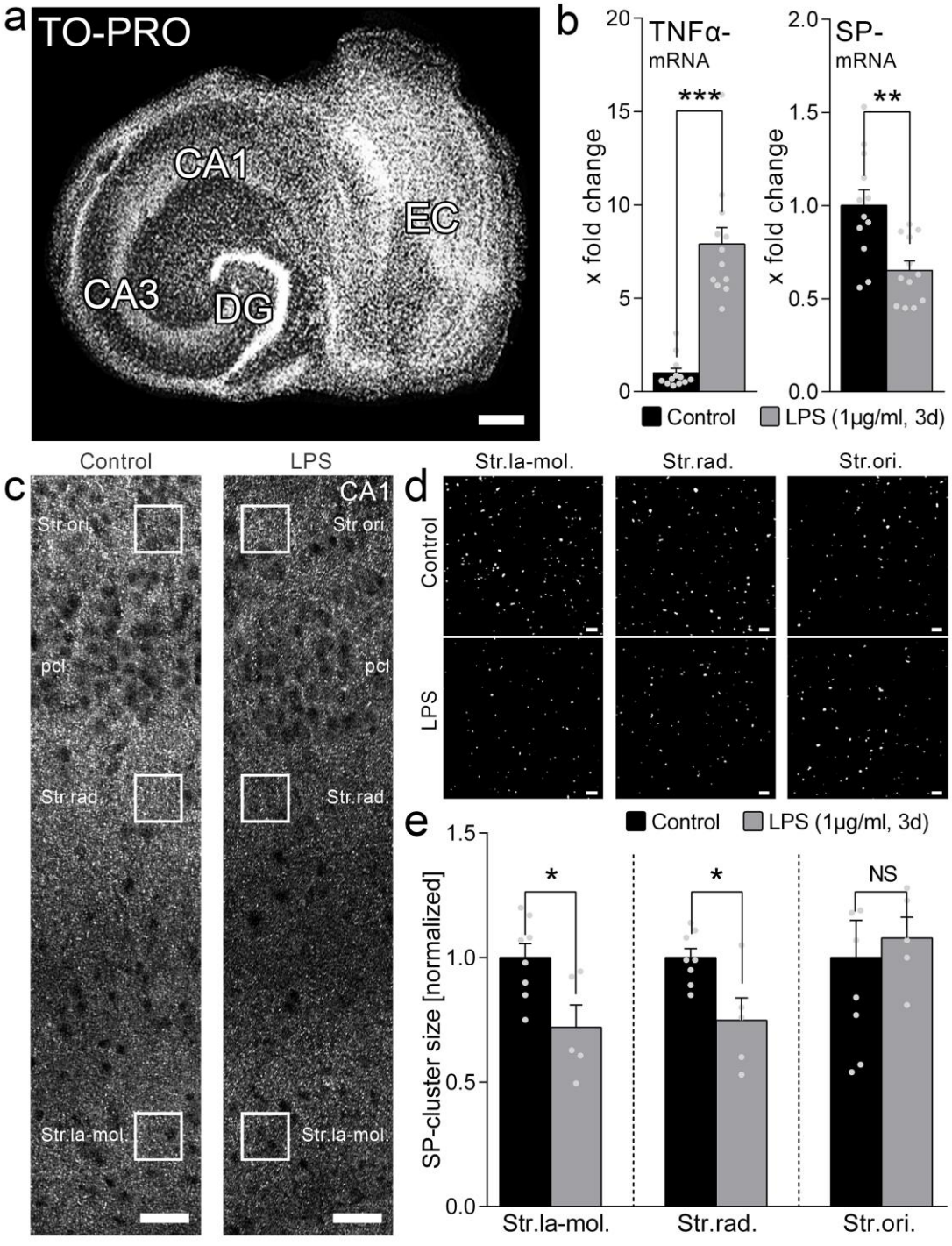

Figure 15. SP-mRNA as well as SP-protein cluster sizes are reduced upon LPS-treatment in mouse organotypic entorhinal hippocampal slice cultures (OTCs). (a) TO-PRO® staining of an OTC. DG = dentate gyrus, EC = entorhinal cortex, CA = Cornu Ammonis. Scale bar: 200 µm. **(b)** Analysis of TNFα- and SP-mRNA expression following LPS treatment (1 µg/ml, 3 d) using quantitative RT-PCR (n = 12 per group; **p < 0.01, ***p < 0.001, Mann-Whitney test). **(c)** SP-cluster were analyzed within the hippocampal area CA1 in selected regions at high magnification (indicated by white squares) within the lamina of Str.oriens (Str.ori.), Str.radiatum (Str.rad.) and Stratum lacunosum moleculare (Str.la-mol.). Pyramidal cell layer, pcl; Scale bar: 30 µm. **(d)** Higher magnification of selected regions showing SP-clusters in white. Scale bar: 2 µm. **(e)** SP-cluster sizes were significantly reduced in Str.la-mol. and Str.rad. but not in Str.ori. upon three days of LPS treatment compared to vehicle-treated controls. SP-cluster numbers were not significantly changed following LPS-treatment ($n_{Control}$ = 8; n_{LPS} = 5; Values represent mean ± SEM; Mann-Whitney test; *p < 0.05; **p < 0.01; NS = not significant).

5.2.3 *In vitro* LPS treatment has no apparent effect on cell viability

Although inflammatory reactions are considered to be protective responses which repair and recycle damaged tissue (Wyss-Coray & Mucke 2002), strong inflammation inhibits cell-regeneration and induces cell death, e.g. through excess release of neurotoxic factors (Lull & Block 2010; Das Sarma 2014; for detailed reviews see also Ransohoff 2016; Chen et al. 2016). Since a significant reduction in SP-cluster numbers was observed after LPS treatment *in vitro*, it had to be excluded that LPS triggered cell death, which would have trivially explained the LPS-induced reduction of SP-mRNA and protein levels. Hence, cell viability was monitored via propidium iodide (PI) nuclear staining in hippocampal area CA1. The plasma membrane of vital cells is impermeable to PI. In degenerated and dead cells with damaged cell membranes, PI enters the cell and intercalates with the DNA in the nucleus (Figure 16a). As a positive control, and to demonstrate the applicability of this method in slice culture preparations, one group was fixed with PFA before PI-staining. Since PFA destroys membrane integrity, all cells should be PI-positive in this group. As a second positive control, another group was treated with a high dose of NMDA (50 µM, 4 h) which induces apoptosis by excess influx of calcium (reviewed by Orrenius et al. 2003). Indeed, in response to a high dose of NMDA, about 20% (19.56 ± 5.3%) cells in the hippocampal CA1 region were PI positive compared to vehicle-treated controls. Interestingly, in the LPS-treated group only a

minority of 0.01 ± 0.004% was PI positive, compared to vehicle-treated controls (0.06 ± 0.01%; Figure 16b-d). These data show that LPS (1 µg/ml; 3 d) does not induce prominent cell death which could explain the LPS-induced reduction of SP. Hence, other mechanisms, i.e. specific signaling pathways mediated by LPS, are likely to be involved in affecting synaptic structure and function, i.e. SP properties and synaptic plasticity.

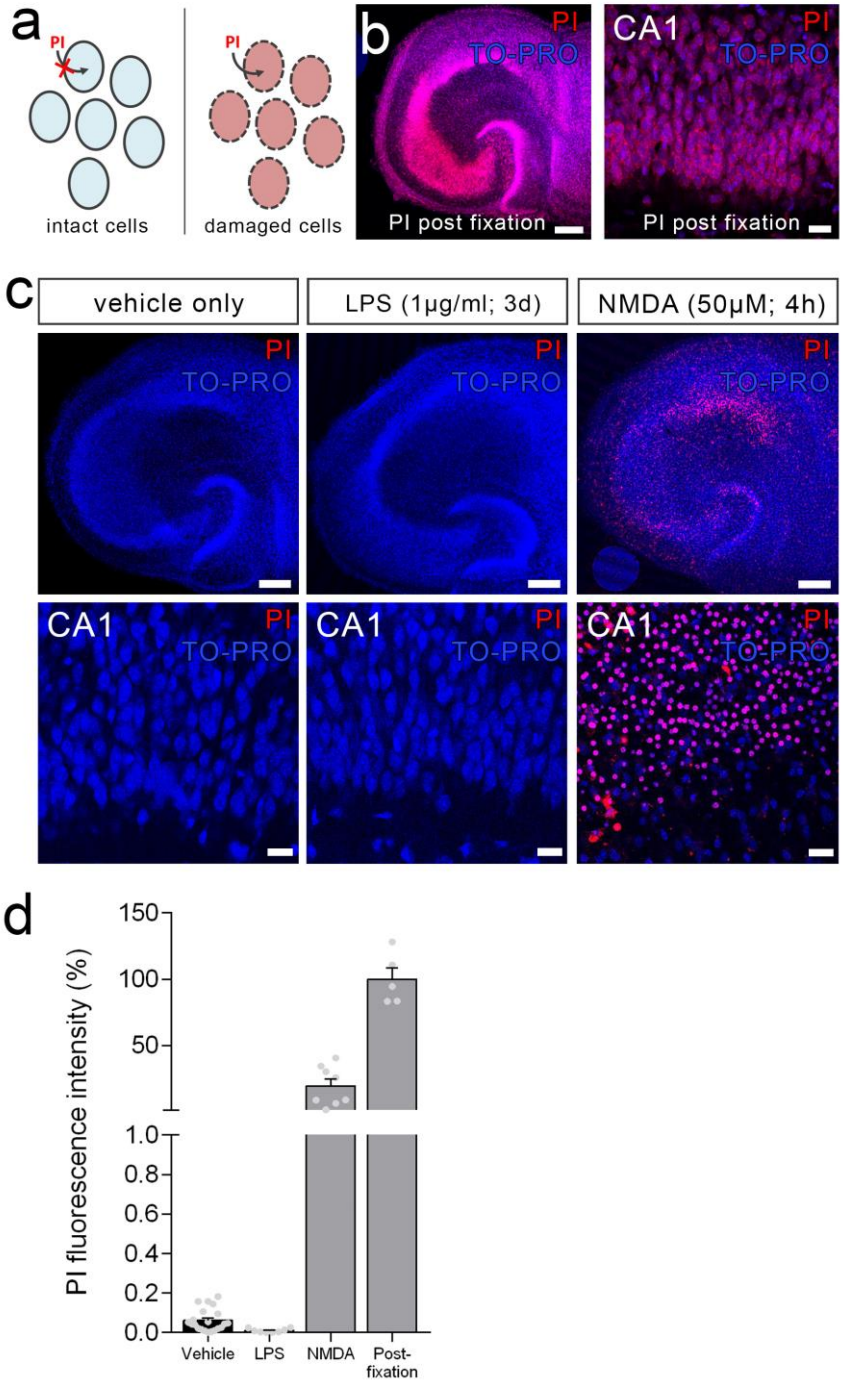

Figure 16. LPS-treatment does not lead to neuronal cell death in OTCs. (a) Schematic illustrating the principle of propidium iodide (PI) staining: Vital plasma membranes are impermeable to PI (left). Only under conditions when the cell membrane is damaged, PI is able to enter the cytosol (right). (b+c) PI staining (red) of entorhinal hippocampal slice cultures following PFA-fixation **(b)** as well as LPS (1 µg/ml; 3 d) and NMDA (50 µM; 4 h) treatment versus a vehicle-treated control **(c).** TO-PRO®-nuclear stain (blue) illustrates the cytoarchitecture of the hippocampus (left in 'b', top row in 'c') and in higher magnification the CA1 region (right in 'b', bottom row in 'c'). Scale bars in b: left = 200 µm, right = 20 µm; Scale bars in c: top row = 200 µm, bottom row = 20 µm). **(d)** Quantification of PI fluorescence of area CA1 ($n_{vehicle}$ = 21; n_{LPS} = 8; n_{NMDA} = 8; $n_{Postfix}$ = 5; Error bars represent SEM).

5.2.4 SP is neither affected in TNFα- nor TNFR-deficient mice upon LPS treatment

Neuroinflammation involves the production of various pro-inflammatory and neurotoxic mediators (Teeling & Perry 2009; Glass et al. 2010). Among them is the chemokine TNFα which is markedly increased following LPS treatment (Strehl et al. 2014). To elucidate whether TNFα is involved in LPS-mediated alteration in SP expression, LPS treatment and SP-cluster analysis were repeated in cultures prepared from mice lacking TNFα (referred to as TNF KO-mice). Interestingly, LPS treatment of TNF KO cultures did not result in a significant decrease in SP-cluster size (Figure 17a; normalized values: SP KO, $Control_{Str.la\text{-}mol.}$ = 1.00 ± 0.04; $LPS_{Str.la\text{-}mol.}$ = 1.17 ± 0.08; $p > 0.1$; $Control_{Str.rad.}$ = 1.00 ± 0.04; $LPS_{Str.rad.}$ = 1.00 ± 0.04; $p > 0.80$; $Control_{Str.ori.}$ = 1.00 ± 0.05; $LPS_{Str.ori.}$ = 1.00 ± 0.06; $p > 0.95$) or cluster numbers (Figure 17a; normalized values: SP KO, $Control_{Str.la\text{-}mol.}$ = 1.00 ± 0.14; $LPS_{Str.la\text{-}mol.}$ = 1.04 ± 0.15; $p > 0.74$; $Control_{Str.rad.}$ = 1.00 ± 0.13; $LPS_{Str.rad.}$ = 1.12 ± 0.17; $p > 0.78$; $Control_{Str.ori.}$ = 1.00 ± 0.12; $LPS_{Str.ori.}$ = 1.10 ± 0.13; $p > 0.74$). Parallel experiments conducted in wildtype littermates showed the expected and significant lamina-specific reduction of SP-cluster sizes in hippocampal CA1-layers stratum lacunosum moleculare (-20 ± 4%, $p < 0.01$) and stratum radiatum (-14 ± 6%, $p < 0.05$) (Figure 17b), while SP-cluster sizes in the stratum oriens remained unaffected by LPS treatment (-8 ± 7%, $p > 0.70$). Analysis of SP-cluster numbers yielded a similar picture to the experiments performed in C57BL/6 cultures, except that the reduction of SP in stratum oriens reached significance in wildtype littermates (Str.la-mol. = -40 ± 8%, $p < 0.01$;

Str.rad. = -25 ± 14%, $p < 0.05$; Str. ori = -9 ± 17%, $p > 0.71$). To further validate this finding and to exclude off-target effects of TNFα, the exact same experiment in cultures prepared from mice lacking the respective TNFα receptors, TNFR1/2 was performed. Similar to the results obtained in TNFα-deficient slice cultures, LPS treatment (1 µg/ml, 3 d) performed in TNF1/2-KO cultures did not alter SP-cluster sizes and numbers (Figure 17c; normalized cluster sizes: $Control_{Str.la\text{-}mol.} = 1.00 \pm 0.07$; $LPS_{Str.la\text{-}mol.} = 1.01 \pm 0.05$; $p > 0.71$; $Control_{Str.rad.} = 1.00 \pm 0.06$; $LPS_{Str.rad.} = 1.05 \pm 0.03$; $p > 0.70$; $Control_{Str.ori.} = 1.00 \pm 0.06$; $LPS_{Str.ori.} = 1.14 \pm 0.10$; $p > 0.52$; normalized cluster numbers: $Control_{Str.la\text{-}mol.} = 1.00 \pm 0.19$; $LPS_{Str.la\text{-}mol.} = 0.86 \pm 0.09$; $p > 0.50$; $Control_{Str.rad.} = 1.00 \pm 0.27$; $LPS_{Str.rad.} = 0.91 \pm 0.14$; $p > 0.99$; $Control_{Str.ori.} = 1.00 \pm 0.26$; $LPS_{Str.ori.} = 1.04 \pm 0.12$; $p > 0.43$). These data suggest that LPS exerts its effects on SP by enhancing the expression of TNFα.

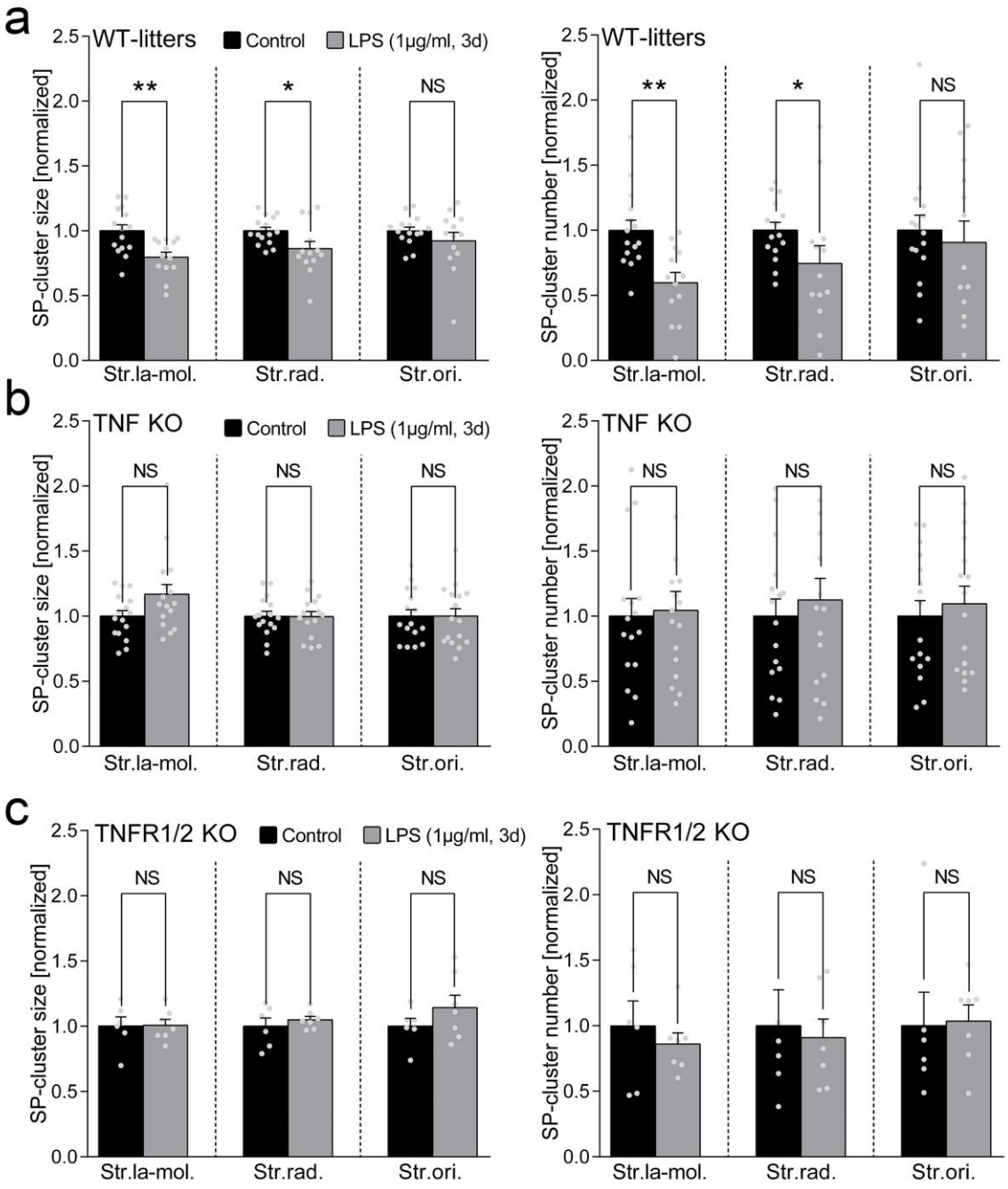

Figure 17. LPS-induced reduction of SP-cluster sizes is dependent on TNFα-signaling. SP-clusters were analyzed within the hippocampal area CA1 in selected regions within the lamina of Str.oriens (Str.ori.), Str.radiatum (Str.rad.), and Stratum lacunosum moleculare (Str.la-mol.). **(a)** SP-cluster sizes were significantly reduced in Str.la-mol. and Str.rad., but not in Str.ori. of wildtype littermate cultures upon LPS treatment (1 µM, 3 d) compared to vehicle-treated controls ($n_{Control}$ = 15, n_{LPS} = 13, Mann-Whitney test; *p < 0.05; **p < 0.01, NS = not significant). **(b+c)** Neither SP-cluster sizes nor numbers were significantly altered in cultures lacking either TNFα protein or the TNFα receptors TNFR1/2 following LPS-treatment (1 µM, 3 d) compared to vehicle-treated controls (TNF KO: n = 16 per group; TNFR1/2 KO: $n_{Control}$ = 6; n_{LPS} = 7; Values represent mean ± SEM; Mann-Whitney test; NS = not significant).

5.2.5 Role of glial cells in the synthesis of TNFα following LPS treatment

Neurons, astrocytes, and microglia are capable of producing TNFα upon appropriate physiological and pathological stimuli (Chung & Benveniste 1990; Rogers et al. 1996; Breder et al. 1993). More recent studies show that microglia mainly express TNFα under conditions of neuroinflammation (Hanisch 2002; Welser-alves & Milner 2013). To determine the source of TNFα produced in response to LPS treatment, a TNFα reporter mice line, referred to as tg(TNF-eGFP), was used. These mice express GFP under the control of the TNFα-promoter and hence allow for the visualization of TNFα-expressing cells (Figure 18a). To identify microglia and astrocytes slice cultures prepared from tg(TNF-eGFP) were immunostained for Iba1 and GFAP respectively upon LPS treatment (1 µg/ml; 3 d),

In a first step, GFP-expression was quantified. Consistent with the qPCR data a considerable increase in GFP-fluorescence (+23 ± 3 fold, $p < 0.001$) was detected in LPS-treated cultures compared to vehicle-treated controls (Figure 18b). In the next step the source of TNFα-expression was determined by assessing co-localization of GFP/Iba1 and GFP/GFAP. Interestingly, cells expressing GFP co-localized with Iba1 and almost no GFP-positive cells co-localized with GFAP (Figure 18c). This suggests that Iba1-positive microglial cells are the major source of TNFα in the experimental setting of OTCs. No evidence for a neuronal source of TNFα was obtained after carefully examining Iba1-negative and GFAP-negative cells in the stratum pyramidale. This observation was confirmed by Pearson's correlation analysis (Pearson's r: Iba1/GFP = 0.77 ± 0.01; GFAP/GFP = 0.06 ± 0.02; Figure 18d/e). Taken together, these experiments show that microglia are a major source for TNFα upon direct application of LPS to slice culture preparations.

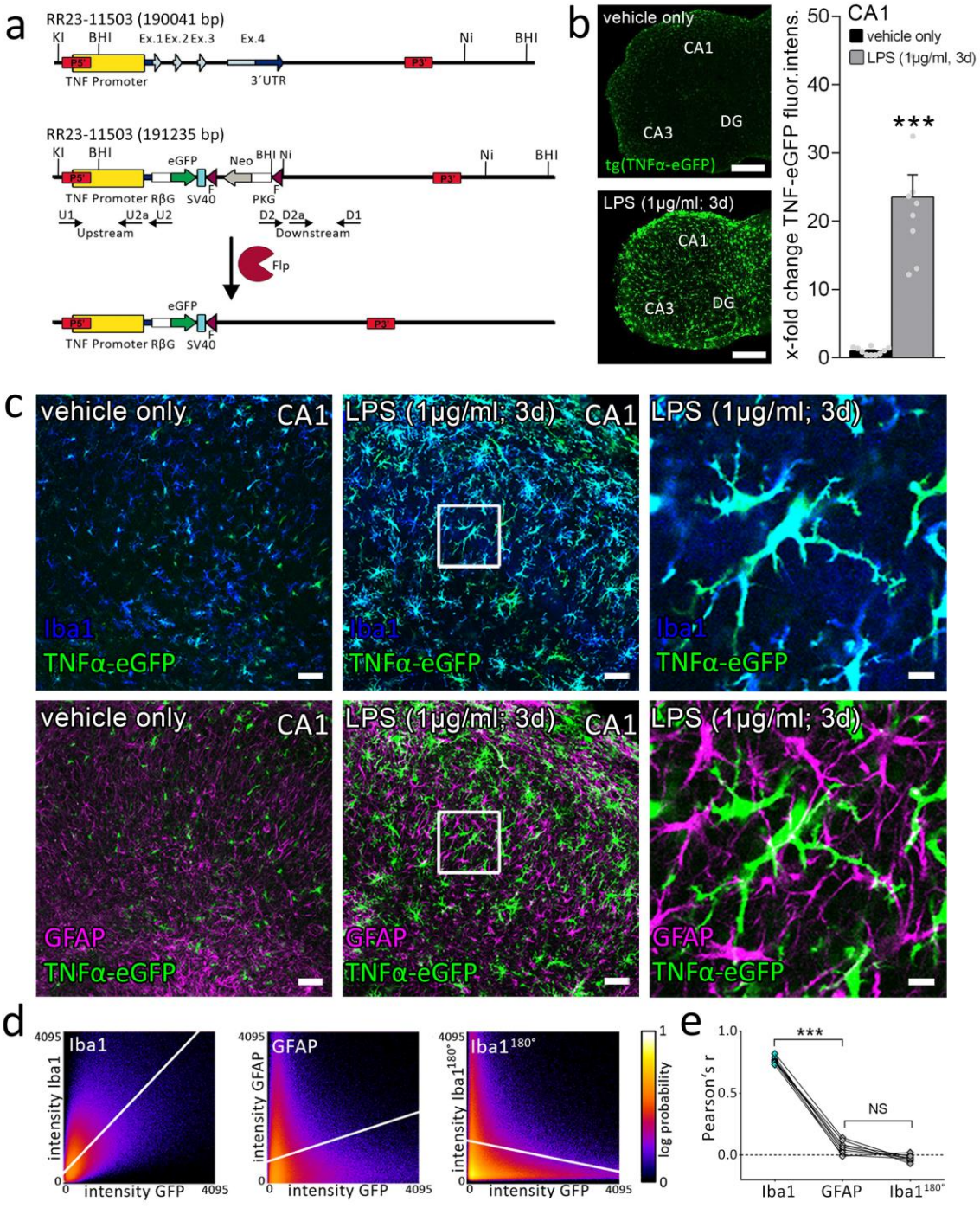
a
RR23-11503 (190041 bp)
KI BHI Ex.1 Ex.2 Ex.3 Ex.4 Ni BHI
TNF Promoter
3´UTR
RR23-11503 (191235 bp)
eGFP Neo BHI Ni
TNF Promoter RβG SV40 PKG
U1 U2a U2 Upstream
D2 D2a D1 Downstream
Flp
b
vehicle only
CA1
CA3
DG
tg(TNFα-eGFP)
LPS (1µg/ml; 3d)
x-fold change TNF-eGFP fluor.intens.
vehicle only
LPS (1µg/ml, 3d)
***
c
vehicle only
LPS (1µg/ml; 3d)
CA1
Iba1
GFAP
TNFα-eGFP
d
intensity Iba1
intensity GFAP
intensity Iba1180°
intensity GFP
log probability
e
Pearson's r
***
NS
Iba1
GFAP
Iba1180°

Figure 18. Microglial cells represent the major source of TNFα synthesis following LPS treatment. (a) Gene draft of tg(TNF-eGFP) reporter mice expressing GFP controlled by the TNFα promoter. **(b)** Left: Hippocampal region of OTCs prepared from tg(TNF-eGFP) mice. GFP-expression (green) in vehicle-treated control compared to a culture treated three days with LPS (1 µg/ml). Scale bar: 300 µm. Right: Increased normalized GFP fluorescence intensity of tg(TNF-eGFP) cultures following LPS-treatment ($n_{Control}$ = 10, n_{LPS} = 9; Mann-Whitney test). **(c)** Immuno-histochemical staining of tg(TNF-eGFP) mice against Iba1 (blue) and GFAP (magenta). Colocalization with GFP fluorescence (cyan) indicates that TNFα-production is mainly active in Iba1-positive cells. Selected regions (white squares) are displayed in higher magnification (right). Left scale bar: 50 µm, right scale bar: 10 µm. **(d)** Scatter plots visualizing colocalization of Iba1 vs. GFP (left), GFAP vs. GFP (middle) and random Iba1 distribution (by 180 degree rotation) vs. GFP (right). **(e)** Pearson's correlation of co-localization analysis (n = 9 per group; values represent mean ± SEM; Mann-Whitney test; ***p < 0.001, NS = not significant).

5.2.6 Depletion of microglia prevents LPS-induced TNFα increase

To eliminate microglia, OTCs were treated with liposome-encapsulated clodronic acid (1 mg/ml, 24 h; FormuMax), a highly hydrophilic cell membrane impermeable bisphosphate, which is taken up by cells via phagocytosis. Since in hippocampal slice cultures microglia are the only cells with phagocytic activity, clodronic acid selectively affects microglia (Russell & Rogers 1999, Mönkkönen et al. 1994; Ylitalo et al. 1998). Upon internalization of the lipid vesicles, lysosomal activity within the cytoplasma of microglia releases clodronic acid which causes irreversible cell damage (van Rooijen et al. 1996). To visualize microglial cells and to monitor microglia elimination, these experiments were performed in OTCs prepared from the transgenic mouse line tg(Iba1-EGFP) which expresses GFP under the control of the Iba1 promoter (Hirasawa et al. 2005; Figure 19a). Indeed, treatment with liposome-encapsulated clodronic acid markedly reduced the GFP signal, while untreated cultures as well as control cultures treated with empty liposomes did not show a visible reduction of GFP-expression, which would have indicated an elimination of microglial cells (Figure 19a).

To assess the role of microglia in LPS-caused effects on TNFα- and SP gene expression, a quantitative RT-PCR was performed in the presence or absence of clodronic acid. As expected, LPS treatment in cultures exposed to empty liposomes increased TNFα levels significantly (+8.7 ± 0.6 fold; Figure 19b). As anticipated, only a small and not significant increase of TNFα-mRNA was detected upon LPS treatment in clodronic acid-exposed cultures

(+1.9 ± 0.9 fold), confirming the results performed in cultures from tg(TNF-eGFP) mice (Figure 18), that microglia are the major source of TNFα following *in vitro* LPS treatment.

Next mRNA-expression of SP from the same set of cultures was analyzed. Interestingly, while SP-mRNA level was reduced upon LPS treatment in the vehicle-treated group (-35 ± 5%), no apparent difference was observed in the clodronic acid-treated groups where microglia had been eliminated (+1.4 ± 7%). However, it is important to note that overall SP-mRNA levels were already reduced in these groups by about 10% (Figure 19b). Furthermore, upon LPS treatment only a slight and not significant decrease of SP-mRNA was detected in the group treated with empty liposomes (-7 ± 3%), even though microglia should be intact in these cultures (c.f., Figure 19a, middle panel). While these results support the major conclusion that microglial TNFα regulates SP, it was decided not to follow up on this line of research, also considering that clodronic acid and liposomes may have additional effects in OTC preparations.

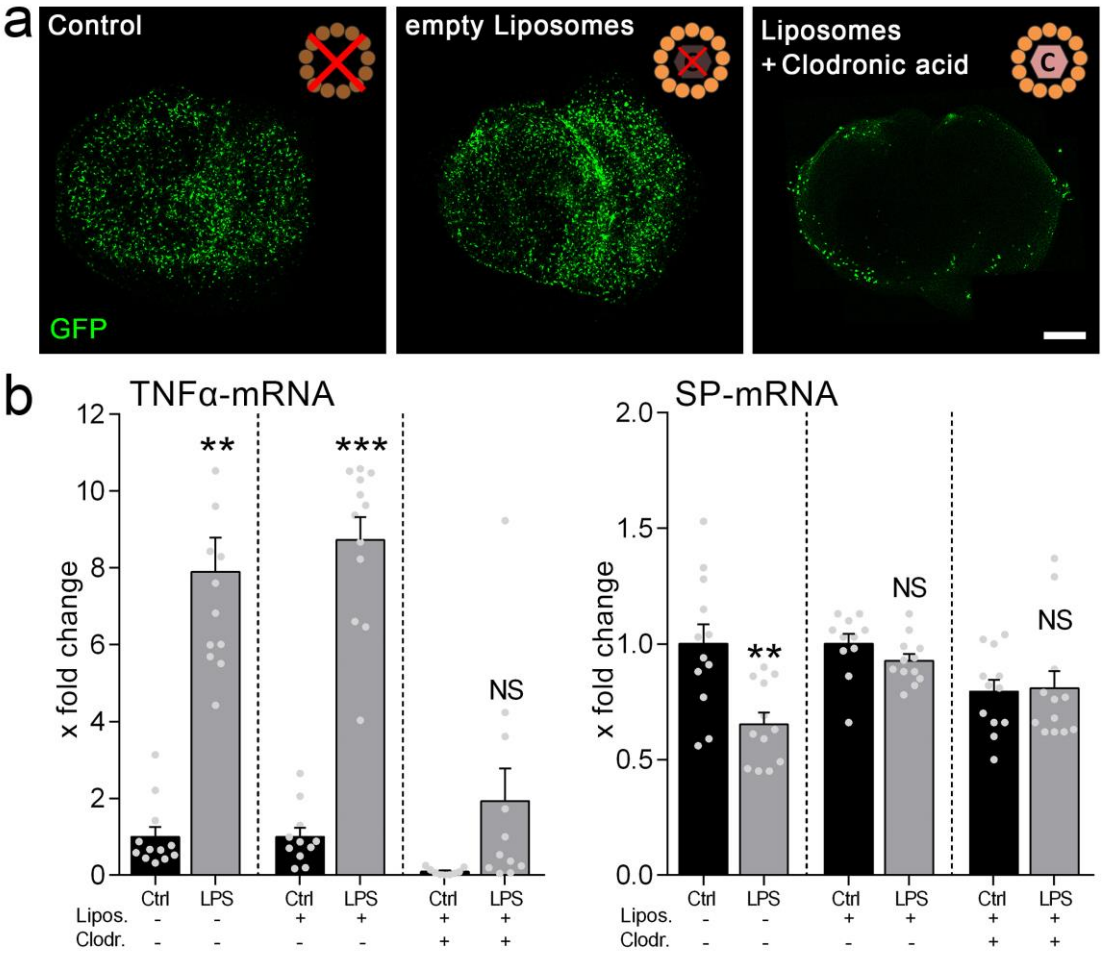

Figure 19. Elimination of microglial cells using clodronic acid prevents an increase of TNFα-mRNA and likely blocks downregulation of SP-mRNA. (a) OTCs prepared from the transgenic mouse line tg(Iba1-eGFP) were used to visualize microglial cells and to monitor microglial elimination. GFP-fluorescence (green) of OTCs treated with vehicle (left), empty liposomes (middle), and liposomes-encapsulated clodronic acid (1 mg/ml; right). Scale bar: 300 µm. **(b)** Normalized TNFα-mRNA expression. Treatment conditions are indicated: Lipos. = empty liposomes, Clodr. = liposome encapsulated clodronic acid. n = 9 - 12 cultures per group; Values represent mean ± SEM; Mann-Whitney test; **p < 0.01; ***p < 0.001; NS = not significant.

5.3 Role of SP in RA-dependent synaptic plasticity

The second part of the thesis addresses the role of RA in SP-mediated homeostatic synaptic plasticity and neuroinflammation. Because previous work in the group on SP and homeostatic plasticity was carried out on dentate granule cells, I decided to also focus these experiments on the dentate gyrus.

5.3.1 4 h RA treatment neither increases synaptic strength nor changes SP-clusters

The effects of RA on SP expression and synaptic transmission were examined in the dentate gyrus of three-week old entorhino-hippocampal slice culture preparations. Four hours after RA (1 µM) application, cultures were fixed and immunostained for SP. In these experiments, SP-cluster sizes and numbers did not change significantly in the RA group (Figure 20c/d). Also, RA did not increase mEPSC-amplitude after a 4 hours treatment (Figure 20a/b). Rather, a slight but significant decrease in mEPSC amplitude was observed in these experiments (Control = 12.87 ± 0.48 pA; RA = 11.48 ± 0.47 pA; $p < 0.05$; Mann-Whitney test) (Figure 20a/b). Interestingly, mEPSC-frequency was significantly increased following 4 hours RA treatment (Control = 1.24 ± 0.11 pA; RA = 1.94 ± 0.18 pA; $p < 0.01$; Mann-Whitney test; Figure 20a/b). Hence, four hours RA treatment is not sufficient to induce strengthening of excitatory synaptic transmission and changes in SP expression in dentate granule cells of three-week-old entorhino-hippocampal slice cultures.

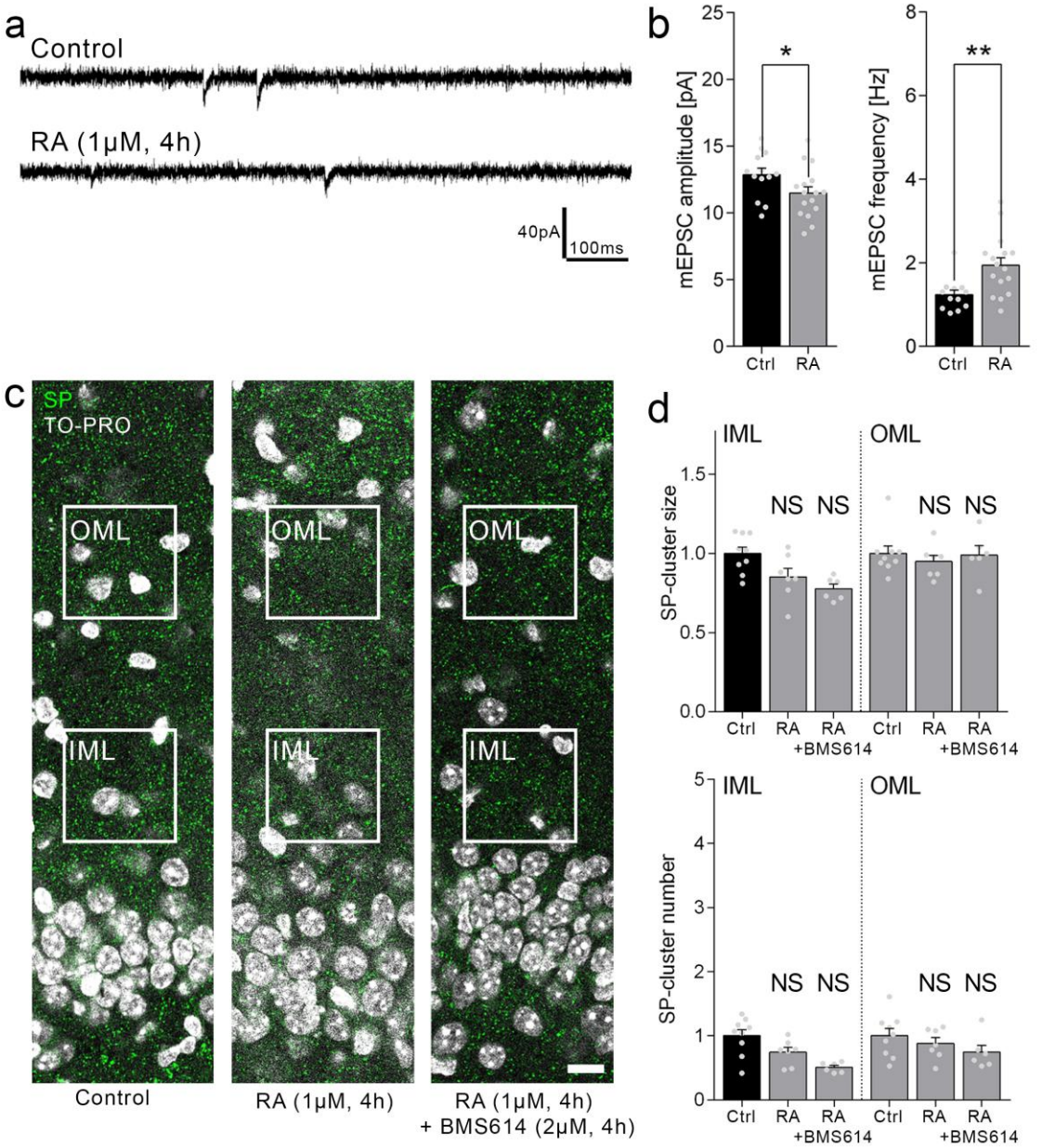

Figure 20. Short-term treatment of entorhino-hippocampal organotypic slice cultures with RA (1 µM, 4 h) has neither an effect on mEPSCs nor on SP-clusters. (a) Sample traces related to **(b)** amplitude and frequency analysis of mEPSC recordings from hippocampal dentate granule cells upon 4 hours RA treatment (1 µM) vs. an untreated control ($n_{Control}$ = 13; n_{RA} = 16). **(c)** Immunostainings showing a segment of the suprapyramidal dentate gyrus from organotypic hippocampal slice cultures either untreated, treated with RA (1 µM) alone or in parallel with BMS614 (2 µM). Exemplary regions of interest selected for SP-cluster analysis are indicated by white squares. IML = inner molecular layer, OML = outer molecular layer. Scale bar: 10 µm. **(d)** SP-cluster analysis in the IML and OML of the dentate gyrus ($n_{Control}$ = 9; RA, n_{RA} = 7; $n_{RA+BMS614}$ = 6. Values represent mean ± SEM; Mann-Whitney test, *p<0.05; **p<0.01; NS = not significant. Individual data points are indicated by gray dots.

5.3.2 3 days RA treatment increases SP-cluster sizes *in vivo* and *in vitro*

Next, the duration of RA treatment was increased to three days. Indeed, prolonged RA treatment increased SP-cluster sizes. While a slight but not significant increase in the IML was observed, SP-cluster sizes in the OML were significantly increased in RA-treated cultures (1.41 ± 0.12 fold; $p < 0.05$; $n_{Control} = 6$; $n_{RA} = 7$; Mann-Whitney test). SP-cluster number was also not significantly changed in the IML, but it was significantly increased in the OML (2.55 ± 0.38 fold; $p < 0.01$; $n_{Control} = 6$; $n_{RA} = 7$; Mann-Whitney test).

It has been shown that RA exerts its effects on synaptic plasticity via the RA-receptor RARα. To test whether RA acts on SP via RARα, another set of cultures was treated for three days with RA (1 µM) together with BMS614 (2 µM), a selective antagonist of RARα ($K_i = 2.5$ nM). BMS614 indeed prevented the increase in SP-cluster sizes and numbers seen in the RA-treated group (Figure 21a-c), while having no apparent affect in BMS614-only-treated cultures.

Effects of RA on global changes of SP levels were also tested. For this purpose, quantitative RT-PCR and western blot were performed with whole entorhino-hippocampal slices. Interestingly, analysis of protein- and mRNA-expression revealed no significant changes in total protein- and mRNA-levels in slice culture preparations upon RA treatment (Figure 21d/e), indicating that RA modulates SP rather locally, either by re-distributing soluble SP from the cytosol to pre-existing clusters and/or through post-transcriptional mechanisms. To confirm the validity of these *in vitro* results, *in vivo,* i.p. injections of RA were carried out. 6-month-old C57BL/6J mice were injected i.p. with RA (10 mg/kg) and SP-clusters were analyzed three days later in the DG of horizontal brain slices. RA treatment significantly increased SP-cluster sizes in the IML and OML of the DG (IML: 1.33 ± 0.03 fold; $p < 0.01$; OML: 1.25 ± 0.06 fold; $p < 0.05$; $n_{Control} = 10$; $n_{RA} = 8$; Mann-Whitney test). SP-cluster numbers remained unchanged in the IML while SP-numbers within the OML were significantly increased (2.13 ± 0.20 fold; $p < 0.001$; $n_{Control} = 10$; $n_{RA} = 8$; Mann-Whitney test) (Figure 22). Together, these experiments provided robust experimental evidence that RA affects SP, both *in vitro* and *in vivo*.

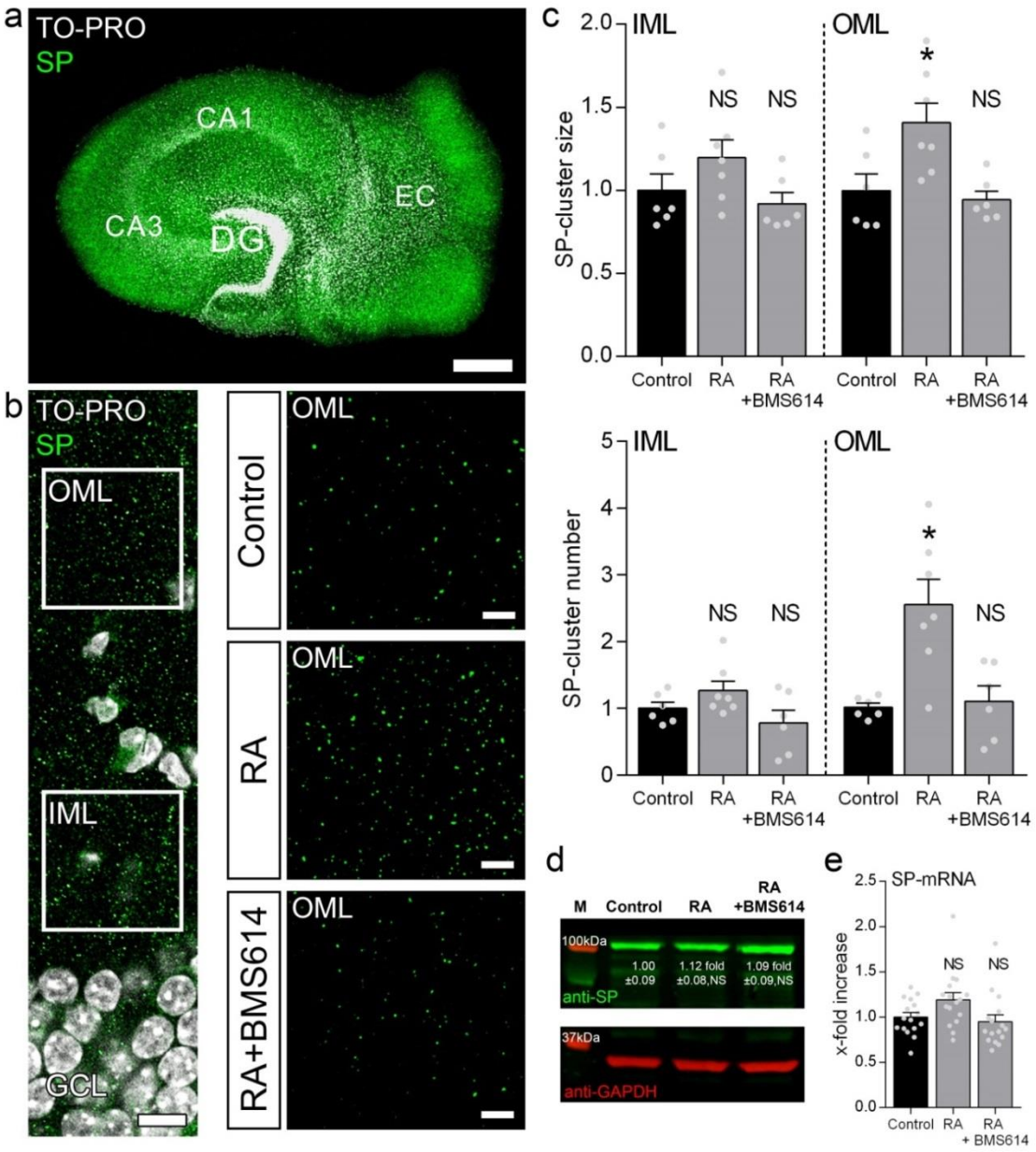

Figure 21. Long-term RA treatment (1 µM, 3 d) increases SP-cluster sizes and numbers in a region specific fashion while global SP-protein and SP-mRNA expression remain unaffected. (a) SP-immunostaining (green) of a mouse entorhino hippocampal OTC. TO-PRO® nuclear stain (white). DG = dentate gyrus, EC = entorhinal cortex, CA = Cornu Ammonis. Scale bar: 300 µm. **(b)** Immunostainings showing a segment of the DG from an untreated slice culture. Exemplary regions of interest selected for SP-cluster analysis are indicated by white squares and illustrated in higher magnification (right) for the corresponding treatment conditions. IML = inner molecular layer, OML = outer molecular layer. Left scale bar: 10 µm, right scale bar: 4 µm. **(c)** SP-cluster analysis in the IML and OML of the DG ($n_{Control}$ = 6; n_{RA}, = 7; $n_{RA+BMS614}$ = 6) **(d)** Western blot showing SP-protein expression (green) from total OTCs. GAPDH (red) was used as reference. Normalized x-fold fluorescence change (top line), standard error of the mean (SEM, bottom line). $n_{Control}$ = 9, n_{RA} = 10, $n_{RA+BMS614}$ = 10. **(e)** Quantitative RT-PCR analysis showing SP-mRNA expression of total OTCs (n = 16 cultures per group). Kruskal-Wallis test; Values represent mean ± SEM; *p < 0.05; NS = not significant. Individual data points are indicated by gray dots.

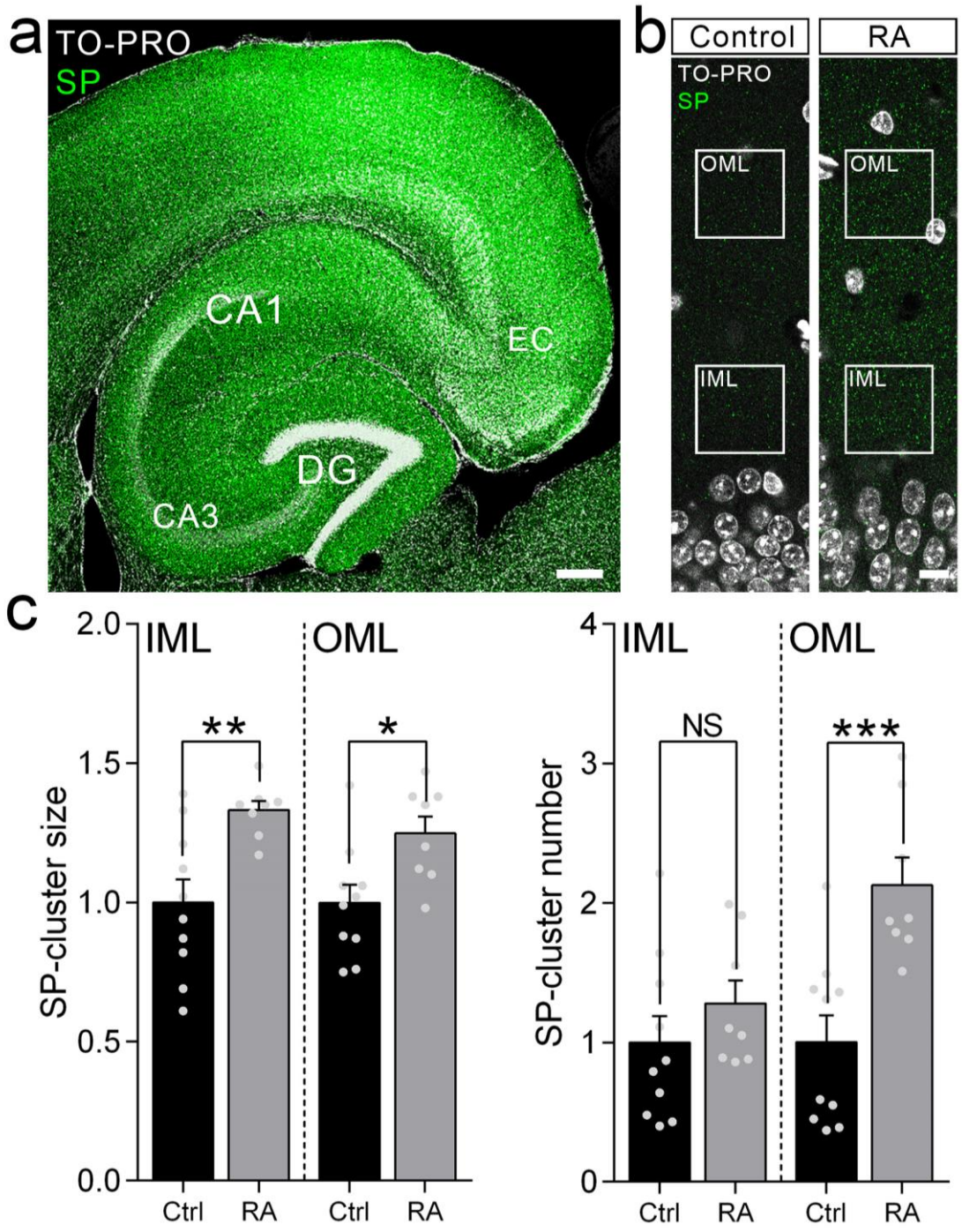

Figure 22. RA (10 mg/kg, 3 d) injected intraperitoneally significantly increased SP-cluster sizes in the molecular layer of the dentate gyrus *in vivo*. (a) Mouse horizontal brain slice showing the entorhino-hippocampal formation. Synaptopodin (SP, green) and TO-PRO® nuclear stain (white). DG = dentate gyrus, EC = entorhinal cortex, CA = Cornu Ammonis. Scale bar: 300 µm. **(b)** Immunostainings showing a segment of the DG from mice injected with RA (10 mg/ kg i.p.) compared to untreated controls. Exemplary regions of interest selected for SP-cluster analysis are indicated by white squares. IML = inner molecular layer, OML = outer molecular layer. Scale bar: 10 µm. **(c)** SP-cluster analysis of the IML and OML of the DG (Control, n = 10; RA, n = 8; values represent mean ± SEM; Mann-Whitney test, *p<0.05; **p<0.01; ***p < 0.001; NS = not significant. Individual data points are indicated by gray dots.

5.3.3 RA treatment increases mEPSC amplitude of cultured dentate granule cells

What are the functional consequences of the RA-mediated increase in SP-cluster sizes? Three-week-old OTCs were exposed to RA (1 µM; 3 d) and mEPSCs were recorded from dentate granule cells. Interestingly, under these conditions mEPSC amplitudes were markedly increased (Control: 12.31 ± 0.30 pA, n = 26; RA: 16.68 ± 0.70 pA, n = 19; $p < 0.001$; Kruskal-Wallis test followed by Dunn's *post hoc* test; Figure 23). Surprisingly mEPSC amplitudes after application of RA together with the RARα antagonist BMS614 were even significantly reduced (RA+BMS614: 10.45 ± 0.23 pA, n = 10; $p < 0.05$; Figure 23). mEPSC frequencies did not change, neither by RA

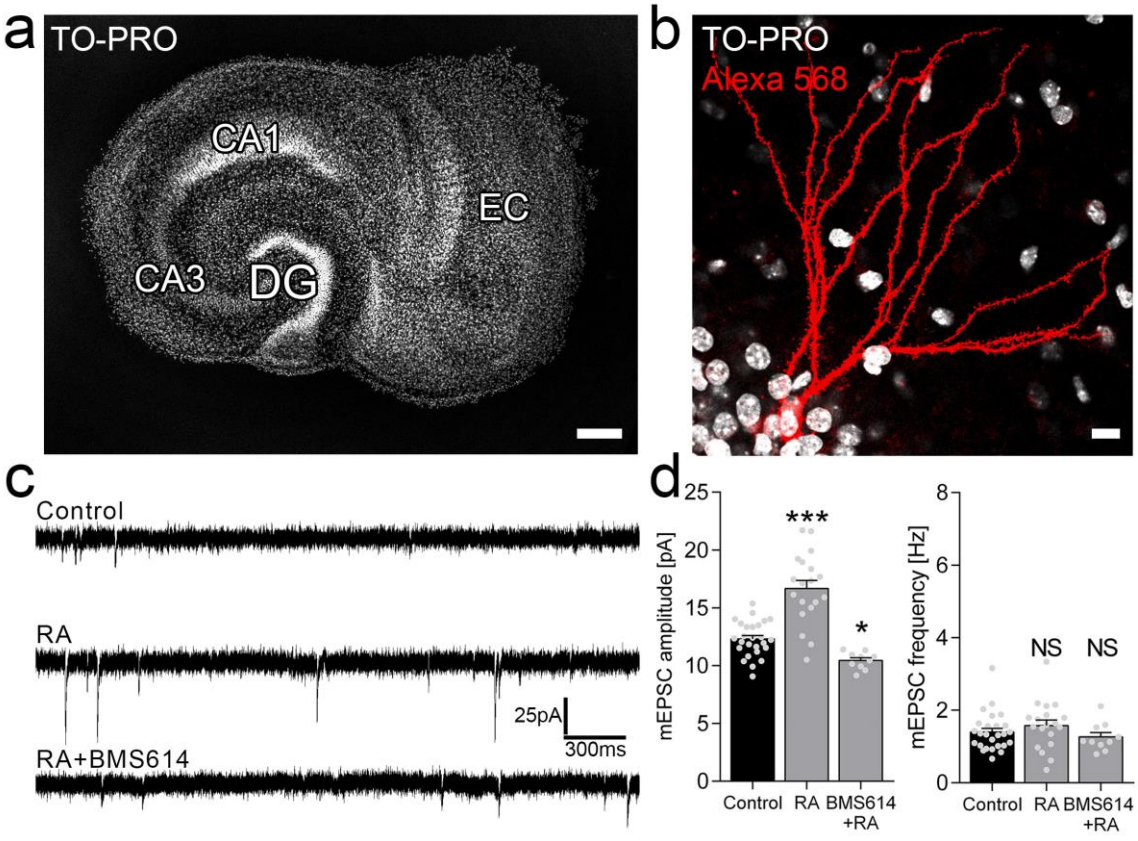

Figure 23. Prolonged RA treatment increases synaptic strength of hippocampal dentate granule cells. (a) TO-PRO® staining of an OTC. DG = dentate gyrus, EC = entorhinal cortex, CA = Cornu Ammonis. Scale bar: 200 µm. **(b)** Alexa-568/ Biocytin-filled, strepatavidin-568 conjugate counterstained dentate granule cell (red). TO-PRO® nuclear staining (white). Scale bar: 10 µm. **(c)** Sample traces related to **(d)** amplitude and frequency analysis of mEPSC recordings from hippocampal dentate granule cells following RA treatment (1 µM; 3 d) alone and in parallel with the RARα antagonist BMS614 (2 µM) vs. an untreated control ($n_{Control} = 26$; $n_{RA} = 19$; $n_{RA+BMS614} = 10$; Values represent mean ± SEM; Mann-Whitney test; ***$p < 0.001$; *$p < 0.05$; NS = not significant).

treatment alone nor subsequently applied together with BMS614. Hence, it can be concluded that RA (1 µM; 3 d) induces an increase in excitatory synaptic strength of cultured dentate granule cells which is accompanied by an increase in SP-cluster sizes.

5.3.4 RA does not increase mEPSC amplitude in SP-deficient slice cultures

To determine whether SP is involved in RA-mediated synaptic adaptation, mEPSC recordings were repeated in three-week-old entorhino-hippocampal slice cultures prepared from SP-deficient mice (SP KO). Interestingly, RA did not significantly change mEPSC amplitudes of SP-deficient dentate granule cells ($Control_{SPKO}$: 12.38 ± 0.47 pA, n = 10; RA_{SPKO}: 13.23 ± 0.61 pA, n = 12), while a significant increase in mEPSC amplitudes was detected in age- and time-matched wildtype (WT) cultures ($Control_{WT}$: 14.36 ± 0.71 pA, n = 12; RA_{WT}: 17.72 ± 0.78 pA, n = 11; $p < 0.01$; Mann-Whitney test). No changes in mEPSC frequencies were seen in these experiments (Figure 24). Thus, SP is required for RA-dependent excitatory synaptic strengthening to occur.

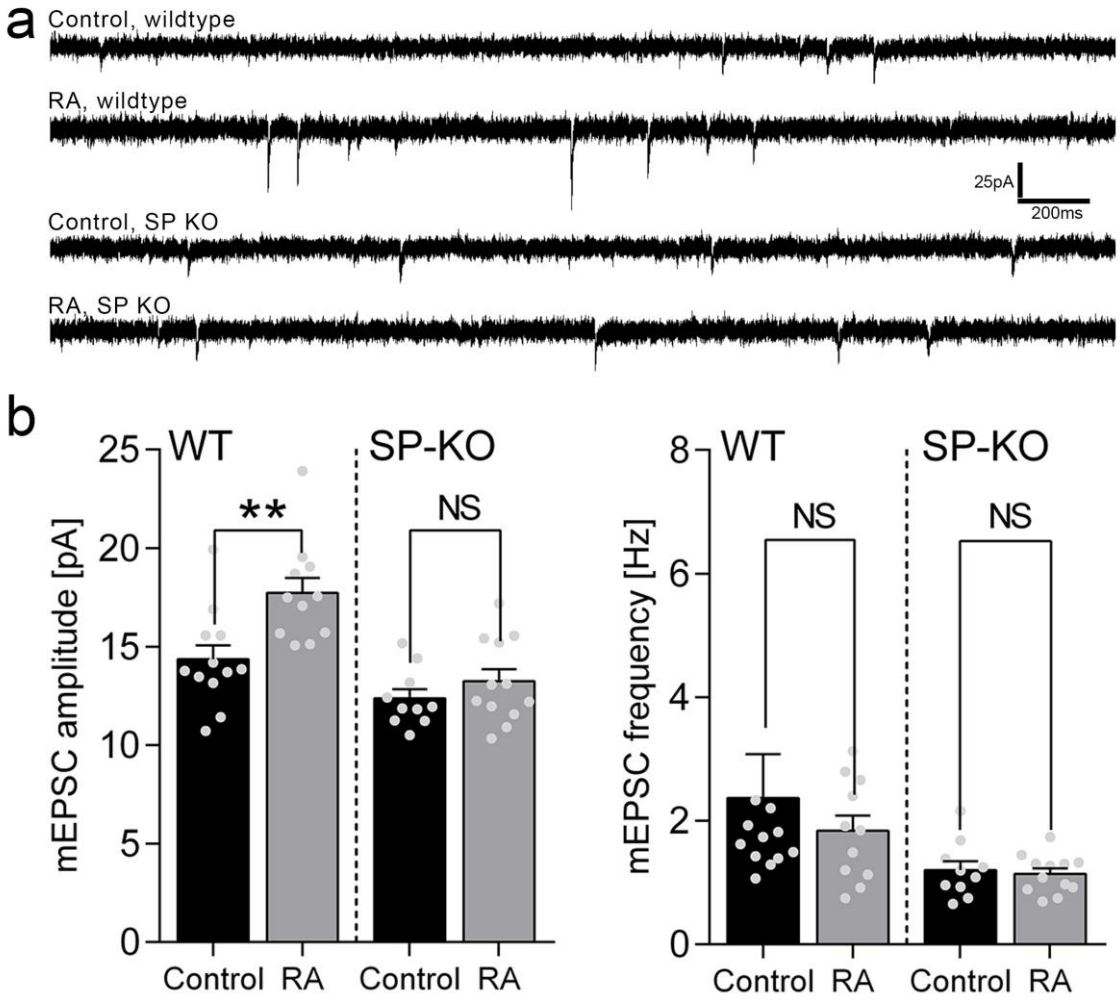

Figure 24. RA-mediated synaptic strengthening is prevented in SP-deficient cultures. (a) Sample traces related to **(b)** amplitude and frequency analysis of mEPSC recordings from hippocampal dentate granule cells following RA treatment (1 µM; 3 d) compared to untreated controls of SP KO cultures and wildtype littermates. Wildtype: $n_{Control} = 12$, $n_{RA} = 11$; SP KO: $n_{Control} = 10$, $n_{RA} = 12$; Values represent mean ± SEM; Mann-Whitney test; $^{**}p < 0.01$; NS = not significant. Individual data points are indicated by gray dots; one data point in (b) out of the axis limits.

5.3.5 Prolonged RA-mediated synaptic plasticity resembles a homeostatic mechanism

Application of TTX is a classic experimental approach to induce homeostasis (Turrigiano et al. 1998; Vlachos et al. 2013). To test whether RA-mediated effects on synaptic plasticity represent a homeostatic mechanism, in a first step cultures were treated with TTX (2 µM) for three days alone or in presence of the RARα antagonist BMS614 (2 µM). Indeed, prolonged activity blockade induced homeostatic synaptic scaling, which was prevented by the RARα antagonist BMS614 (Figure 25a+b; Control = 9.722 ± 0.66 pA, n = 10; TTX = 17.91 ± 1.51 pA, n = 8; TTX + BMS614 = 11.89 ± 0.70 pA, n = 11). Surprisingly, also the frequencies were increased during TTX-treatments, however only significant when RARα was blocked by BMS614 (Control = 1.38 ± 0.41 Hz, n = 10; TTX = 3.89 ± 2.02 Hz, n = 8; TTX + BMS614 = 3.301 ± 0.84 Hz, n = 11; Figure 25a+b).

Blockade of N-methyl D aspartate receptor channels (NMDARs) induces homeostatic synaptic plasticity that depends on local protein synthesis (Sutton et al. 2006). In contrast, inhibition of NMDARs is expected to prevent the expression of associative plasticity. In order to further elucidate the nature of RA-dependent synaptic strengthening, NMDARs were blocked with APV during RA treatment.

In presence of RA (1 µM) and APV (50 µM), excitatory synapses are strengthened, as indicated by a significant increase of mEPSC amplitudes (Control = 11.01 ± 0.54 pA, n = 7; RA = 13.56 ± 0.68 pA, n = 5; RA + APV = 14.98 ± 1.05 pA, n = 9; Figure 25c+d). Frequencies were not significantly altered, neither by RA treatment alone nor in parallel with APV (Control = 2.03 ± 0.12 Hz, n = 7; RA = 1.38 ± 0.13 Hz, n = 5; RA + APV = 2.28 ± 0.30 Hz, n = 9; Figure 25c+d). Thus, RA- and APV-induced effects on post-synaptic excitability are rather homeostatic and not associative in OTCs.

Taken together, these results suggest that synaptic modifications induced by three days of RA treatment in dentate granule cells resemble a homeostatic mechanism. The observation that blockade of RARα prevents TTX-induced homeostatic synaptic scaling further supports an endogenous source of RA in

OTC preparations. Also, these experiments substantiate the overall understanding that RA is a key player for the expression of homeostatic synaptic plasticity.

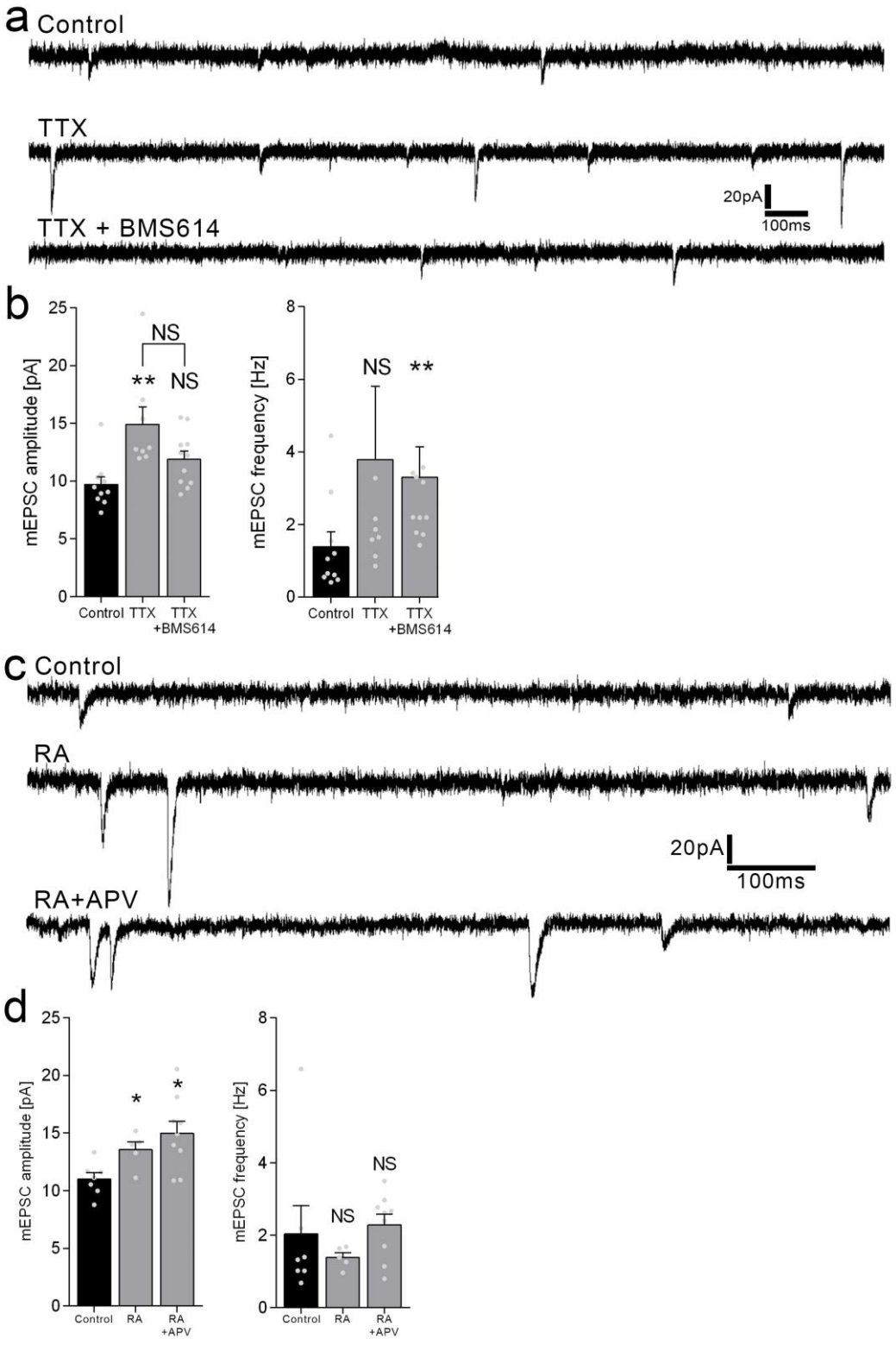

Figure 25. RA-dependent synaptc plasticity represents a homeostatic mechanism. (a+b) TTX-induced homeostatic synaptic plasticity of dentate granule cells is prevented by blockade of RARα with BMS614. mEPSC recordings from wildtype cultures, either untreated (control), treated with TTX (2 µM) alone or together with BMS614 (2 µM, 3 d). **(a)** Sample traces related to **(b)** amplitude and frequency analysis of mEPSC recordings. Control, n = 10; TTX, n = 8; TTX + BMS614, n = 11; values represent mean ± SEM; Mann-Whitney test. (c+d) RA-induced synaptic strengthening is occluded by simultaneous treatment with APV (50 µM). mEPSC recordings from wildtype cultures, either untreated (control), treated with RA (1 µM; 3 d) alone or together with APV (50 µM; 3 d). **(c)** Sample traces related to **(d)** amplitude and frequency analysis of mEPSC recordings. Control, n = 7; RA, n = 5; RA + APV, n = 9; Values represent mean ± SEM; Mann-Whitney test. *p < 0.05; **p < 0.01. NS = not significant. Individual data points are indicated by gray dots; two data points in (b) out of the axis limits.

5.3.6 GluA2-lacking AMPARs mediate RA-dependent synaptic strengthening

Because (i) local protein synthesis of GluA1 favors the insertion of calcium-permeable AMPARs (Sutton et al. 2006), (ii) RA mediates local protein synthesis of GluA1 (Poon & Chen 2008; Aoto et al. 2008), and (iii) SP has been linked to GluA1-dependent synaptic plasticity (Vlachos et al. 2009), it was hypothesized that the RA-induced, SP-dependent increase in mEPSC amplitudes may depend on the insertion of GluA2-lacking calcium-permeable AMPARs. Indeed, blockade of GluA2-lacking AMPARs with the polyamine N-acetyl spermine (NASPM, 100 µM) during mEPSC recordings masked increased mEPSC amplitude in wildtype cultures, while having no apparent effect in SP KO (WT: Control = 12.07 ± 0.50 pA, n = 7; RA = 11.09 ± 0.62 pA, n = 11; SP KO: Control = 11.79 ± 0.69 pA, n =11; RA = 10.56 ± 2.39 pA, n = 9; Figure 26). Frequencies were not significantly altered during these experiments (WT: Control = 2.48 ± 0.59 Hz, n = 7; RA = 1.48 ± 0.22 Hz, n = 11; SP KO: Control = 2.10 ± 0.28 Hz, n =11; RA = 1.65 ± 0.26 Hz, n = 9; Figure 26). These data support the notion that RA-mediated synaptic adaptations require SP and are mainly caused by regulation of postsynaptic GluA1 AMAPR subunits.

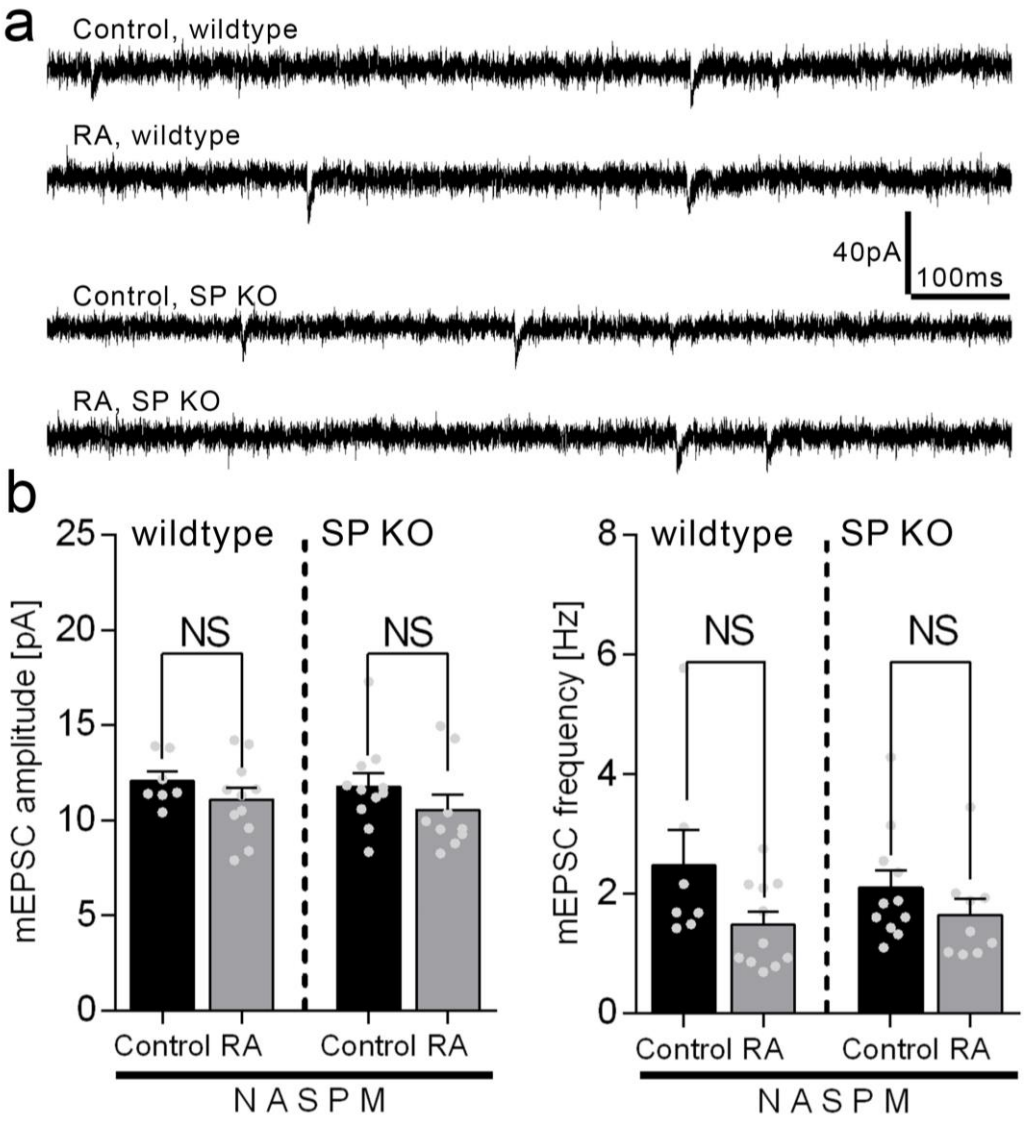

Figure 26. RA-induced synaptic strengthening is crucially dependent on GluA2-lacking AMPA receptors. (a+b) mEPSC recordings from wildtype (WT) and SP KO entorhino-hippocampal organotypic slice cultures, either untreated (control) or treated with RA (1 µM, 3 d), recorded in the presence of 1-Naphthyl acetyl spermine trihydrochloride (NASPM, 100 µM) in order to block GluA2-lacking AMPA receptors. **(a)** Sample traces related to **(b)** amplitude and frequency analysis of mEPSC recordings. Wildtype: $n_{Control}$ = 7; n_{RA} = 11; SP KO: $n_{Control}$ = 11, n_{RA} = 9; Values represent mean ± SEM; Kruskal-Wallis test, NS = not significant. Individual data points are indicated by gray dots.

5.3.7 RA-mediated effects on SP-clusters and synaptic strength are protein synthesis-dependent

Previous work has shown that the effect of RA on synaptic strength is protein synthesis-dependent (Aoto et al. 2008). Based on the experiments described above, it appeared likely that the RA-mediated effects on mEPSCs

and SP might also depend on mRNA translation. Therefore, mEPSC recordings were conducted in slice cultures challenged with the protein synthesis blocker anisomycin (10 µM) during prolonged RA treatment (1 µM, 3 d). Indeed, in the presence of anisomycin, RA had no apparent effect on mEPSC amplitude or frequency (Control = 10.62 ± 0.42 pA; RA + anisomycin = 10.59 ± 0.40 pA; n = 11 per group; Figure 27b+c). As expected, RA increased mEPSC amplitudes significantly in experiments conducted in parallel without anisomycin (Control = 10.62 ± 0.42 pA; RA = 15.63 ± 0.68 pA; n = 11 per group). Notably, anisomycin *per se* did not affect synaptic transmission (anisomycin = 10.94 ± 0.59 pA, n = 11; Figure 27b+c).

Similar effects were observed in the context of RA-mediated changes in SP. Anisomycin prevented the RA-mediated increase in SP-cluster size in the OML (Figure 27d). Interestingly, SP-cluster numbers are reduced when challenged with anisomycin alone and in the presence of RA (Figure 27d). This clearly shows that protein synthesis is necessary for effects on SP and synaptic strength induced by three days of RA treatment (Maghsoodi et al. 2008; Poon & Chen 2008; Arendt et al. 2015b).

To ensure that prolonged inhibition of protein synthesis does not affect cell viability PI stainings following three days of anisomycin (10 µM) treatment were performed. No differences between control- and anisomycin-treated groups were detected, hence confirming that protein synthesis blockade does not affect cell viability or induced cell death, which could trivially explain the obtained findings (Figure 27e).

Taken together, these results demonstrate that synaptic modifications triggered by prolonged RA treatment depend on protein synthesis and are thus consistent with the previously proposed role of RA/RARα in mediating local protein synthesis. It is therefore conceivable that SP-mRNA translation is also regulated in an RA-dependent manner.

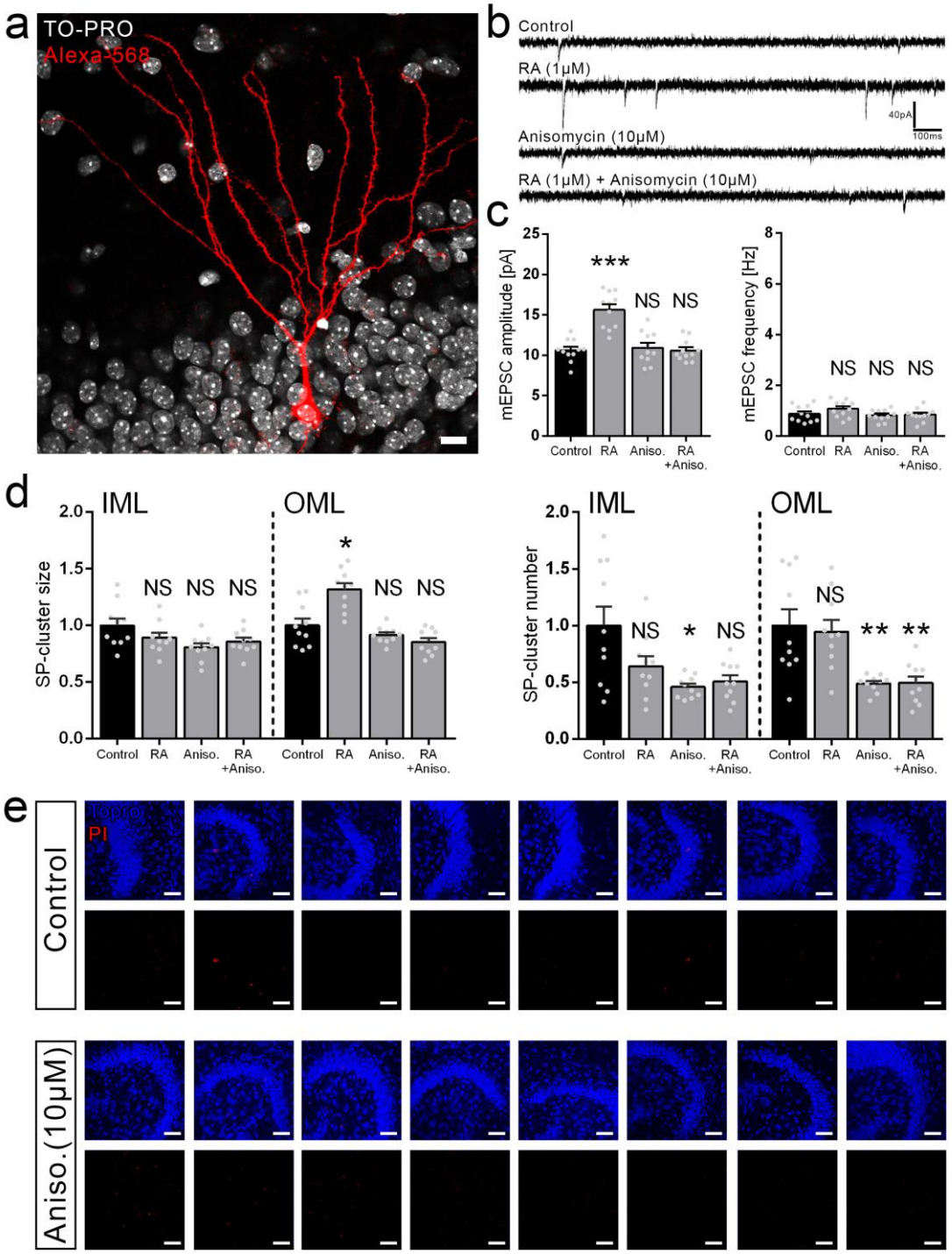

Figure 27. Blockade of protein synthesis prevents the RA-induced synaptic strengthening and the increase of SP-clusters. (a) Alexa-568/ Biocytin-filled, strepatavidin-568 conjugate counterstained dentate granule cell (red). TO-PRO® nuclear staining (white) Scale bar: 10 µm. **(b)** Sample traces related to **(c)** amplitude and frequency analysis of mEPSC recordings from OTCs treated with RA (1 µM) and/ or anisomycin (10 µM) for 3 d. n = 11 cells per group; Values represent mean ± SEM; Mann-Whitney test. **(d)** Analysis of SP-cluster sizes and number within the inner- and outer molecular layer (IML/ OML) of the DG from OTCs treated with RA (1 µM) and/ or anisomycin (10 µM) for 3 days. **(e)** Propidium iodide staining (red) following anisomycin treatment (10 µM; 3 d) compared to untreated controls. TO-PRO® nuclear stain (blue). Scale bar: 50 µm. *p < 0.05, **p < 0.01, ***p < 0.001; NS = not significant. Individual data points are indicated by gray dots.

5.3.8 Lack of SP-3'UTR prevents increase of mEPSCs upon prolonged RA treatment

Modifications of synaptic strength mediated by RA have been shown to depend on the regulation of mRNA-translation via the RA-receptor RARα. A region at the C-terminus of RARα, the so called F-domain, equips RARα with the ability to target and silence specific mRNAs (Poon & Chen 2008). Poon and Chen (2008) identified two groups of RARα binding sequences (motifs 1 and 2) within the 5'UTR of GluA1, GluA2, and eukaryotic elongation factor 2 (eEF2) that share a specific sequence homology (Table 26; illustrated in Figure 28a). It appears that presence of both sequence motifs is required for a binding of RARα to its target mRNA (Poon & Chen 2008).

Motif1:	Motif2:
1 **CA** | AA | **TC**	1 **GG** | A | **G** | A | **G**
2 **CA** | AC | **TC**	2 **GG** | A | **G** | G | **G**
3 **CA** | AT | **TC**	3 **GG** | A | **G** | C | **G**
4 **CA** | CA | **TC**	4 **GG** | A | **G** | T | **G**
5 **CA** | CC | **TC**	5 **GG** | C | **G** | A | **G**
6 **CA** | CT | **TC**	6 **GG** | C | **G** | G | **G**
7 **CA** | GA | **TC**	7 **GG** | C | **G** | C | **G**
8 **CA** | GC | **TC**	8 **GG** | C | **G** | T | **G**
9 **CA** | GT | **TC**	9 **GG** | G | **G** | A | **G**
	10 **GG** | G | **G** | G | **G**
	11 **GG** | G | **G** | C | **G**
	12 **GG** | G | **G** | T | **G**
	13 **GG** | T | **G** | A | **G**
	14 **GG** | T | **G** | G | **G**
	15 **GG** | T | **G** | C | **G**
	16 **GG** | T | **G** | T | **G**

Table 26. Possible nucleotide composition for motif 1 and 2. As published by Poon and Chen (2008) two groups of RARα binding motifs have been identified which share a specific sequence homology. Conserved nucleotides are shown in bold letters.

Hence, the murine SP-mRNA sequence (accession number NM_001109975.1) was screened for the published RARα binding motifs (Table 26). Indeed, several of such motifs within the mRNA of SP were found (for a detailed overview, see Table 27). Interestingly, the great majority of these motifs was localized to the 3'UTR of SP-mRNA (5'UTR: 8; CDS: 13; 3'UTR: 24 motifs) (summarized in Figure 28b). Therefore it appeared likely that a potential interaction between RARα protein and SP-mRNA exists.

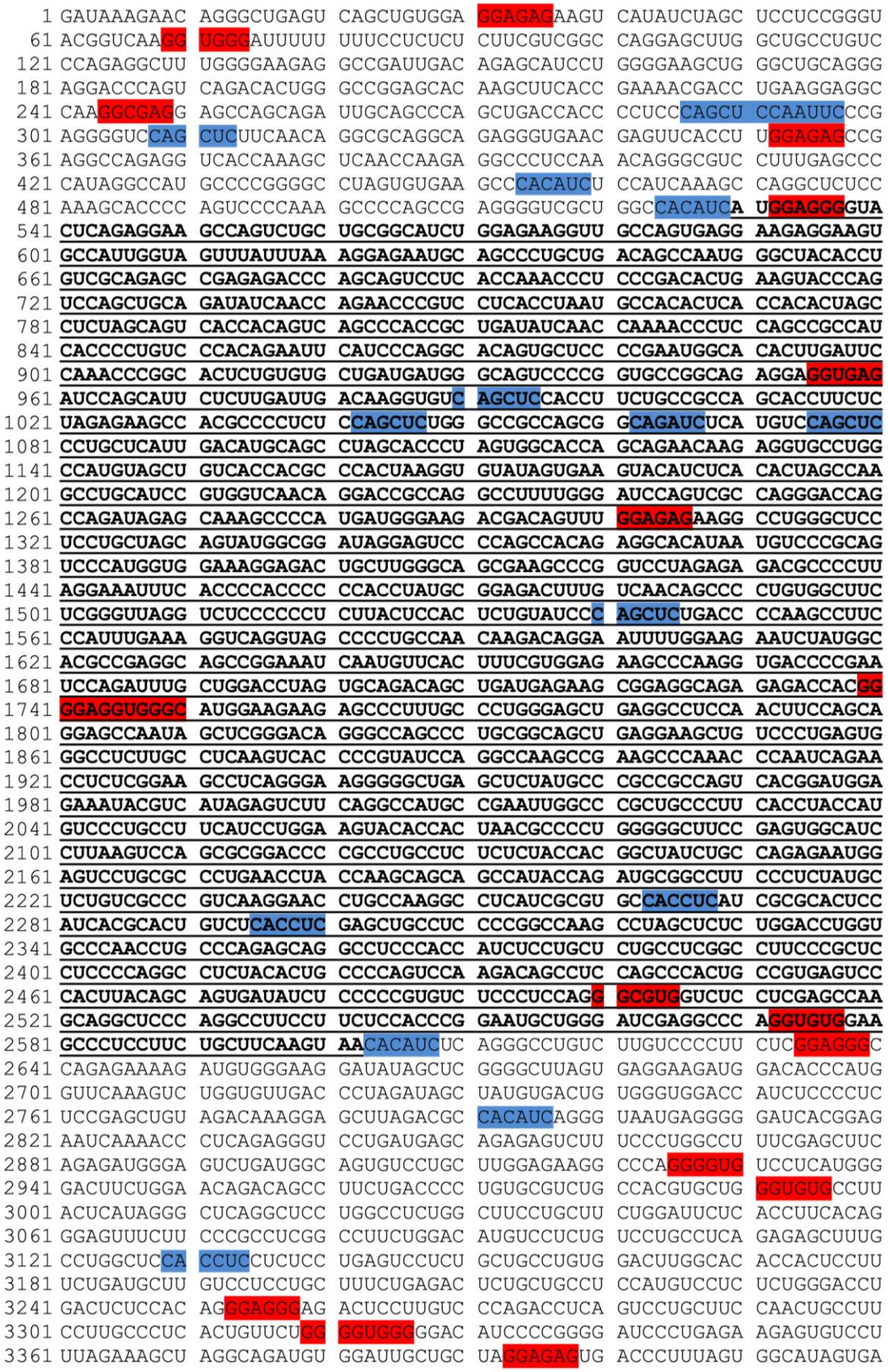

3421 CCUCAGACAA GAACUCCCUG GUUGAAAGAA GCCACCUCGA UGCAAAGGCU CAAGGUCCAG
3481 GGAGAGACAA CAGAGGAGUG UCCAAGACUU GCCCACACCU CCUCCCAUUU GCUGGGGGAG
3541 CUUUGGCCAA UUCACUCCUU UCUAGGUCUU AGUUUUCCCA UGUACACAGG GUCCUCUAGU
3601 UGUGAAAAUC ACUCAAGAUU GAGAGAACAG GCUGGCAUAG UGGGAUAAAG GGCCCAAAAG
3661 CAAGGAGACU GUCGUAUAGA AAGAAAGUGG ACAGGAUGCU ACUGAGGGAC AGAGAAGUUA
3721 GCUUUUCUUG AGAGCGGCCU GGGGUGGUUG GGUUGGAAGA AGCUGCUGCA GCGGCUAUAG
3781 UCAGAAGCCC CGGUUGGGCC AGCUUAAGCU UGGGACCCGC UGGUGACAGU GGCUCAGAAG
3841 AGGGACAGAA AAGCCUUGGA CUUAGAUCUG GGUUCUAACA GACUGAAUGU GCACCUUGGG
3901 UCUCAGACUC AGUUUCCCCG UUCAUACAUA CAGGGAGUAU GAAGUCAGGU AGCCUAAGAU
3961 CUCCCACUCC CUGCCUCCCU UUGACGUGGU ACAGCCACCC CCACCCACCC CGCCCCCGAA
4021 CUAGCCUUUU UGGGGGAGUG AGAAUACAGA UACAAGAAGA CAGACACAUU UAGAUGGAAU
4081 CUUACCACGA CUUGAGGCUA GGACCACCCA CUUCCUCUUU CCCAGCCCUA UUUCUGGGAU
4141 CCCAGAGGGG CAGGGGUGGU GGAGGCGGUG CCGGGACUUG GCUGAGUGCA GUUUGAGCUC
4201 UAGGCUUGUC UCCAUGGGAA CAGGAGGGGU GCCUUGUCAG CAAGCUCAUC CGCACAGAAG
4261 AGGGAAGAGG GAGAUGCGUG GGGAAACUGA GUGAGUCGGA UUCCUCCAGG CCAGGUCUUC
4321 CCAGAACAGA GUCAGCCUCU AGUAGACCCU GCUCUUUUGC CCCUGGGGCG GGGAGGGUUG
4381 GCAGUGGUGG GGCCCAUCCU CUAUCCUGUA GCUCCUGCCG CUGCGAGGCU GAACUCUUUG
4441 GUCCUGCCUC CCGUUCUCAA UACACUCUGU CUCAAAUCUA AAAAAAAAAA AAAAAA

Table 27. mRNA sequence of murine SP. SP-mRNA **(**NM_001109975.1) was screened for the nucleotide combinations of RARα-binding motifs 1 and 2 as published by Poon & Chen (2008). Motif 1 is highlighted in blue, motif 2 is highlighted in red. Coding sequence is underlined and displayed with bold letters.

To address the role of SP-3'UTR in transducing RA-mediated effects on synaptic strength, the tg(Thy1-GFP/SP) x SP KO mouse line was used (Vlachos et al. 2013). Since tg(Thy1-GFP/SP) x SP KO mice are generated on a SP KO background, they lack endogenous SP but instead express a genetically modified GFP-tagged version of SP lacking the 3'UTR (Figure 28c+d). Thus, the question was addressed whether a potential interaction between RARα protein and a sequence motif localized within the 3'UTR of SP-mRNA is required to mediate the effects of RA on synaptic strengthening. Cultures prepared from tg(Thy1-GFP/SP) x SP KO mice were treated with RA (1 µM, 3 d) and mEPSCs were recorded. Interestingly, prolonged RA treatment did not increase excitatory synaptic strength of dentate granule cells from slice cultures lacking the SP-3'UTR, as indicated by unaltered mEPSC amplitudes (Control: 14.06 ± 0.95 pA; RA: 14.36 ± 0.88 pA; n = 10 cells per group; Figure 28e+f) and frequencies (Control: 2.55 ± 0.34 Hz; RA: 2.29 ± 0.32 Hz, n = 10 cells per group; Figure 28e+f). These data support the idea that RARα protein might interact with SP by binding to the 3'UTR of SP-mRNA.

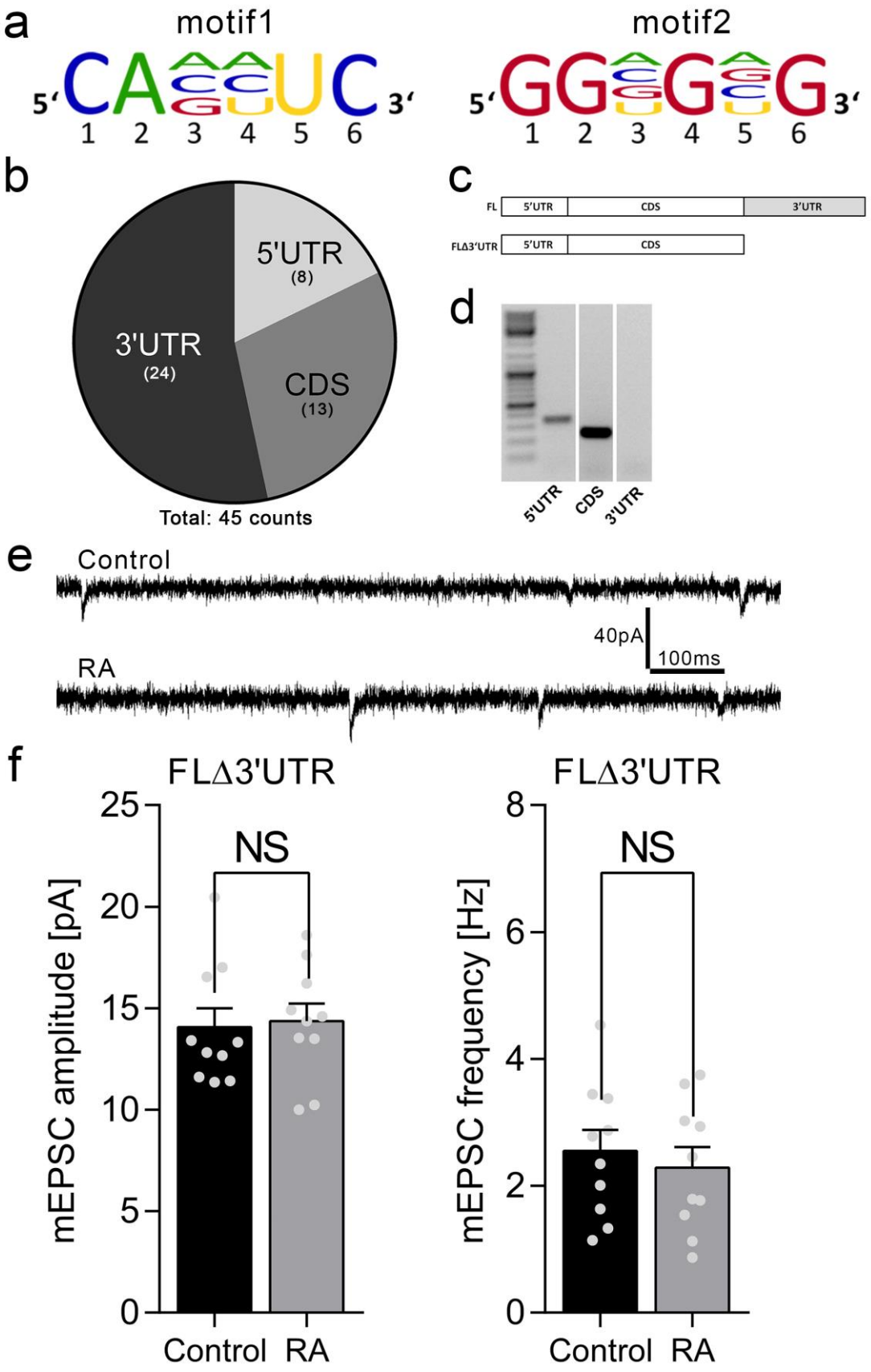
a
motif1
5'
3'
1 2 3 4 5 6
motif2
5'
3'
1 2 3 4 5 6
b
5'UTR
(8)
CDS
(13)
3'UTR
(24)
Total: 45 counts
c
FL
5'UTR
CDS
3'UTR
FLΔ3'UTR
5'UTR
CDS
d
5'UTR
CDS
3'UTR
e
Control
40pA
100ms
RA
f
FLΔ3'UTR
NS
mEPSC amplitude [pA]
25
20
15
10
5
0
Control
RA
FLΔ3'UTR
NS
mEPSC frequency [Hz]
8
6
4
2
0
Control
RA

Figure 28. Dentate granule cells lacking the SP-3'UTR do not increase synaptic strength upon three days RA treatment. (a) Sequences of RARα-binding motifs 1 and 2 as identified by Poon & Chen (2008) (see also Table 26+27). **(b)** Percentage distribution of motifs 1 and 2 within SP-mRNA as shown in Table 27. UTR = untranslated region, CDS = coding sequence. **(c)** Schematic showing the full-length (FL) mRNA sequence of SP and the truncated transcript from the tg(Thy1-GFP/SP) x SP KO-mouse line (FLΔ3'UTR) which is lacking the 3'UTR. **(d)** Verification of SP-mRNA sequence of tg(Thy1-GFP/SP) x SP KO mice using standard RT-PCR confirms that 3'UTR is missing. **(e+f)** mEPSC recordings from tg(Thy1-GFP/SP) x SP KO cultures expressing the truncated SP-mRNA (FLΔ3'UTR), either untreated (control) or treated with RA (1 µM, 3 d). **(e)** Sample traces related to **(f)** amplitude and frequency analysis of mEPSC recordings. n = 10 cells per group; Values represent mean ± SEM; Mann-Whitney test; NS = not significant. Individual data points are indicated by gray dots.

5.3.9 Possible interaction of RA-receptor alpha with SP-mRNA

It has been shown that RARα transcript and RARα protein are abundant in hippocampal pyramidal cells (Krezel et al. 1999; Zetterström et al. 1999). Furthermore RARα protein not only localizes to the nucleus and soma, but also at high levels within dendrites of pyramidal cells (Poon & Chen 2008). Immunostainings performed in slice culture preparations confirmed that RARα protein is present in CA1/ CA3 regions as well as in the granule cell layer and molecular layer of the dentate gyrus (Figure 29).

To verify a direct interaction between SP-mRNA and RARα protein, a pull-down experiment was performed using RNA-immunoprecipitation (RIP) followed by standard as well as quantitative RT-PCR to detect transcripts bound by RARα protein. An input sample collected prior to RIP reaction containing a pool of all hippocampal mRNA species served as a positive control. Furthermore, the ribosomal protein SNRNP70 that is known to bind to U1snRNA was used as a positive control and to verify the RIP workflow. Antibodies against the IgG epitope served as a negative control since they should not bind to any transcript present. As expected, standard RT-PCR showed a bright signal for U1snRNA within the positive controls of the input sample and the SNRNP70 fraction, while only a weak signal appeared in the negative control and the RARα fraction. Intriguingly, a weak but visible signal was observed for SP in the RARα fraction that was similar to the input sample, while no SP transcript was detected in the negative IgG or in the SNRNP70 fraction (Figure 30a). Indeed, this result could be confirmed using quantitative RT-PCR showing a high abundance of SP-

mRNA in the RARα fraction of wildtype cultures compared to a 74 – 90% decreased signal in the negative controls of input sample and SNRNP70 fraction (Figure 30b). Surprisingly, analysis of SP-mRNA/ RARα-protein RNA-immunoprecipitation of cultures lacking the SP-3'UTR showed similar results (Figure 30b). This indicates that other bindings sites might be present upstream of the 3'UTR, which are inactive or at least not sufficient to regulate RARα-dependent SP-mRNA translation. Taken together, these results indicate that a direct interaction between SP-mRNA and RARα protein appears very likely, even though the precise localization of a RARα-binding motif within the SP-mRNA warrants further investigations.

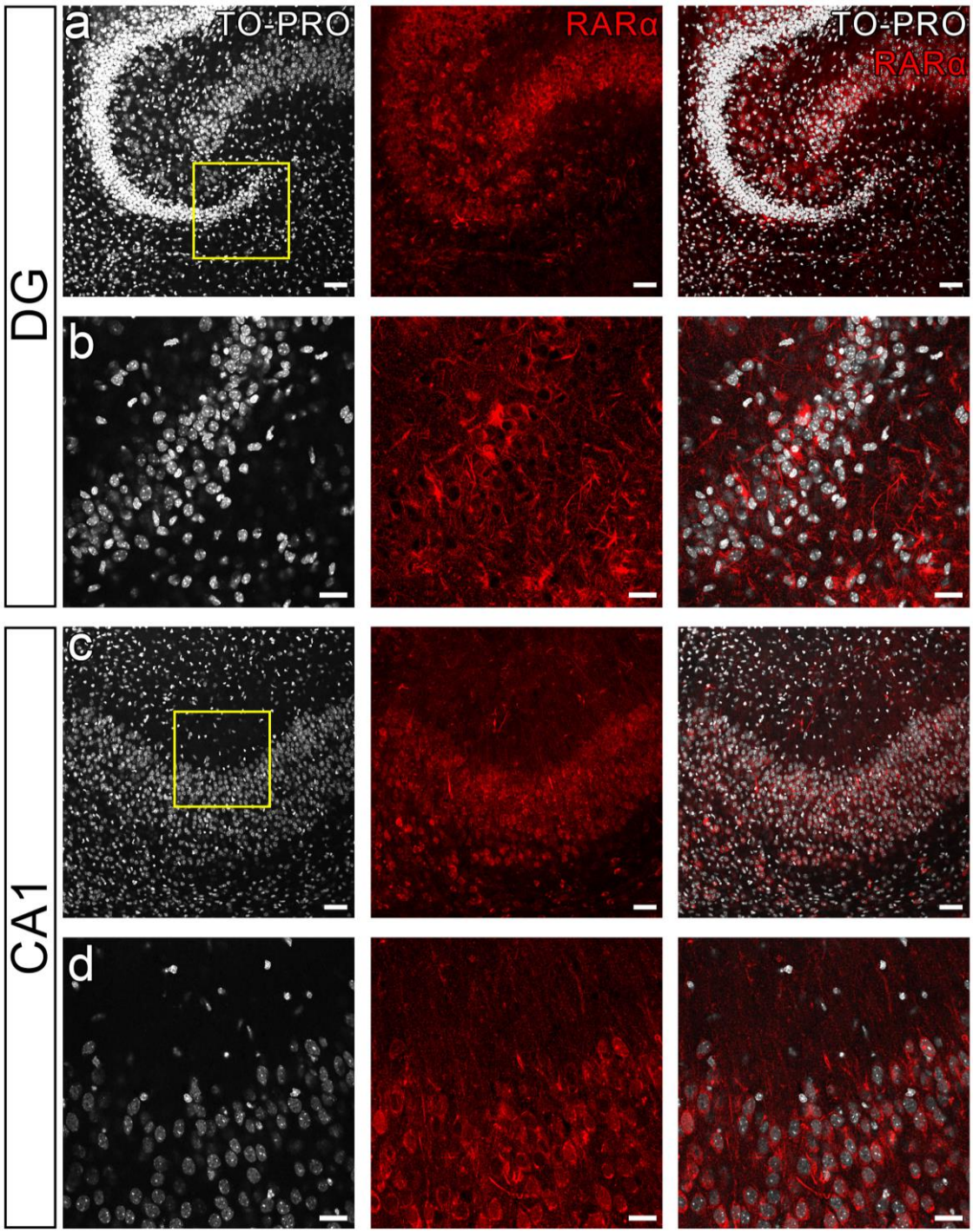

Figure 29. Immunohistochemical staining of OTCs showing the distribution of RARα in the hippocampal regions of dentate gyrus (DG) and CA1. (a+c) Overview image showing the expression of RARα (red) within the DG and CA1 region of OTCs. TO-PRO® nuclear stain in white. Regions highlighted by yellow squares are shown in higher magnification in **(b)** and **(d)**. Scale bars in 'a' and 'c': 50 µm; Scale bars in 'b' and 'd': 20 µm.

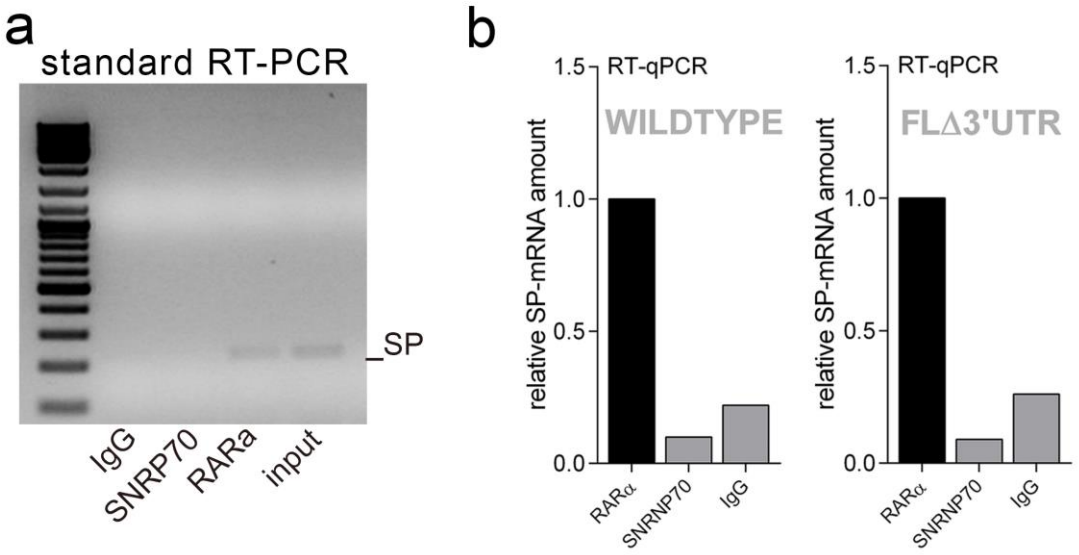

Figure 30. Retinoic acid receptor alpha (RARα) might regulate SP by binding to its mRNA. (a) Qualitative analysis using standard RT-PCR **(b)** and quantitative RT-PCR of SP-transcripts co-immunoprecipitated with IgG antibody, SNRNP70, and RARα protein. ‚Input' represents a sample containing all mRNA collected before immunoprecipitation and served as a positive control.

5.3.10 RA restores SP-mRNA levels upon LPS treatment *in vitro*

Finally, this thesis aimed at investigating RA as a possible intervention to compensate for defects in synaptic function, e.g. that were caused by inflammatory processes. Cultures were treated with LPS (1 µg/ml) and RA (1 µM) in parallel for three days and mRNA levels for TNFα and SP were analyzed. As expected LPS treatment lead to a considerable increase of TNFα-mRNA expression (18 ± 2 fold) while simultaneously causing a

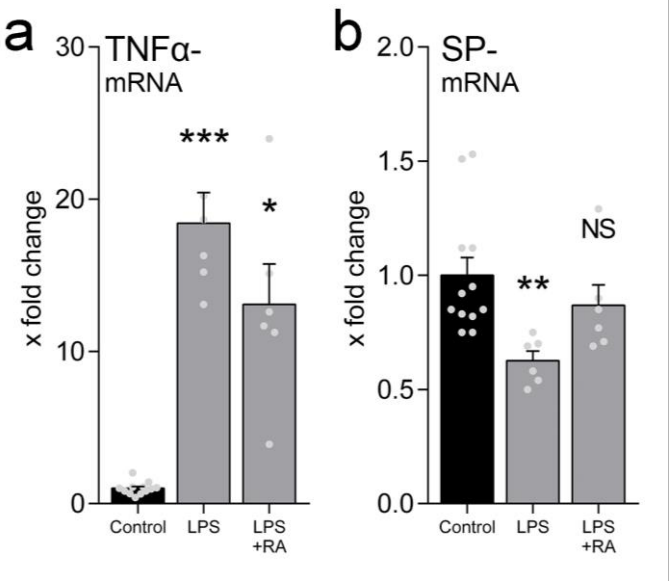

Figure 31. RA prevents downregulation of SP-mRNA expression following LPS-treatment (1 µM; 3 d). Relative quantification of **(a)** TNFα- and **(b)** SP-mRNA expression normalized to GAPDH ($n_{Control}$ = 12, n_{LPS} = 6; n_{LPS+RA} = 6; Kruskal-Wallis test; Values represent mean ± SEM; *p < 0.05; **p < 0.01).

significant reduction in SP-mRNA levels (63 ± 4%) compared to a vehicle-treated control (Figure 31a). Even though an increase in TNFα-mRNA expression is still detected after LPS in the presence of RA (13 ± 3 fold), RA prevented the LPS-induced reduction of SP-mRNA levels (87 ± 9%) (Figure 31b). These data suggest that RA could serve as a potential approach to restore synaptic function upon neuroinflammation by compensating for reduced SP-mRNA levels. However, since SP-mRNA levels are changed, it appears to be a different mechanism that is not necessarily related to RA-mediated protein synthesis.

6. Discussion

6.2 Role of SP in neuroinflammation

The first part of this thesis addresses the question how neuroinflammation affects the ability of hippocampal CA1 pyramidal neurons to express synaptic plasticity *in vivo* (classic electric/tetanic-LTP) and aimed at elucidating the neuronal targets through which pro-inflammatory cytokines elicit their detrimental effects on synaptic plasticity. Studying the effects of systemic inflammation, this thesis shows for the first time that systemically applied LPS reduces SP-mRNA levels as well as SP-protein in the brain, which is accompanied by alterations in LTP. The established *in vitro* LPS model disclosed that TNFα plays a crucial role in mediating inflammation-caused defects on synaptic neurotransmission and SP expression, since lack of TNFα restores synaptic plasticity and SP expression under conditions of neuroinflammation. SP could be identified as an important neuronal target through which TNFα asserts its negative effects on brain function under inflammatory conditions.

6.2.1 Role of SP and TNFα in LPS-induced effects of synaptic plasticity

Numerous inflammatory mediators, mainly cytokines are released during inflammation and affect synaptic function (Vereker 2000; for reviews see Allan & Rothwell 2001; Dantzer et al. 2008; Filippo et al. 2008; Trotta et al. 2014; Yang & Chen 2008). The investigation of the mechanisms through which these factors affect neural function is challenging, mainly because inflammatory signaling cascades can have various and also opposing effects (Sriram & O'Callaghan 2007). For example, basal release of TNFα from glial cells has been shown to be necessary to regulate synaptic scaling and to influence homeostatic synaptic plasticity (Beattie 2002; Stellwagen & Malenka 2006; Steinmetz & Turrigiano 2010; Becker et al. 2013; Pribiag & Stellwagen 2013; for a recent review on TNFα, see Santello & Volterra 2012), while excess release of TNFα within brain tissue has been shown to have pathogenic effects (Wang

et al. 2002; Mehta et al. 2016). Furthermore, besides its role in homeostatic synaptic plasticity TNFα has been shown to be involved in associative forms of synaptic plasticity (Butler et al. 2004; Cunningham et al. 1996).

Interestingly, SP has also been shown to be involved in mediating associative and homeostatic synaptic plasticity (Vlachos 2012). SP is crucial for the induction of LTP (Deller et al. 2003; Jedlicka et al. 2009; Vlachos et al. 2009; Yamazaki et al. 2001; Zhang et al. 2013) and LTD (Holbro et al. 2009). While these studies correlate SP-function with associative synaptic plasticity, Vlachos et al. (2013) suggested a role for SP also in homeostatic synaptic plasticity.

It has been further suggested that elevated TNFα levels increase the expression and incorporation of NMDARs and AMPARs to synapses while simultaneously decreasing $GABA_A$ receptor expression, resulting in a net increase of the excitation/ inhibition ratio in a model of acute neuroinflammation (Stellwagen et al. 2005; also reviewed by Olmos & Lladó 2014). The results, however, do not provide any evidence that LPS-triggered upregulation of TNFα affects synaptic neurotransmission since mEPSC amplitudes remain unaltered upon LPS treatment under baseline conditions. The release of inflammatory mediators can in turn act on astrocytes to induce secondary inflammatory actions (Saijo et al. 2009). This is remarkable since astrocytes are largely involved in Ca^{2+} homeostasis under baseline and conditions of activity (reviewed in detail by Volterra et al. 2014).

Furthermore, this thesis discloses that downstream of TNFα production, the TNF receptors TNFR1/2 are necessary for mediating the inflammatory effects on SP expression. However, follow-up experiments are necessary to provide a precise description as to whether and how the complex TNFα-signaling cascade (as described previously; Figure 4) interferes with synaptic plasticity.

6.2.2 Role of SP in LPS-induced effects of synaptic plasticity

Within the hippocampus, SP is distributed in a lamina-specific fashion (Bas Orth et al. 2005) and it has been shown that SP is regulated in an activity-

dependent manner (Okubo-Suzuki et al. 2008; Vlachos et al. 2013; Vlachos et al. 2009; Yamazaki et al. 2001). For example, an increase of SP-mRNA and protein levels have been reported upon the induction of LTP (Fukazawa et al. 2003; Yamazaki et al. 2001). Since changes in SP-protein have been reported in absence of SP-mRNA changes, it is plausible that SP might be regulated both, on the (post-) transcriptional as well as (post-) translational level. Since SP-cluster size was not reduced in all layers of the hippocampal formation equally, it is plausible to assume that global factors (acting on the mRNA level) and local factors regulating protein translation or protein assembly may act together to control SP abundance under inflammatory conditions.

6.2.3 LPS acts directly on neural tissue to affect plasticity

Under physiological conditions, the blood brain barrier (BBB) is a tight barrier for peripheral molecules, and evidence has been provided that only very limited amounts of systemically applied LPS are able to cross the BBB (Banks & Robinson 2010). However, under conditions of neuroinflammation the BBB breaks down and its permeability is markedly increased (Erickson & Banks 2011). It is therefore possible that LPS exerts its effects on SP and synaptic plasticity directly. *In vitro* experiments performed in organotypic entorhino-hippocampal slice preparations support this idea (Figure 15). It has been shown that LPS binds to the transmembrane TLR4. Interactions with TLR4 trigger the production of pro-inflammatory cytokines in microglia by regulating gene expression (for reviews, see Rathinam & Fitzgerald 2013; Trotta et al. 2014). Quantitative RT-PCR results of this thesis confirm that LPS indeed increases mRNA levels of TNFα in the hippocampus. It has also been suggested that breakdown of the BBB and rupture of brain endothelial cells leads to activation and entrance of coagulation factors to the brain tissue, thereby affecting synaptic plasticity (Shikamoto & Morita 1999; Gingrich et al. 2000; Maggio et al. 2013). Particularly thrombin has been shown to impair the ability of neurons to adapt their synaptic strength upon activation by saturating NMDAR-dependent synaptic plasticity mechanisms via the activation of protease activated receptor

PAR1 (Maggio et al. 2013). It has further been reported that thrombin facilitates inflammation (Esmon 2013). To which extent blood components like thrombin are involved in modulating inflammation-caused effects on synaptic function remains to be further investigated. The LPS *in vitro* model established in this thesis appears as an optimal means to address this question, since the BBB is absent in organotypic preparations. Hence, peripheral molecules can be applied directly to study its effects on brain tissue structure and function. Independently of these considerations, the data reveal that LPS applied *in vitro* is sufficient to modulate SP-distribution and synaptic plasticity in a similar extent than *in vivo* – even layer specificity is preserved.

6.2.4 Role of inflammation-induced cell death

Numerous studies show that inflammation leads to tissue damage and cell death. The destructive property of inflammation is caused by various molecules and pathways: complement proteins (Kalfayan & Kidd 1952), cationic proteins (Clark & Klebanoff 1975), cytokines (Carswell et al. 1975; Laster et al. 1988), or reactive oxygen species (Badwey & Karnovsky 1980; Carson et al. 2006; reviewed in detail by Wallach et al. 2014). Especially members of two cytokine families promote inflammation induced cell death: the TNF family and the interferons (Wallach et al. 1999). The results of this study however provide evidence that conditions of prolonged LPS exposure do not lead to cell degeneration or death in OTCs. This does not exclude the possibility that peripheral stimuli e.g. triggered by activation of distinct cells of the immune system e.g. lymphocytes which are absent in slice preparations, might be involved in triggering cell detrimental actions. However, it seems rather unlikely that LPS directly causes cell death since LPS (1 µg/ml) did not show any apparent increase of PI fluorescence (Figure 16). Finally, it is conceivable that activation of pathways promoting cell survival act in parallel with neuroinflammation to prevent cell death.

6.2.5 Source of LPS-induced TNFα in OTCs

What is the source of TNFα? Inflammation of brain tissue is generally accompanied by the activation of glial cells (Perry & Teeling 2013) and the production of inflammatory mediators such as eicosanoids, acute-phase proteins, complements and cytokines (Barone & Feuerstein 1999; Allan & Rothwell 2001). In particular microglial cells contribute to the production of reactive oxygen species, nitrogen, TNFα, and glutamate, which are neurotoxic when released at high concentrations (Qian et al. 2007; Gordon et al. 2012; also reviewed by González et al. 2014). Immunohistochemical data obtained from tg(TNF-GFP) mice disclose that TNFα released upon LPS-induced neuroinflammation is produced primarily by microglial cells. Within the brain of mice, Toll-like receptor 4 (TLR4) – the receptor that binds and mediates the downstream effects of LPS, e.g. the production of TNFα – is exclusively expressed by microglial cells (Vaure & Liu 2014). This further corroborates the finding that microglia are the major source of TNFα expression and that the increase of TNFα might be regulated by TLR4.

6.2.6 Role of microglia in LPS-induced effects on synapse function

Unfortunately further validation of the contribution of microglia to the regulation of SP expression during neuroinflammation by pharmacologically eliminating microglia using liposome-encapsulated clodronic acid turned out to be technical challenging (Figure 19): First, the observation that empty liposomes affect the regulation of SP-mRNA expression upon LPS treatment makes it difficult to interpret the obtained results, especially since TNFα-expression was as expected in these experiments, i.e. there was an upregulation of TNFα-mRNA by LPS in presence of empty liposome and no LPS-effect on TNFα-mRNA in the presence of clodronic acid. Second, clodronic acid itself and/ or the elimination of microglia seem to have a downregulating effect on SP-mRNA expression under baseline conditions. Besides clodronic acid, other approaches might turn out to be successful. The colony-stimulating factor 1 receptor (CSF1R) for instance is essential to maintain the viability of

microglia, which can be blocked by PLX3397, leading to an almost complete elimination of microglia from brain tissue (Dagher et al. 2015). Taken together, with the data obtained using clodronic acid to eliminate microglia from OTCs, one can only speculate whether the presence of microglia is required to maintain physiological SP homeostasis.

6.2.7 Role of mechanisms acting on site to modulate synaptic plasticity

The presented data hold that the inflammatory cascade triggered by LPS finally meets at post-synapses regulating expression of SP, thereby affecting neural function. The observation that SP-protein expression is not regulated homogeneously across different hippocampal regions raises the intriguing possibility that local mechanisms acting on site of synaptic plasticity are involved in modulating SP turn-over (Figure 32). Thus, it is conceivable that inflammatory processes mediated by TNFα might affect local protein synthesis, which has been shown to be crucial for synaptic function (Sutton & Schuman 2006). Besides, at least so far not identified processes responsible for SP degradation or redistribution might also explain the layer-specific expression of SP under inflammatory conditions.

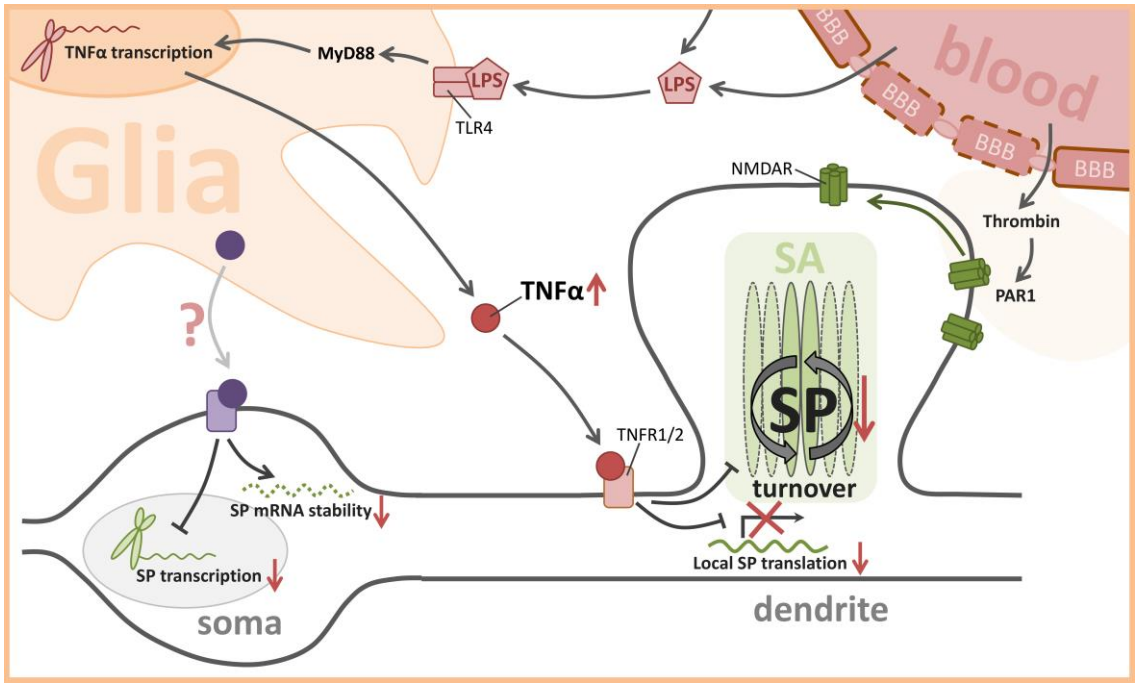

Figure 32. Suggested mechanism of LPS-induced effects on neural function. LPS exerts its effects mainly via interacting with the TLR4 which is located at cell surface of microglia. Binding to TLR4 triggers a MyD88-dependent signaling cascade that induces expression and release of TNFα and other pro-inflammatory cytokines. TNFα in turn activates a TNFR1/2-dependent pathway that is necessary for the observed lamina-specific downregulation of SP-protein. This study suggests a TNFα-dependent pathway that might affect SP-composition i.e. turn-over and/or local protein synthesis of SP at synapses. SP-mRNA has been shown to be downregulated in a global fashion upon LPS-treatment. Whether TNFR1/2 or a so far unidentified mechanism is responsible for SP-mRNA downregulation warrants further investigations. LPS-treatment also effects the vascular system. In case of systemic inflammation, the peripheral immune response leads to a permeabilization of the blood brain barrier (BBB), thereby increasing the passage for pro-inflammatory substances. Also, passage of thrombin is facilitated under inflammatory conditions, affecting NMDA receptor composition on synapses in a PAR1-dependent manner that might contribute to the observed defects in synaptic plasticity, i.e. LTP. SP = synaptopodin, SA = spine apparatus, LPS = lipopolysaccharide, TLR4 = toll-like receptor 4, TNFα = tumor necrosis factor alpha, NMDAR = NMDA receptor, TNFR1/2 = TNF receptor 1 and 2, PAR1 = protease activated receptor 1.

6.2.8 Conclusion

This thesis identifies SP as a neural target of LPS-triggered and TNFα-mediated neuroinflammation. Alterations of SP crucially affect the ability of neurons to express synaptic plasticity. This might explain why processes required for learning and memory are disturbed under pathologic conditions that involve neuroinflammation. The role of other cytokines remains to be investigated. The LPS *in vitro* model introduced in this thesis appears to be an excellent attempt especially in this regard.

6.3 Role of SP in RA-dependent synaptic plasticity

In the second part of this thesis, the role of RA in regulating SP-dependent synaptic plasticity was addressed. Prolonged RA treatment leads to an increase in excitatory synaptic strength of dentate granule cells, which depends on the presence of SP. Subsequently, this thesis demonstrates that RA increases SP-abundance at synapses *in vitro* and *in vivo*.

6.3.1 Role of RA in local protein synthesis and SP expression

Evidence has been provided that RA mediates its synaptic effects via disinhibition of mRNA translation in dendrites through its receptor RARα (e.g. (Aoto et al. 2008; Poon & Chen 2008; Chen et al. 2012) and that these actions are independent from nuclear gene regulation (Aoto et al. 2008; Maghsoodi et al. 2008). In this context, it has been shown that RARα binds to a specific sequence motif within the mRNA of GluA1, a subunit of the AMPAR channel (Poon & Chen 2008). It appeared likely that RA regulates the expression of SP in a similar fashion. Indeed, total hippocampal SP-mRNA levels remain unchanged after RA treatment, indicating that SP is regulated post transcriptional and/ or translational. Indeed, blockade of mRNA translation using anisomycin during RA treatment suggests that protein synthesis is necessary for RA-mediated effects on SP expression. In a first attempt to clarify a possible direct interaction between RARα protein and the SP-transcript, several sequence elements within the SP-mRNA have been identified which have great consensus with the RARα-binding motif Poon and Chen (2008) identified within the GluA1-mRNA (Poon & Chen 2008). RNA-immunoprecipitation (RIP) experiments revealed that SP-mRNA is associated with RARα protein (Figure 30). Interestingly, mEPSC recordings performed in tg(Thy1-GFP/SP) x SP KO cultures lacking the 3'UTR of SP-mRNA seem to confirm the relevance of SP-3'UTR in RA-mediated effects on synaptic strength, since these cultures show no alteration in mEPSC amplitude upon RA exposure. However, RIP experiments performed with tg(Thy1-GFP/SP) x SP KO cultures indicate that despite the lack of 3'UTR, SP-transcripts are co-immunoprecipitated to a similar amount than the SP full-length variant from wildtype mice. This appears somehow puzzling, but might be explained by a binding site of RARα localized within the 5'UTR or coding sequence of SP-mRNA which is not involved in or silenced during RA-mediated synaptic strengthening. This idea is in line with previous observations made by Aoto and colleagues (2008), who could demonstrate that despite an interaction of RARα with the mRNA of GluA2, regulation of mRNA translation remains unaffected (Aoto et al. 2008). However, it has to be admitted that the final evidence of a regulation of SP expression via

an interaction of RARα with the SP-3'UTR is currently missing. This might be achieved in future experiments using rescue experiments with a mouse line expressing the full-length transgene of Thy1-GFP/SP. Furthermore, post-translational modifications of RARα that fine-tune the mRNA regulation, such as phosphorylation, are plausible. Interestingly, previous studies investigating phosphorylation of RARα identified sites within the ligand-binding domain and F-domain (Rochette-Egly et al. 1997). Finally, it still cannot be excluded that the SP-3'UTR is part of another regulatory pathway affecting synaptic neurotransmission which is independent from RA – this, however, remains hypothetic at present and warrants further investigations.

6.3.2 Effects of short- vs. long-term RA treatment on synaptic plasticity

This thesis shows that RA increases excitatory synaptic strength when applied for a prolonged period of three days. Short-term treatment however, does not affect mEPSC amplitudes. This is surprising since previous data show that short-term exposure of RA (30 min to 2 hours) increases excitatory synaptic strength (Aoto et al. 2008; Arendt et al. 2015b). However, neural cell types of this study versus previous studies on RA/RARα signaling are distinct. While Aoto and colleagues (2008) investigated RA-mediated synaptic plasticity in hippocampal CA1 neurons, experiments in this study have been performed in dentate granule cells, since SP-dependent synaptic plasticity has been best studied in the dentate gyrus (Vlachos et al. 2013). The findings of this thesis suggest that RA might act through two different pathways in CA1 neurons versus dentate granule cells. While regulation of synaptic strength in CA1 neurons appears to be sensitive to short-term RA treatment (Aoto et al. 2008; Arendt et al. 2015b; long-term effects of RA need to be investigated), dentate granule cells exclusively respond to prolonged application of RA. Both mechanisms have in common that they show clear characteristics of homeostatic synaptic plasticity. Furthermore, such time-dependent differences on the ability of neurons to express homeostatic synaptic plasticity have been demonstrated previously. For example, it has been shown that rapid activity

blockade induced by TTX leads to synaptic strengthening only when NMDAR channels are blocked simultaneously, while prolonged TTX treatment induces synaptic scaling irrespective of NMDARs (Sutton & Schuman 2006).

6.3.3 Validation of RA-mediated effects using BMS614

RA-mediated regulation of synaptic strength within the hippocampus has been shown to crucially depend on RARα (Maghsoodi et al. 2008; Aoto et al. 2008; Arendt et al. 2015a/b). To verify RARα dependency of RA-effects within entorhino-hippocampal OTCs, experiments were conducted in presence of the RARα specific antagonist BMS614. Indeed, BMS614 showed to prevent both the RA-mediated increase of SP-cluster size as well as the increase in mEPSC amplitudes (Figure 21, Figure 22, Figure 23). Surprisingly, mEPSC amplitudes were significantly decreased in presence of both RA and the RARα antagonist. This indicates a potential contribution of endogenous RA to synaptic strength of hippocampal dentate granule cells under control conditions. Together, these results clearly show and verify the crucial dependency of RA-mediated effects on RARα in OTCs.

6.3.4 Role of RA in homeostatic synaptic plasticity

This thesis provides evidence that similarly to hippocampal CA1 neurons, homeostatic synaptic plasticity in dentate granule cells crucially depends on RA/ RARα-signaling. This is supported by two main findings: First, blockade of RARα prevented prolonged TTX-induced synaptic scaling. Second, an associative and NMDAR-dependent mechanism could be excluded, since synaptic scaling induced by RA is not prevented by the simultaneous blockade of NMDARs with APV.

Several studies have demonstrated that activity-dependent homeostatic synaptic scaling involves the incorporation of polyamine-sensitive GluA1 receptor subunits, while Ca^{2+}-impermeable GluA2 receptor subunits remain unchanged (Ju et al. 2004; Shepherd et al. 2006; Sutton & Schuman 2006; Thiagarajan et al. 2005). There is also evidence that acute RA treatment

increases the GluA1/GluA2 ratio (Aoto et al. 2008). mEPSC data obtained from recordings in the presence of NASPM, however, confirm that also prolonged RA treatment acts by increasing the GluA1 levels while keeping GluA2 subunits unchanged.

Besides its role in homeostatic synaptic plasticity, this thesis provides evidence that SP-dependent RARα/ RA-signaling might also be involved in changing the efficiency of neurons to perform synaptic plasticity, also referred to as metaplasticity, a term originally coined by Abraham & Bear (1996). LTP experiments performed by collaborators in Israel (Strehl et al. 2017; unpublished data) in acute hippocampal slice cultures provide initial evidence that RA may affect the ability to express LTP. This RA-mediated from of metaplasticity is not observed in SP KO mice. These data support a role for SP-dependent RA/RARα-signaling in metaplasticity.

6.3.5 Mechanism of SP-dependent and RA-induced synaptic plasticity

Regarding the control of RA-induced synaptic plasticity, the regulation of local SP expression is suggested to be important for the accumulation of AMPARs within synapses. In this scenario and in line with the general understanding of RA/RARα signaling in the field, RA disinhibits the expression of GluA1 subunits, thereby increasing the presence of GluA1 containing, calcium-permeable AMPARs in the postsynaptic membrane (Aoto et al. 2008) (Figure 33). However, the sole increase of AMPAR number within dendrites is not sufficient to potentiate synapses (Schnell et al. 2002) and additional steps are required to stabilize receptors at the post-synaptic membrane. Thus, concomitant to an increase of GluA1, RA/RARα enhances SP-mRNA expression, thereby locally strengthening the SA, which might promote the incorporation and stabilization of AMPARs at synapses (Figure 33). Indeed, due to its association with the actin-cytoskeleton and actin-modulating proteins (Mundel et al. 1997), SP has been proposed to be involved in spine motility, and AMPAR trafficking and anchoring (Wyszynski et al. 1997, 1998). Furthermore, the SA has been suggested to be involved in modulating dendritic calcium

concentrations (Fifkova et al. 1983). Interestingly, increase of calcium from internal stores within individual spines is sufficient to increase GluA1 subunits in the post-synaptic membrane (Korkotian and Segal 2007) and depends on F-actin, a component of the actin-cytoskeleton (Vlachos et al. 2009). In turn, increased calcium concentrations within spines, triggered by influx through incorporated AMPARs as well as internal stores, might provide a negative feed-back mechanism by silencing CaN activity and thus RA synthesis (Arendt et al. 2015b). Control of internal calcium stores by SP/SA might be necessary for the RA/RARα mechanism to be functional. Besides, SP/SA-dependent regulation of AMPAR accumulation might also involve the so-called post-synaptic density (PSD), a structure localized in close contact with the post-synaptic membrane (Bats et al. 2007). Interestingly, SP has been shown to be associated with the PSD , which suggests a possible mechanism through which SP might control the incorporation and stabilization of AMPARs (Mundel et al. 1997). Indeed it has been reported that the SA might be involved in regulating molecule translocation to the synaptic zone via an association to the PSD (Segal et al. 2010). Taken together, the proposed mechanism suggests that RA/RARα activity promotes SP-dependent regulation in a feedforward fashion by facilitating the expression of SP, thereby potentiating the incorporation and stabilization of AMPARs.

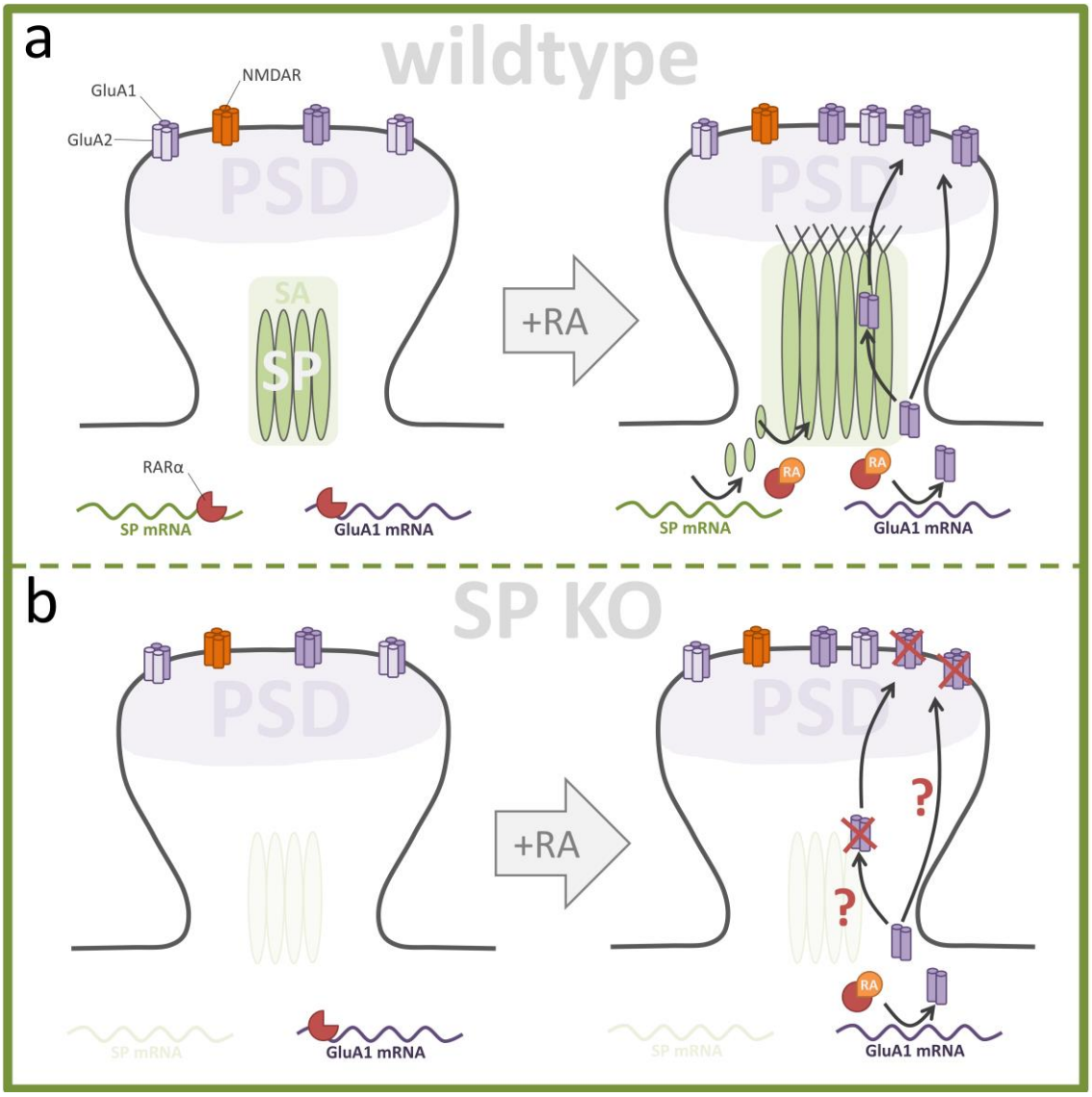

Figure 33. Suggested mechanism of SP-dependent RA/RARα signaling. (a) In absence of RA, SP- as well as GluA1-mRNA translation within dendrites are blocked by RARα. RA synthesis, which has been shown to be triggered by decreased network activity (i.e. reduced calcium concentrations), binds to and releases RARα, thereby initiating protein synthesis. SP is an essential component of the spine apparatus (SA) and has been suggested to be involved in AMPA receptor trafficking and anchoring. Furthermore, SP has been shown to interact with the post-synaptic density (PSD), which represents a possible mechanism how SP stabilizes synapses and regulates incorporation of synaptic proteins like GluA1 into synapses. **(b)** Indeed, neurons of SP-deficient mice do not perform RA-mediated synaptic strengthening. This might be explained by a failure to incorporate and stabilize AMPA receptors into the post-synaptic membrane, which in turn is suggested to depend on the SA and SP. GluA1/2 = glutamate receptor ionotropic AMPA subtype 1/2, NMDAR = NMDA receptor, SP = synaptopodin, RA = retinoic acid, RARα = retinoic acid receptor alpha.

6.3.6 Outlook and future direction

Neural function and synaptic plasticity in particular are regulated by various mechanisms involving thousands of proteins and genes that encode these proteins. RA-signaling refers to a mechanism that is important to initiate and sustain local homeostatic synaptic plasticity and this thesis denotes that SP is an elementary component of this pathway. This thesis was driven by the motivation to identify and investigate novel pathways and regulatory proteins that contribute to future clinical approaches aiming to improve impaired brain function. Intriguingly it was possible to show that inflammation-induced down-regulation of SP can be recovered by means of RA treatment. Hence, therapies involving RA might be one of several approaches to restore brain function. This investigation, however, is at its very beginning, opening key questions for establishing follow-up experiments: What are the interactions of SP within dendrites that lead to synaptic strengthening under RA treatment? Is there a role for SP in regulating turn-over of synaptic proteins like GluA1? Where within the mRNA of SP is the RARα binding element exactly located?

Altogether, this work could show that SP is both fundamentally involved in synaptic plasticity under pathological conditions induced by neuroinflammation as well as under physiological conditions by regulating and sustaining synaptic functioning by means of the RA/RARα system.

6.4 Clinical relevance of this thesis

6.4.1 Applicability of OTCs for the investigation of SP-mediated synaptic plasticity

Most experiments in this thesis have been performed using OTCs. In general, the use of organotypic tissue to study neural function is well established (Aptowicz et al. 2004; Karmarkar & Buonomano, 2006; Vlachos et al. 2013; Arendt et al. 2015b). Nevertheless, applicability of the use of OTCs has to be carefully determined. This is crucial, especially when results obtained

from OTCs are transferred to the *in vivo* situation and when a potential clinical relevance is evaluated. For example OTCs lack cortical connection (except for EC projections), endocrine, and blood supply. Indeed, quantification of SP-levels examined in brains obtained from mice injected versus OTCs treated with LPS and/or RA revealed a comparable change of SP-clusters within the hippocampus (Figure 15). Thus, since the *in vitro* results resemble the results *in vivo*, other factors seem not to play a role in affecting SP expression. Furthermore, the finding that blockade of RARα during TTX treatment blocks synaptic scaling indicates that endogenous RA is supposed to be present in OTCs (Figure 25). Taken together, this warrants the use of OTCs in assessing the effects of LPS and RA on SP-mediated synaptic plasticity.

6.4.2 Clinical relevance of the TNFα pathway

Synaptic plasticity is controlled by various functional molecules and signaling pathways. Among those molecules this thesis focuses on the cytokine TNFα and shows that increased levels of the pro-inflammatory cytokine TNFα regulate LPS-induced reduction in SP expression and impair synaptic plasticity. Other studies confirm that even though basal release of cytokines like TNFα is necessary for normal cell and tissue function, increased TNFα levels have pathogenic effects (Wang et al. 2002; Mehta et al. 2016). This raises the opportunity that BBB-permeable drugs with antagonistic effects on TNFα activity might turn out to have beneficial effects in cases of alterations in synaptic plasticity that are associated with neuroinflammation e.g. in case of stroke, brain or spinal cord injury, or Alzheimer's disease.

Interestingly, and consistent with the previous *in vivo* findings, showing that LPS impairs the ability of the hippocampal CA1 neurons to express LTP and reduces SP-clusters, this thesis provides evidence that the lack of TNFα not prevents the reduction of SP-cluster size by LPS in TNF KO cultures. This indicates that TNFα might play a crucial role in an inflammatory cascade that mediates defects in neural function and suggests that SP is linked to this pathway. It is tempting to speculate that TNFα inhibitors might improve the condition of patients diagnosed with neurodegenerative diseases accompanied

by inflammatory processes, even though the inhibition of TNFα might also imply unforeseen side effects due to the interference with its physiological functions. Future *in vivo* studies could show whether a direct blockade of TNFα might restore the ability of neurons to perform synaptic plasticity. Intriguingly, a nested case control study demonstrated that patients diagnosed with rheumatic arthritis, which represents a status of chronic inflammation, had an increased risk of Alzheimer's disease and that treatment with the TNFα inhibitor etanercept lowered the risk of Alzheimer's disease in the studied rheumatic arthritis population significantly (Chou et al. 2016).

6.4.3 SP and RA as potential therapeutic targets

The role of SP in synaptic plasticity and the observed LPS-triggered downregulation of its expression that is accompanied by alterations in synaptic plasticity, indicates that SP itself could meet the criteria of a therapeutic target. Indeed it has been shown that SP is reduced in patients with Alzheimer's disease (Arnold et al. 2013; Counts et al. 2014) and it further could be demonstrated that activation of the immune system (mainly mediated by glial cells) contributes to the pathogenesis of the disease (Broussard et al. 2012; R. Zhang et al. 2013). Approaches aiming at increasing SP-levels might therefore turn out to be beneficial in cases of inflammation-caused defects in synaptic plasticity.

This thesis provides evidence that RA is crucially involved in regulating homeostatic synaptic plasticity (Maghsoodi et al. 2008; Aoto et al. 2008; Sarti et al. 2012; Arendt et al. 2015b) by upregulating SP abundance at synapses. Therefore RA appears as a promising candidate to compensate for inflammation-caused defects in synaptic plasticity by regulating SP expression. Besides, it has been shown that RA also affects TNFα by decreasing its transcription (Dheen et al. 2005; Nozaki et al. 2006). Intriguingly, this thesis demonstrates that concomitant RA treatment downregulates TNFα expression as well as impedes the LPS-induced downregulation of SP-mRNA. Interestingly, the SP-transcript is altered under RA treatment in these experiments. This

indicates a genomic regulation and is thus distinct from the previously described transcriptional regulation. This displays that RA effects on SP are sufficient to compensate for the inflammation-triggered imbalance of SP homeostasis which prompts the hypothesis that RA treatment might be a suitable clinical approach to compensate for inflammation-caused synaptic dysregulation. However, to which extent RA might improve synaptic plasticity necessitates further investigations. In general clinical use of RA has to be assessed carefully due to a variety of adverse events that have been reported from patients under RA treatment and due to its teratogenic potential (Katz et al. 1999; Pearce et al. 2006).

6.4.4 Repetitive magnetic stimulation as an approach to treat and monitor neuroinflammation

Repetitive magnetic stimulation (rMS) represents a non-invasive brain stimulation technique that proved clinical success in diagnosing and treating distinct neurological disorders (Barker et al. 1985; Ridding & Rothwell 2007; Lefaucheur et al. 2014; for reviews, see e.g., Dayan et al. 2013; Rothwell 2012; Schulz et al. 2013). Recent data provide evidence, that rMS increases overall neural network activity by modulating the excitation/ inhibition balance (Lenz et al. 2015; Lenz et al. 2016) and that rMS induces NMDAR-dependent LTP (Vlachos et al. 2012; see also Müller-Dahlhaus & Vlachos 2013; Lenz & Vlachos 2016; Vlachos et al. 2017). Furthermore, clinical (Cantarero et al. 2013) as well as pre-clinical studies (Vlachos et al. 2012; Lenz et al. 2015; Lenz et al. 2016) provide evidence, that rMS can modulate neuronal connections leading to long-lasting changes of synaptic strength. How rMS can be used as a therapeutic means to compensate for disturbed synaptic function by upregulating SP-protein and SP-mRNA amount remains to be investigated. So far it is not clear whether changes in neural activity might be beneficial in the case of neuroinflammation.

A major challenge in the clinics remains the fact that non-invasive diagnostic approaches to monitor therapy success in cases of

neuroinflammation are not available at present. Thus rMS appears as a promising approach e.g. to monitor studies aiming at improving clinical endpoints under conditions of neuroinflammation.

6.4.5 Conclusion

Taken together, this work substantially contributes to the understanding of a broad spectrum of neurological diseases which are accompanied and/ or caused by inflammation of brain tissue, and provides possible targets for therapeutic interventions. I am confident that the presented results will attract other scientists and physicians aiming to improve the outcome of patients diagnosed with neuropathologies that involve inflammatory responses like Alzheimer's disease, multiple sclerosis, epilepsy, or stroke by targeting SP expression and SP-mediated synaptic plasticity.

7. References

Abbott, N.J., Ronnback, L., and Hansson, E. (2006). Astrocyte-endothelial interactions at the blood-brain barrier. Nature reviews Neuroscience 7, 41-53.

Abraham, W.C., and Bear, M.F. (1996). Metaplasticity: the plasticity of synaptic plasticity. Trends in Neurosciences 19, 126-130.

Allan, S.M., and Rothwell, N.J. (2001). Cytokines and acute neurodegeneration. Nature reviews Neuroscience 2, 734-744.

Alvarez, A., Cacabelos, R., Sanpedro, C., Garcia-Fantini, M., and Aleixandre, M. (2007). Serum TNF-alpha levels are increased and correlate negatively with free IGF-I in Alzheimer disease. Neurobiology of Aging 28, 533-536.

Amaral, D.G., and Witter, M.P. (1989). The three-dimensional organization of the hippocampal formation: a review of anatomical data. Neuroscience 31, 571-591.

Andersen, P., Morris, R., Amaral, D., and Tim Bliss, J.O.K. (2007). The Hippocampus Book (Oxford University Press).

Aoto, J., Nam, C.I., Poon, M.M., Ting, P., and Chen, L. (2008). Synaptic signaling by all-trans retinoic acid in homeostatic synaptic plasticity. Neuron 60, 308-320.

Aptowicz, C.O., Kunkler, P.E., and Kraig, R.P. (2004). Homeostatic plasticity in hippocampal slice cultures involves changes in voltage-gated Na+ channel expression. Brain Research 998, 155-163.

Arendt, K.L., Zhang, Y., Jurado, S., Malenka, R.C., Sudhof, T.C., and Chen, L. (2015a). Retinoic Acid and LTP Recruit Postsynaptic AMPA Receptors Using Distinct SNARE-Dependent Mechanisms. Neuron 86, 442-456.

Arendt, K.L., Zhang, Z., Ganesan, S., Hintze, M., Shin, M.M., Tang, Y., Cho, A., Graef, I.A., and Chen, L. (2015b). Calcineurin mediates homeostatic synaptic plasticity by regulating retinoic acid synthesis. Proceedings of the National Academy of Sciences of the United States of America 112, E5744-5752.

Arnold, S.E., Louneva, N., Cao, K., Wang, L.S., Han, L.Y., Wolk, D.A., Negash, S., Leurgans, S.E., Schneider, J.A., Buchman, A.S., et al. (2013). Cellular, synaptic, and biochemical features of resilient cognition in Alzheimer's disease. Neurobiology of Aging 34, 157-168.

Asanuma, K., Kim, K., Oh, J., Giardino, L., Chabanis, S., Faul, C., Reiser, J., and Mundel, P. (2005). Synaptopodin regulates the actin-bundling activity of alpha-actinin in an isoform-specific manner. J Clin Invest 115, 1188-1198.

Badwey, J.A., and Karnovsky, M.L. (1980). Active oxygen species and the functions of phagocytic leukocytes. Annu Rev Biochem 49, 695-726.

Banks, W.A., and Robinson, S.M. (2010). Minimal penetration of lipopolysaccharide across the murine blood-brain barrier. Brain, behavior, and immunity 24, 102-109.

Barger, S.W., and Basile, A.S. (2001). Activation of microglia by secreted amyloid precursor protein evokes release of glutamate by cystine exchange and attenuates synaptic function. Journal of Neurochemistry 76, 846-854.

Barker, A.T., Jalinous, R., and Freeston, I.L. (1985). Non-invasive magnetic stimulation of human motor cortex. Lancet 1, 1106-1107.

Barone, F.C., and Feuerstein, G.Z. (1999). Inflammatory mediators and stroke: new opportunities for novel therapeutics. J Cereb Blood Flow Metab 19, 819-834.

Bas Orth, C., Schultz, C., Muller, C.M., Frotscher, M., and Deller, T. (2007). Loss of the cisternal organelle in the axon initial segment of cortical neurons in synaptopodin-deficient mice. The Journal of comparative neurology 504, 441-449.

Bas Orth, C., Vlachos, A., Del Turco, D., Burbach, G.J., Haas, C.A., Mundel, P., Feng, G., Frotscher, M., and Deller, T. (2005). Lamina-specific distribution of Synaptopodin, an actin-associated molecule essential for the spine apparatus, in identified principal cell dendrites of the mouse hippocampus. The Journal of comparative neurology 487, 227-239.

Bats, C., Groc, L., and Choquet, D. (2007). The interaction between Stargazin and PSD-95 regulates AMPA receptor surface trafficking. Neuron 53, 719-734.

Beattie, E.C., Stellwagen, D., Morishita, W., Bresnahan, J.C., Ha, B.K., Von Zastrow, M., Beattie, M.S., and Malenka, R.C. (2002a). Control of synaptic strength by glial TNFalpha. Science 295, 2282-2285.

Beattie, M.S., Hermann, G.E., Rogers, R.C., and Bresnahan, J.C. (2002b). Cell death in models of spinal cord injury. Progress in Brain Research 137, 37-47.

Becker, D., Zahn, N., Deller, T., and Vlachos, A. (2013). Tumor necrosis factor alpha maintains denervation-induced homeostatic synaptic plasticity of mouse dentate granule cells. Frontiers in cellular neuroscience 7, 257.

Bedi, S.S., Hetz, R., Thomas, C., Smith, P., Olsen, A.B., Williams, S., Xue, H., Aroom, K., Uray, K., Hamilton, J., et al. (2013). Intravenous multipotent adult progenitor cell therapy attenuates activated microglial/macrophage response and improves spatial learning after traumatic brain injury. Stem cells translational medicine 2, 953-960.

Begley, D.J., and Brightman, M.W. (2003). Structural and functional aspects of the blood-brain barrier. Prog Drug Res 61, 39-78.

Bi, G., and Poo, M. (2001). Synaptic modification by correlated activity: Hebb's postulate revisited. Annual review of neuroscience 24, 139-166.

Bliss, T.V., and Collingridge, G.L. (1993). A synaptic model of memory: long-term potentiation in the hippocampus. Nature 361, 31-39.

Bliss, T.V., and Lomo, T. (1973). Long-lasting potentiation of synaptic transmission in the dentate area of the anaesthetized rabbit following stimulation of the perforant path. J Physiol 232, 331-356.

Block, M.L., Zecca, L., and Hong, J.S. (2007). Microglia-mediated neurotoxicity: uncovering the molecular mechanisms. Nature reviews Neuroscience 8, 57-69.

Breder, C.D., Tsujimoto, M., Terano, Y., Scott, D.W., and Saper, C.B. (1993). Distribution and characterization of tumor necrosis factor-alpha-like immunoreactivity in the murine central nervous system. The Journal of comparative neurology 337, 543-567.

Broussard, G.J., Mytar, J., Li, R.C., and Klapstein, G.J. (2012). The role of inflammatory processes in Alzheimer's disease. Inflammopharmacology 20, 109-126.

Burguillos, M.A., Deierborg, T., Kavanagh, E., Persson, A., Hajji, N., Garcia-Quintanilla, A., Cano, J., Brundin, P., Englund, E., Venero, J.L., et al. (2011). Caspase signalling controls microglia activation and neurotoxicity. Nature 472, 319-324.

Burnashev, N., Monyer, H., Seeburg, P.H., and Sakmann, B. (1992). Divalent ion permeability of AMPA receptor channels is dominated by the edited form of a single subunit. Neuron 8, 189-198.

Butler, M.P., O'Connor, J.J., and Moynagh, P.N. (2004). Dissection of tumor-necrosis factor-alpha inhibition of long-term potentiation (LTP) reveals a p38 mitogen-activated protein kinase-dependent mechanism which maps to early-but not late-phase LTP. Neuroscience 124, 319-326.

Cambiaghi, M. (2017). Andreas Vesalius (1514-1564). J Neurol 264, 1828-1830.

Cantarero, G., Tang, B., O'Malley, R., Salas, R., and Celnik, P. (2013). Motor learning interference is proportional to occlusion of LTP-like plasticity. The Journal of neuroscience : the official journal of the Society for Neuroscience 33, 4634-4641.

Carson, M.J., Thrash, J.C., and Walter, B. (2006). The cellular response in neuroinflammation: The role of leukocytes, microglia and astrocytes in neuronal death and survival. Clin Neurosci Res 6, 237-245.

Carswell, E.A., Old, L.J., Kassel, R.L., Green, S., Fiore, N., and Williamson, B. (1975). An endotoxin-induced serum factor that causes necrosis of tumors. Proceedings of the National Academy of Sciences of the United States of America 72, 3666-3670.

Catorce, M.N., and Gevorkian, G. (2016). LPS-induced Murine Neuroinflammation Model: Main Features and Suitability for Pre-clinical Assessment of Nutraceuticals. Curr Neuropharmacol 14, 155-164.

Ceulemans, A.G., Zgavc, T., Kooijman, R., Hachimi-Idrissi, S., Sarre, S., and Michotte, Y. (2010). The dual role of the neuroinflammatory response after ischemic stroke: modulatory effects of hypothermia. Journal of Neuroinflammation 7, 74.

Chapman, T.R., Barrientos, R.M., Ahrendsen, J.T., Maier, S.F., and Patterson, S.L. (2010). Synaptic correlates of increased cognitive vulnerability with aging: peripheral immune challenge and aging interact to disrupt theta-burst late-phase long-term potentiation in hippocampal area CA1. The

Journal of neuroscience: the official journal of the Society for Neuroscience 30, 7598-7603.

Chen, L., Lau, A.G., and Sarti, F. (2014). Synaptic retinoic acid signaling and homeostatic synaptic plasticity. Neuropharmacology 78, 3-12.

Chen, W.W., Zhang, X., and Huang, W.J. (2016). Role of neuroinflammation in neurodegenerative diseases (Review). Molecular Medicine Reports 13, 3391-3396.

Chou, R.C., Kane, M., Ghimire, S., Gautam, S., and Gui, J. (2016). Treatment for Rheumatoid Arthritis and Risk of Alzheimer's Disease: A Nested Case-Control Analysis. CNS Drugs 30, 1111-1120.

Chung, I.Y., and Benveniste, E.N. (1990). Tumor necrosis factor-alpha production by astrocytes. Induction by lipopolysaccharide, IFN-gamma, and IL-1 beta. Journal of Immunology 144, 2999-3007.

Clark, R.A., and Klebanoff, S.J. (1975). Neutrophil-mediated tumor cell cytotoxicity: role of the peroxidase system. J Exp Med 141, 1442-1447.

Collingridge, G.L., Peineau, S., Howland, J.G., and Wang, Y.T. (2010). Long-term depression in the CNS. Nature reviews Neuroscience 11, 459-473.

Conrad, L.C., Leonard, C.M., and Pfaff, D.W. (1974). Connections of the median and dorsal raphe nuclei in the rat: an autoradiographic and degeneration study. The Journal of comparative neurology 156, 179-205.

Cooper, L.N., and Bear, M.F. (2012). The BCM theory of synapse modification at 30: interaction of theory with experiment. Nature reviews Neuroscience 13, 798-810.

Counts, S.E., Alldred, M.J., Che, S., Ginsberg, S.D., and Mufson, E.J. (2014). Synaptic gene dysregulation within hippocampal CA1 pyramidal neurons in mild cognitive impairment. Neuropharmacology 79, 172-179.

Cunningham, A.J., Murray, C.A., O'Neill, L.A., Lynch, M.A., and O'Connor, J.J. (1996). Interleukin-1 beta (IL-1 beta) and tumour necrosis factor (TNF) inhibit long-term potentiation in the rat dentate gyrus in vitro. Neuroscience Letters 203, 17-20.

Dagher, N.N., Najafi, A.R., Kayala, K.M., Elmore, M.R., White, T.E., Medeiros, R., West, B.L., and Green, K.N. (2015). Colony-stimulating factor 1 receptor inhibition prevents microglial plaque association and improves cognition in 3xTg-AD mice. Journal of Neuroinflammation 12, 139.

Dantzer, R., O'Connor, J.C., Freund, G.G., Johnson, R.W., and Kelley, K.W. (2008). From inflammation to sickness and depression: when the immune system subjugates the brain. Nature reviews Neuroscience 9, 46-56.

Das Sarma, J. (2014). Microglia-mediated neuroinflammation is an amplifier of virus-induced neuropathology. Journal of NeuroVirology 20, 122-136.

Dayan, E., Censor, N., Buch, E.R., Sandrini, M., and Cohen, L.G. (2013). Noninvasive brain stimulation: from physiology to network dynamics and back. Nature Neuroscience 16, 838-844.

Deller, T., Korte, M., Chabanis, S., Drakew, A., Schwegler, H., Stefani, G.G., Zuniga, A., Schwarz, K., Bonhoeffer, T., Zeller, R., et al. (2003). Synaptopodin-deficient mice lack a spine apparatus and show deficits in synaptic plasticity. Proceedings of the National Academy of Sciences of the United States of America 100, 10494-10499.

Deller, T., Martinez, A., Nitsch, R., and Frotscher, M. (1996). A novel entorhinal projection to the rat dentate gyrus: direct innervation of proximal dendrites and cell bodies of granule cells and GABAergic neurons. The Journal of neuroscience : the official journal of the Society for Neuroscience 16, 3322-3333.

Deller, T., Merten, T., Roth, S.U., Mundel, P., and Frotscher, M. (2000). Actin-associated protein synaptopodin in the rat hippocampal formation: localization in the spine neck and close association with the spine apparatus of principal neurons. The Journal of comparative neurology 418, 164-181.

Dheen, S.T., Jun, Y., Yan, Z., Tay, S.S., and Ling, E.A. (2005). Retinoic acid inhibits expression of TNF-alpha and iNOS in activated rat microglia. Glia 50, 21-31.

Di Filippo, M., Sarchielli, P., Picconi, B., and Calabresi, P. (2008). Neuroinflammation and synaptic plasticity: theoretical basis for a novel, immune-centred, therapeutic approach to neurological disorders. Trends Pharmacol Sci 29, 402-412.

Dunn, K.W., Kamocka, M.M., and McDonald, J.H. (2011). A practical guide to evaluating colocalization in biological microscopy. Am J Physiol Cell Physiol 300, C723-742.

Ekdahl, C.T., Kokaia, Z., and Lindvall, O. (2009). Brain inflammation and adult neurogenesis: the dual role of microglia. Neuroscience 158, 1021-1029.

Erickson, M.A., and Banks, W.A. (2011). Cytokine and chemokine responses in serum and brain after single and repeated injections of lipopolysaccharide: multiplex quantification with path analysis. Brain, behavior, and immunity 25, 1637-1648.

Esmon, C.T. (2014). Targeting factor Xa and thrombin: impact on coagulation and beyond. Thrombosis and Haemostasis 111, 625-633.

Fifkova, E., Markham, J.A., and Delay, R.J. (1983). Calcium in the spine apparatus of dendritic spines in the dentate molecular layer. Brain Research 266, 163-168.

Fleige, S., and Pfaffl, M.W. (2006). RNA integrity and the effect on the real-time qRT-PCR performance. Molecular Aspects of Medicine 27, 126-139.

Frotscher, M., Seress, L., Schwerdtfeger, W.K., and Buhl, E. (1991). The mossy cells of the fascia dentata: a comparative study of their fine structure and synaptic connections in rodents and primates. The Journal of comparative neurology 312, 145-163.

Fukazawa, Y., Saitoh, Y., Ozawa, F., Ohta, Y., Mizuno, K., and Inokuchi, K. (2003). Hippocampal LTP is accompanied by enhanced F-actin content within the dendritic spine that is essential for late LTP maintenance in vivo. Neuron 38, 447-460.

Gaillard, P.J., de Boer, A.B., and Breimer, D.D. (2003). Pharmacological investigations on lipopolysaccharide-induced permeability changes in the blood-brain barrier in vitro. Microvascular Research 65, 24-31.

Gao, R., and Penzes, P. (2015). Common mechanisms of excitatory and inhibitory imbalance in schizophrenia and autism spectrum disorders. Curr Mol Med 15, 146-167.

Gingrich, M.B., Junge, C.E., Lyuboslavsky, P., and Traynelis, S.F. (2000). Potentiation of NMDA receptor function by the serine protease thrombin. The Journal of neuroscience : the official journal of the Society for Neuroscience 20, 4582-4595.

Glass, C.K., Saijo, K., Winner, B., Marchetto, M.C., and Gage, F.H. (2010). Mechanisms underlying inflammation in neurodegeneration. Cell 140, 918-934.

Goel, A., Jiang, B., Xu, L.W., Song, L., Kirkwood, A., and Lee, H.K. (2006). Cross-modal regulation of synaptic AMPA receptors in primary sensory cortices by visual experience. Nature Neuroscience 9, 1001-1003.

Goel, A., Xu, L.W., Snyder, K.P., Song, L., Goenaga-Vazquez, Y., Megill, A., Takamiya, K., Huganir, R.L., and Lee, H.K. (2011). Phosphorylation of AMPA receptors is required for sensory deprivation-induced homeostatic synaptic plasticity. PLoS ONE 6, e18264.

Goncalves, M.B., Clarke, E., Hobbs, C., Malmqvist, T., Deacon, R., Jack, J., and Corcoran, J.P. (2013). Amyloid beta inhibits retinoic acid synthesis exacerbating Alzheimer disease pathology which can be attenuated by an retinoic acid receptor alpha agonist. The European journal of neuroscience 37, 1182-1192.

Gonzalez, H., Elgueta, D., Montoya, A., and Pacheco, R. (2014). Neuroimmune regulation of microglial activity involved in neuroinflammation and neurodegenerative diseases. Journal of Neuroimmunology 274, 1-13.

Gordon, R., Anantharam, V., Kanthasamy, A.G., and Kanthasamy, A. (2012). Proteolytic activation of proapoptotic kinase protein kinase Cdelta by tumor necrosis factor alpha death receptor signaling in dopaminergic neurons during neuroinflammation. Journal of Neuroinflammation 9, 82.

Hafting, T., Fyhn, M., Molden, S., Moser, M.B., and Moser, E.I. (2005). Microstructure of a spatial map in the entorhinal cortex. Nature 436, 801-806.

Hanisch, U.K. (2002). Microglia as a source and target of cytokines. Glia 40, 140-155.

Hartman, K.N., Pal, S.K., Burrone, J., and Murthy, V.N. (2006). Activity-dependent regulation of inhibitory synaptic transmission in hippocampal neurons. Nature Neuroscience 9, 642-649.

Hebb, D.O. (1949). Organization of behavior: A neuropsychological theory. The Journal of Comparative Neurology, 1-335.

Heppner, F.L., Ransohoff, R.M., and Becher, B. (2015). Immune attack: the role of inflammation in Alzheimer disease. Nature reviews Neuroscience 16, 358-372.

Hirasawa, T., Ohsawa, K., Imai, Y., Ondo, Y., Akazawa, C., Uchino, S., and Kohsaka, S. (2005). Visualization of microglia in living tissues using Iba1-EGFP transgenic mice. J Neurosci Res 81, 357-362.

Holbro, N., Grunditz, A., and Oertner, T.G. (2009). Differential distribution of endoplasmic reticulum controls metabotropic signaling and plasticity at hippocampal synapses. Proceedings of the National Academy of Sciences of the United States of America 106, 15055-15060.

Jedlicka, P., Schwarzacher, S.W., Winkels, R., Kienzler, F., Frotscher, M., Bramham, C.R., Schultz, C., Bas Orth, C., and Deller, T. (2009). Impairment of in vivo theta-burst long-term potentiation and network excitability in the dentate gyrus of synaptopodin-deficient mice lacking the spine apparatus and the cisternal organelle. Hippocampus 19, 130-140.

Jedlicka, P., Vlachos, A., Schwarzacher, S.W., and Deller, T. (2008). A role for the spine apparatus in LTP and spatial learning. Behavioural Brain Research 192, 12-19.

Ju, W., Morishita, W., Tsui, J., Gaietta, G., Deerinck, T.J., Adams, S.R., Garner, C.C., Tsien, R.Y., Ellisman, M.H., and Malenka, R.C. (2004). Activity-dependent regulation of dendritic synthesis and trafficking of AMPA receptors. Nature Neuroscience 7, 244-253.

Kagan, J.C., Su, T., Horng, T., Chow, A., Akira, S., and Medzhitov, R. (2008). TRAM couples endocytosis of Toll-like receptor 4 to the induction of interferon-beta. Nat Immunol 9, 361-368.

Kalfayan, B., and Kidd, J.G. (1953). Structural changes produced in Brown-Pearce carcinoma cells by means of a specific antibody and complement. J Exp Med 97, 145-162.

Kandel, E. (2006). In Search of Memory: The Emergence of a New Science of Mind ({W. W. Norton}).

Kandel, E., Schwartz, J.H., and Jessell, T. (2000). Principles of Neural Science (McGraw-Hill Medical).

Karmarkar, U.R., and Buonomano, D.V. (2006). Different forms of homeostatic plasticity are engaged with distinct temporal profiles. The European journal of neuroscience 23, 1575-1584.

Katz, H.I., Waalen, J., and Leach, E.E. (1999). Acitretin in psoriasis: an overview of adverse effects. J Am Acad Dermatol 41, S7-S12.

Kazamel, M., and Warren, P.P. (2017). History of electromyography and nerve conduction studies: A tribute to the founding fathers. J Clin Neurosci 43, 54-60.

Kenny, E.F., and O'Neill, L.A.J. (2008). Signalling adaptors used by Toll-like receptors: An update. Cytokine 43, 342-349.

Kettenmann, H., Hanisch, U.K., Noda, M., and Verkhratsky, A. (2011). Physiology of microglia. Physiological Reviews 91, 461-553.

Kim, C.H. (2011). Retinoic acid, immunity, and inflammation. Vitam Horm 86, 83-101.

Kohler, C. (1985). Intrinsic projections of the retrohippocampal region in the rat brain. I. The subicular complex. The Journal of comparative neurology 236, 504-522.

Korkotian, E., Frotscher, M., and Segal, M. (2014). Synaptopodin regulates spine plasticity: mediation by calcium stores. The Journal of neuroscience : the official journal of the Society for Neuroscience 34, 11641-11651.

Korkotian, E., and Segal, M. (2007). Morphological constraints on calcium dependent glutamate receptor trafficking into individual dendritic spine. Cell Calcium 42, 41-57.

Krezel, W., Kastner, P., and Chambon, P. (1999). Differential expression of retinoid receptors in the adult mouse central nervous system. Neuroscience 89, 1291-1300.

Laster, S.M., Wood, J.G., and Gooding, L.R. (1988). Tumor necrosis factor can induce both apoptic and necrotic forms of cell lysis. Journal of Immunology 141, 2629-2634.

Lee, H.K. (2012). Ca-permeable AMPA receptors in homeostatic synaptic plasticity. Frontiers in Molecular Neuroscience 5, 17.

Lee, S., Varvel, N.H., Konerth, M.E., Xu, G., Cardona, A.E., Ransohoff, R.M., and Lamb, B.T. (2010). CX3CR1 deficiency alters microglial activation and reduces beta-amyloid deposition in two Alzheimer's disease mouse models. The American Journal of Pathology 177, 2549-2562.

Lefaucheur, J.P., Andre-Obadia, N., Antal, A., Ayache, S.S., Baeken, C., Benninger, D.H., Cantello, R.M., Cincotta, M., de Carvalho, M., De Ridder, D., et al. (2014). Evidence-based guidelines on the therapeutic use of repetitive transcranial magnetic stimulation (rTMS). Clin Neurophysiol 125, 2150-2206.

Lenz, M., Galanis, C., Muller-Dahlhaus, F., Opitz, A., Wierenga, C.J., Szabo, G., Ziemann, U., Deller, T., Funke, K., and Vlachos, A. (2016). Repetitive

magnetic stimulation induces plasticity of inhibitory synapses. Nature communications 7, 10020.

Lenz, M., Platschek, S., Priesemann, V., Becker, D., Willems, L.M., Ziemann, U., Deller, T., Muller-Dahlhaus, F., Jedlicka, P., and Vlachos, A. (2015). Repetitive magnetic stimulation induces plasticity of excitatory postsynapses on proximal dendrites of cultured mouse CA1 pyramidal neurons. Brain Struct Funct 220, 3323-3337.

Lenz, M., and Vlachos, A. (2016). Releasing the Cortical Brake by Non-Invasive Electromagnetic Stimulation? rTMS Induces LTD of GABAergic Neurotransmission. Front Neural Circuits 10, 96.

Lerouge, I., and Vanderleyden, J. (2002). O-antigen structural variation: mechanisms and possible roles in animal/plant–microbe interactions. FEMS Microbiology Reviews 26, 17-47.

Lissin, D.V., Gomperts, S.N., Carroll, R.C., Christine, C.W., Kalman, D., Kitamura, M., Hardy, S., Nicoll, R.A., Malenka, R.C., and von Zastrow, M. (1998). Activity differentially regulates the surface expression of synaptic AMPA and NMDA glutamate receptors. Proceedings of the National Academy of Sciences of the United States of America 95, 7097-7102.

Loughlin, S.E., Foote, S.L., and Grzanna, R. (1986). Efferent projections of nucleus locus coeruleus: morphologic subpopulations have different efferent targets. Neuroscience 18, 307-319.

Lu, Y.C., Yeh, W.C., and Ohashi, P.S. (2008). LPS/TLR4 signal transduction pathway. Cytokine 42, 145-151.

Lull, M.E., and Block, M.L. (2010). Microglial activation and chronic neurodegeneration. Neurotherapeutics : the journal of the American Society for Experimental NeuroTherapeutics 7, 354-365.

Maden, M. (2002). Retinoid signalling in the development of the central nervous system. Nature reviews Neuroscience 3, 843-853.

Maffei, A., Nataraj, K., Nelson, S.B., and Turrigiano, G.G. (2006). Potentiation of cortical inhibition by visual deprivation. Nature 443, 81-84.

Maggio, N., Itsekson, Z., Dominissini, D., Blatt, I., Amariglio, N., Rechavi, G., Tanne, D., and Chapman, J. (2013). Thrombin regulation of synaptic plasticity: implications for physiology and pathology. Experimental Neurology 247, 595-604.

Maghsoodi, B., Poon, M.M., Nam, C.I., Aoto, J., Ting, P., and Chen, L. (2008). Retinoic acid regulates RARalpha-mediated control of translation in dendritic RNA granules during homeostatic synaptic plasticity. Proceedings of the National Academy of Sciences of the United States of America 105, 16015-16020.

McCoy, M.K., and Tansey, M.G. (2008). TNF signaling inhibition in the CNS: implications for normal brain function and neurodegenerative disease. Journal of Neuroinflammation 5, 45.

Mehta, A.K., Gracias, D.T., and Croft, M. (2018). TNF activity and T cells. Cytokine 101, 14-18.

Merrill, J.E. (1991). Effects of interleukin-1 and tumor necrosis factor-alpha on astrocytes, microglia, oligodendrocytes, and glial precursors in vitro. Dev Neurosci 13, 130-137.

Monji, A., Kato, T.A., Mizoguchi, Y., Horikawa, H., Seki, Y., Kasai, M., Yamauchi, Y., Yamada, S., and Kanba, S. (2013). Neuroinflammation in schizophrenia especially focused on the role of microglia. Prog Neuropsychopharmacol Biol Psychiatry 42, 115-121.

Monkkonen, J., Taskinen, M., Auriola, S.O., and Urtti, A. (1994). Growth inhibition of macrophage-like and other cell types by liposome-encapsulated, calcium-bound, and free bisphosphonates in vitro. Journal of Drug Targeting 2, 299-308.

Moser, E.I., Kropff, E., and Moser, M.B. (2008). Place cells, grid cells, and the brain's spatial representation system. Annual review of neuroscience 31, 69-89.

Mosko, S., Lynch, G., and Cotman, C.W. (1973). The distribution of septal projections to the hippocampus of the rat. The Journal of comparative neurology 152, 163-174.

Muller-Dahlhaus, F., and Vlachos, A. (2013). Unraveling the cellular and molecular mechanisms of repetitive magnetic stimulation. Frontiers in Molecular Neuroscience 6, 50.

Mundel, P., Heid, H.W., Mundel, T.M., Kruger, M., Reiser, J., and Kriz, W. (1997). Synaptopodin: an actin-associated protein in telencephalic dendrites and renal podocytes. The Journal of cell biology 139, 193-204.

Nagatsu, T., Mogi, M., Ichinose, H., and Togari, A. (2000). Changes in cytokines and neurotrophins in Parkinson's disease. J Neural Transm Suppl, 277-290.

Neves, G., Cooke, S.F., and Bliss, T.V. (2008). Synaptic plasticity, memory and the hippocampus: a neural network approach to causality. Nature reviews Neuroscience 9, 65-75.

Newpher, T.M., and Ehlers, M.D. (2008). Glutamate receptor dynamics in dendritic microdomains. Neuron 58, 472-497.

Nimmerjahn, A., Kirchhoff, F., and Helmchen, F. (2005). Resting microglial cells are highly dynamic surveillants of brain parenchyma in vivo. Science 308, 1314-1318.

Nozaki, Y., Tamaki, C., Yamagata, T., Sugiyama, M., Ikoma, S., Kinoshita, K., and Funauchi, M. (2006). All-trans-retinoic acid suppresses interferon-gamma and tumor necrosis factor-alpha; a possible therapeutic agent for rheumatoid arthritis. Rheumatology international 26, 810-817.

Nyakas, C., Luiten, P.G., Spencer, D.G., and Traber, J. (1987). Detailed projection patterns of septal and diagonal band efferents to the hippocampus in the rat with emphasis on innervation of CA1 and dentate gyrus. Brain Research Bulletin 18, 533-545.

O'Brien, R.J., Kamboj, S., Ehlers, M.D., Rosen, K.R., Fischbach, G.D., and Huganir, R.L. (1998). Activity-dependent modulation of synaptic AMPA receptor accumulation. Neuron 21, 1067-1078.

O'Keefe, J., and Dostrovsky, J. (1971). The hippocampus as a spatial map. Preliminary evidence from unit activity in the freely-moving rat. Brain Research 34, 171-175.

O'Keefe, J., and Speakman, A. (1987). Single unit activity in the rat hippocampus during a spatial memory task. Experimental brain research 68, 1-27.

Okubo-Suzuki, R., Okada, D., Sekiguchi, M., and Inokuchi, K. (2008). Synaptopodin maintains the neural activity-dependent enlargement of dendritic spines in hippocampal neurons. Molecular and cellular neurosciences 38, 266-276.

Olmos, G., and Llado, J. (2014). Tumor necrosis factor alpha: a link between neuroinflammation and excitotoxicity. Mediators of inflammation 2014, 861231.

Orrenius, S., Zhivotovsky, B., and Nicotera, P. (2003). Regulation of cell death: the calcium-apoptosis link. Nat Rev Mol Cell Biol 4, 552-565.

Pearce, D.J., Higgins, K.B., Stealey, K.H., Balkrishnan, R., Crane, M.M., Camacho, F., Fleischer, A.B., Jr., and Feldman, S.R. (2006). Adverse events from systemic therapies for psoriasis are common in clinical practice. J Dermatolog Treat 17, 288-293.

Perry, V.H., and Teeling, J. (2013). Microglia and macrophages of the central nervous system: the contribution of microglia priming and systemic inflammation to chronic neurodegeneration. Seminars in Immunopathology 35, 601-612.

Pfaffl, M.W. (2001). A new mathematical model for relative quantification in real-time RT-PCR. Nucleic Acids Research 29, e45.

Pickel, V.M., Segal, M., and Bloom, F.E. (1974). A radioautographic study of the efferent pathways of the nucleus locus coeruleus. The Journal of comparative neurology 155, 15-42.

Pickering, M., Cumiskey, D., and O'Connor, J.J. (2005). Actions of TNF-alpha on glutamatergic synaptic transmission in the central nervous system. Experimental physiology 90, 663-670.

Pierce, J.P., van Leyen, K., and McCarthy, J.B. (2000). Translocation machinery for synthesis of integral membrane and secretory proteins in dendritic spines. Nature Neuroscience 3, 311-313.

Poltorak, A., He, X., Smirnova, I., Liu, M.Y., Van Huffel, C., Du, X., Birdwell, D., Alejos, E., Silva, M., Galanos, C., et al. (1998). Defective LPS signaling in C3H/HeJ and C57BL/10ScCr mice: mutations in Tlr4 gene. Science 282, 2085-2088.

Poon, M.M., and Chen, L. (2008). Retinoic acid-gated sequence-specific translational control by RARalpha. Proceedings of the National Academy of Sciences of the United States of America 105, 20303-20308.

Pozo, K., and Goda, Y. (2010). Unraveling mechanisms of homeostatic synaptic plasticity. Neuron 66, 337-351.

Pribiag, H., and Stellwagen, D. (2014). Neuroimmune regulation of homeostatic synaptic plasticity. Neuropharmacology 78, 13-22.

Pyapali, G.K., Turner, D.A., Williams, C.L., Meck, W.H., and Swartzwelder, H.S. (1998). Prenatal dietary choline supplementation decreases the threshold

for induction of long-term potentiation in young adult rats. Journal of neurophysiology 79, 1790-1796.

Qian, L., Tan, K.S., Wei, S.J., Wu, H.M., Xu, Z., Wilson, B., Lu, R.B., Hong, J.S., and Flood, P.M. (2007). Microglia-mediated neurotoxicity is inhibited by morphine through an opioid receptor-independent reduction of NADPH oxidase activity. Journal of Immunology 179, 1198-1209.

Qin, L., Wu, X., Block, M.L., Liu, Y., Breese, G.R., Hong, J.S., Knapp, D.J., and Crews, F.T. (2007). Systemic LPS causes chronic neuroinflammation and progressive neurodegeneration. Glia 55, 453-462.

Raetz, C.R. (1990). Biochemistry of endotoxins. Annu Rev Biochem 59, 129-170.

Ransohoff, R.M. (2016). How neuroinflammation contributes to neurodegeneration. Science 353, 777-783.

Ransohoff, R.M., and Perry, V.H. (2009). Microglial physiology: unique stimuli, specialized responses. Annual Review of Immunology 27, 119-145.

Rathinam, V.A., and Fitzgerald, K.A. (2013). Immunology: Lipopolysaccharide sensing on the inside. Nature 501, 173-175.

Rhee, S.H. (2014). Lipopolysaccharide: basic biochemistry, intracellular signaling, and physiological impacts in the gut. Intest Res 12, 90-95.

Ridding, M.C., and Rothwell, J.C. (2007). Is there a future for therapeutic use of transcranial magnetic stimulation? Nature reviews Neuroscience 8, 559-567.

Rochette-Egly, C., Adam, S., Rossignol, M., Egly, J.M., and Chambon, P. (1997). Stimulation of RAR alpha activation function AF-1 through binding to the general transcription factor TFIIH and phosphorylation by CDK7. Cell 90, 97-107.

Rogers, J., Webster, S., Lue, L.F., Brachova, L., Civin, W.H., Emmerling, M., Shivers, B., Walker, D., and McGeer, P. (1996). Inflammation and Alzheimer's disease pathogenesis. Neurobiology of Aging 17, 681-686.

Rothwell, J.C. (2012). Clinical applications of noninvasive electrical stimulation: problems and potential. Clinical EEG and Neuroscience 43, 209-214.

Russell, R.G., and Rogers, M.J. (1999). Bisphosphonates: from the laboratory to the clinic and back again. Bone 25, 97-106.

Saijo, K., Winner, B., Carson, C.T., Collier, J.G., Boyer, L., Rosenfeld, M.G., Gage, F.H., and Glass, C.K. (2009). A Nurr1/CoREST pathway in microglia and astrocytes protects dopaminergic neurons from inflammation-induced death. Cell 137, 47-59.

Santello, M., and Volterra, A. (2012). TNFalpha in synaptic function: switching gears. Trends in Neurosciences 35, 638-647.

Sarti, F., Schroeder, J., Aoto, J., and Chen, L. (2012). Conditional RARalpha knockout mice reveal acute requirement for retinoic acid and RARalpha in homeostatic plasticity. Frontiers in Molecular Neuroscience 5, 16.

Schindelin, J., Arganda-Carreras, I., Frise, E., Kaynig, V., Longair, M., Pietzsch, T., Preibisch, S., Rueden, C., Saalfeld, S., Schmid, B., et al. (2012). Fiji: an open-source platform for biological-image analysis. Nature Methods 9, 676-682.

Schnell, E., Sizemore, M., Karimzadegan, S., Chen, L., Bredt, D.S., and Nicoll, R.A. (2002). Direct interactions between PSD-95 and stargazin control synaptic AMPA receptor number. Proceedings of the National Academy of Sciences of the United States of America 99, 13902-13907.

Schulz, R., Gerloff, C., and Hummel, F.C. (2013). Non-invasive brain stimulation in neurological diseases. Neuropharmacology 64, 579-587.

Scoville, W.B., and Milner, B. (1957). Loss of recent memory after bilateral hippocampal lesions. J Neurol Neurosurg Psychiatry 20, 11-21.

Sedger, L.M., and McDermott, M.F. (2014). TNF and TNF-receptors: From mediators of cell death and inflammation to therapeutic giants - past, present and future. Cytokine Growth Factor Rev 25, 453-472.

Segal, M., Vlachos, A., and Korkotian, E. (2010). The spine apparatus, synaptopodin, and dendritic spine plasticity. The Neuroscientist : a review journal bringing neurobiology, neurology and psychiatry 16, 125-131.

Seltmann, G., and Holst, O. (2002). The Bacterial Cell Wall. Berlin: Springer.

Shearer, K.D., Stoney, P.N., Morgan, P.J., and McCaffery, P.J. (2012). A vitamin for the brain. Trends in Neurosciences 35, 733-741.

Shechter, R., Miller, O., Yovel, G., Rosenzweig, N., London, A., Ruckh, J., Kim, K.W., Klein, E., Kalchenko, V., Bendel, P., et al. (2013). Recruitment of beneficial M2 macrophages to injured spinal cord is orchestrated by remote brain choroid plexus. Immunity 38, 555-569.

Sheng, M., and Hoogenraad, C.C. (2007). The postsynaptic architecture of excitatory synapses: a more quantitative view. Annu Rev Biochem 76, 823-847.

Shepherd, J.D., Rumbaugh, G., Wu, J., Chowdhury, S., Plath, N., Kuhl, D., Huganir, R.L., and Worley, P.F. (2006). Arc/Arg3.1 mediates homeostatic synaptic scaling of AMPA receptors. Neuron 52, 475-484.

Shikamoto, Y., and Morita, T. (1999). Expression of factor X in both the rat brain and cells of the central nervous system. FEBS Lett 463, 387-389.

Sjostrom, P.J., Rancz, E.A., Roth, A., and Hausser, M. (2008). Dendritic excitability and synaptic plasticity. Physiological Reviews 88, 769-840.

Sommer, B., Kohler, M., Sprengel, R., and Seeburg, P.H. (1991). RNA editing in brain controls a determinant of ion flow in glutamate-gated channels. Cell 67, 11-19.

Sriram, K., and O'Callaghan, J.P. (2007). Divergent roles for tumor necrosis factor-alpha in the brain. J Neuroimmune Pharmacol 2, 140-153.

Steinmetz, C.C., and Turrigiano, G.G. (2010). Tumor necrosis factor-alpha signaling maintains the ability of cortical synapses to express synaptic scaling. The Journal of neuroscience : the official journal of the Society for Neuroscience 30, 14685-14690.

Stellwagen, D., Beattie, E.C., Seo, J.Y., and Malenka, R.C. (2005). Differential regulation of AMPA receptor and GABA receptor trafficking by tumor necrosis factor-alpha. The Journal of neuroscience : the official journal of the Society for Neuroscience 25, 3219-3228.

Stellwagen, D., and Malenka, R.C. (2006). Synaptic scaling mediated by glial TNF-alpha. Nature 440, 1054-1059.

Strange, B.A., Witter, M.P., Lein, E.S., and Moser, E.I. (2014). Functional organization of the hippocampal longitudinal axis. Nature reviews Neuroscience 15, 655-669.

Strehl, A., Lenz, M., Itsekson-Hayosh, Z., Becker, D., Chapman, J., Deller, T., Maggio, N., and Vlachos, A. (2014). Systemic inflammation is associated with a reduction in Synaptopodin expression in the mouse hippocampus. Experimental Neurology 261, 230-235.

Sutton, M.A., Ito, H.T., Cressy, P., Kempf, C., Woo, J.C., and Schuman, E.M. (2006). Miniature neurotransmission stabilizes synaptic function via tonic suppression of local dendritic protein synthesis. Cell 125, 785-799.

Sutton, M.A., and Schuman, E.M. (2006). Dendritic protein synthesis, synaptic plasticity, and memory. Cell 127, 49-58.

Takeuchi, O., and Akira, S. (2010). Pattern recognition receptors and inflammation. Cell 140, 805-820.

Teeling, J.L., and Perry, V.H. (2009). Systemic infection and inflammation in acute CNS injury and chronic neurodegeneration: underlying mechanisms. Neuroscience 158, 1062-1073.

Thiagarajan, T.C., Lindskog, M., and Tsien, R.W. (2005). Adaptation to synaptic inactivity in hippocampal neurons. Neuron 47, 725-737.

Trotta, T., Porro, C., Calvello, R., and Panaro, M.A. (2014). Biological role of Toll-like receptor-4 in the brain. Journal of Neuroimmunology 268, 1-12.

Turrigiano, G.G. (2008). The self-tuning neuron: synaptic scaling of excitatory synapses. Cell 135, 422-435.

Turrigiano, G.G. (2012). Homeostatic synaptic plasticity: local and global mechanisms for stabilizing neuronal function. Cold Spring Harb Perspect Biol 4, a005736.

Turrigiano, G.G., Leslie, K.R., Desai, N.S., Rutherford, L.C., and Nelson, S.B. (1998). Activity-dependent scaling of quantal amplitude in neocortical neurons. Nature 391, 892-896.

van Helden, A.C., and Van Gent, R.H. (1999). The lens production by Christiaan and Constantijn Huygens. Ann Sci 56, 69-79.

van Neerven, S., Regen, T., Wolf, D., Nemes, A., Johann, S., Beyer, C., Hanisch, U.K., and Mey, J. (2010). Inflammatory chemokine release of astrocytes in vitro is reduced by all-trans retinoic acid. Journal of Neurochemistry 114, 1511-1526.

van Rooijen, N., Sanders, A., and van den Berg, T.K. (1996). Apoptosis of macrophages induced by liposome-mediated intracellular delivery of clodronate and propamidine. Journal of Immunological Methods 193, 93-99.

Vaure, C., and Liu, Y. (2014). A comparative review of toll-like receptor 4 expression and functionality in different animal species. Frontiers in Immunology 5, 316.

Vereker, E., Campbell, V., Roche, E., McEntee, E., and Lynch, M.A. (2000). Lipopolysaccharide inhibits long term potentiation in the rat dentate gyrus by activating caspase-1. J Biol Chem 275, 26252-26258.

Vertes, R.P., Fortin, W.J., and Crane, A.M. (1999). Projections of the median raphe nucleus in the rat. The Journal of comparative neurology 407, 555-582.

Vitureira, N., and Goda, Y. (2013). Cell biology in neuroscience: the interplay between Hebbian and homeostatic synaptic plasticity. The Journal of cell biology 203, 175-186.

Vlachos, A. (2012). Synaptopodin and the spine apparatus organelle-regulators of different forms of synaptic plasticity? Ann Anat 194, 317-320.

Vlachos, A., Becker, D., Jedlicka, P., Winkels, R., Roeper, J., and Deller, T. (2012a). Entorhinal denervation induces homeostatic synaptic scaling of excitatory postsynapses of dentate granule cells in mouse organotypic slice cultures. PLoS ONE 7, e32883.

Vlachos, A., Funke, K., and Ziemann, U. (2017). Assessment and modulation of cortical inhibition using transcranial magnetic stimulation, Vol 23.

Vlachos, A., Ikenberg, B., Lenz, M., Becker, D., Reifenberg, K., Bas-Orth, C., and Deller, T. (2013). Synaptopodin regulates denervation-induced homeostatic synaptic plasticity. Proceedings of the National Academy of Sciences of the United States of America 110, 8242-8247.

Vlachos, A., Korkotian, E., Schonfeld, E., Copanaki, E., Deller, T., and Segal, M. (2009). Synaptopodin regulates plasticity of dendritic spines in hippocampal neurons. The Journal of neuroscience : the official journal of the Society for Neuroscience 29, 1017-1033.

Vlachos, A., Muller-Dahlhaus, F., Rosskopp, J., Lenz, M., Ziemann, U., and Deller, T. (2012b). Repetitive magnetic stimulation induces functional and structural plasticity of excitatory postsynapses in mouse organotypic hippocampal slice cultures. The Journal of neuroscience : the official journal of the Society for Neuroscience 32, 17514-17523.

Volterra, A., Liaudet, N., and Savtchouk, I. (2014). Astrocyte Ca(2)(+) signalling: an unexpected complexity. Nature reviews Neuroscience 15, 327-335.

Wallach, D., Kang, T.B., and Kovalenko, A. (2014). Concepts of tissue injury and cell death in inflammation: a historical perspective. Nature reviews Immunology 14, 51-59.

Wallach, D., Varfolomeev, E.E., Malinin, N.L., Goltsev, Y.V., Kovalenko, A.V., and Boldin, M.P. (1999). Tumor necrosis factor receptor and Fas signaling mechanisms. Annual Review of Immunology 17, 331-367.

Wang, J., Asensio, V.C., and Campbell, I.L. (2002). Cytokines and chemokines as mediators of protection and injury in the central nervous system assessed in transgenic mice. Current topics in microbiology and immunology 265, 23-48.

Welser-Alves, J.V., and Milner, R. (2013). Microglia are the major source of TNF-alpha and TGF-beta1 in postnatal glial cultures; regulation by cytokines, lipopolysaccharide, and vitronectin. Neurochem Int 63, 47-53.

Wesselingh, S.L., Power, C., Glass, J.D., Tyor, W.R., McArthur, J.C., Farber, J.M., Griffin, J.W., and Griffin, D.E. (1993). Intracerebral cytokine messenger RNA expression in acquired immunodeficiency syndrome dementia. Ann Neurol 33, 576-582.

Wierenga, C.J., Ibata, K., and Turrigiano, G.G. (2005). Postsynaptic expression of homeostatic plasticity at neocortical synapses. The Journal of neuroscience : the official journal of the Society for Neuroscience 25, 2895-2905.

Wierenga, C.J., Walsh, M.F., and Turrigiano, G.G. (2006). Temporal regulation of the expression locus of homeostatic plasticity. Journal of neurophysiology 96, 2127-2133.

Witter, M.P. (1993). Organization of the entorhinal-hippocampal system: a review of current anatomical data. Hippocampus 3 Spec No, 33-44.

Wolburg, H., and Lippoldt, A. (2002). Tight junctions of the blood-brain barrier: development, composition and regulation. Vascular Pharmacology 38, 323-337.

Wyss-Coray, T., and Mucke, L. (2002). Inflammation in neurodegenerative disease--a double-edged sword. Neuron 35, 419-432.

Wyszynski, M., Lin, J., Rao, A., Nigh, E., Beggs, A.H., Craig, A.M., and Sheng, M. (1997). Competitive binding of alpha-actinin and calmodulin to the NMDA receptor. Nature 385, 439-442.

Wyszynski, M., Kharazia, V., Shanghvi, R., Rao, A., Beggs, A.H., Craig, A.M., Weinberg, R., and Sheng, M. (1998). Differential regional expression and ultrastructural localization of alpha-actinin-2, a putative NMDA receptor-anchoring protein, in rat brain. The Journal of neuroscience : the official journal of the Society for Neuroscience 18, 1383-1392.

Yamazaki, M., Matsuo, R., Fukazawa, Y., Ozawa, F., and Inokuchi, K. (2001). Regulated expression of an actin-associated protein, synaptopodin, during long-term potentiation. Journal of Neurochemistry 79, 192-199.

Yang, H., and Chen, C. (2008). Cyclooxygenase-2 in synaptic signaling. Current Pharmaceutical Design 14, 1443-1451.

Ylitalo, R., Monkkonen, J., and Yla-Herttuala, S. (1998). Effects of liposome-encapsulated bisphosphonates on acetylated LDL metabolism, lipid accumulation and viability of phagocyting cells. Life Sci 62, 413-422.

Yuste, R. (2015). The discovery of dendritic spines by Cajal. Front Neuroanat 9, 18.

Zemelka, A.M. (2017). Alcmaeon of Croton - Father of Neuroscience? Brain, Mind and Senses in the Alcmaeon’s Study, Vol 08.

Zenke, F., Gerstner, W., and Ganguli, S. (2017). The temporal paradox of Hebbian learning and homeostatic plasticity. Current Opinion in Neurobiology 43, 166-176.

Zetterstrom, R.H., Lindqvist, E., Mata de Urquiza, A., Tomac, A., Eriksson, U., Perlmann, T., and Olson, L. (1999). Role of retinoids in the CNS: differential expression of retinoid binding proteins and receptors and evidence for presence of retinoic acid. The European journal of neuroscience 11, 407-416.

Zhang, R., Miller, R.G., Madison, C., Jin, X., Honrada, R., Harris, W., Katz, J., Forshew, D.A., and McGrath, M.S. (2013a). Systemic immune system alterations in early stages of Alzheimer's disease. Journal of Neuroimmunology 256, 38-42.

Zhang, X.L., Poschel, B., Faul, C., Upreti, C., Stanton, P.K., and Mundel, P. (2013b). Essential role for synaptopodin in dendritic spine plasticity of the developing hippocampus. The Journal of Neuroscience 33, 12510-12518.

List of Abbreviations

ACSF	Artificial cerebrospinal fluid
AD	Alzheimer's disease
ALS	Amyotrophic lateral sclerosis
AMPA	α-amino-3-hydroxy-5-methyl-4-isoxazolepropionic acid
AMPAR	α-amino-3-hydroxy-5-methyl-4-isoxazolepropionic acid receptor
APS	Ammonium persulfate
APV	2-Amino-5-phosphonovaleriansäure
BBB	Blood brain barrier
CA	Cornu ammonis
Ca	Calcium
CaCl	Calcium chloride
CaMK	Ca^{2+}/calmodulin-dependent protein kinase
Ca_V	Voltage gated calcium channel
CD14	Cluster of differentiation 14
cDNA	Complementary DNA
CHAPS	Detergent: 3-((3-cholamidopropyl) dimethylammonio)-1-propanesulfonate
CNS	Central nervous system
DG	Dentate gyrus
DIV	Days in vitro
DNA	Deoxyribonucleic acid
Dpi	Days post injection
EC	Entorhinal cortex
EDTA	Ethylenediaminetetraacetic acid
EF1	Elongation factor 1
eGFP	Enhanced green fluorescent protein
FL	Full-length
Fwd	Forward
GABA	γ-aminobutyric acid
GAPDH	Glycerinaldehyd-3-phosphat-Dehydrogenase

GC	Granule cell
GCL	Granule cell layer
GCL	Granule cell layer
GFAP	Glial fibrillary acidic protein
GFP	Green fluorescent protein
GluA1	Glutamate receptor, AMPA type, subunit 1
GluA2	Glutamate receptor, AMPA type, subunit 2
HCl	Hydrochloric acid
HEPES	4-(2-hydroxyethyl)-1-piperazineethanesulfonic acid
Iba1	Ionized calcium-binding adapter molecule 1
IDA	Inflorescence Deficient in Abscission
IgG	Immunoglobulin G
IL-1a/b	Interleukin 1a/b
IL-6	Interleukin 6
IML	Inner molecular layer
KO	Knockout
KOH	Potassium hydroxide
LBP	LPS binding protein
LPS	Lipopolysaccharide
LTD	Long-term depression
LTP	Long-term potentiation
M1	Macrophage phenotype 1
M2	Macrophage phenotype 2
mEPSC	Miniature excitatory postsynaptic current
MERM	Modified Edi’s Recording Medium
MD-2	MD-2 represents a TLR4-associated protein
MgCl	Magnesium chloride
ML	Moleculare layer
MML	Middle molecular layer
mRNA	Messenger ribonucleic acid
MS	Multiple sclerosis
MSO	Maximum stimulator output

mV	Millivolt
MyD88	Myeloid differentiation primary response gene 88
NA	Numerical aperture
NaCl	Sodium chloride
NAD	Nicotinamidadenindinukleotid
NASPM	1-Naphthylacetyl spermine trihydrochloride
NC	Nitrocellulose membrane
NES	Nuclear export sequence
NLS	Nuclear localization sequence
NMDA	N-methyl-D-aspartate
NMDAR	N-methyl-D-aspartate receptor
OD	Optic density
OML	Outer molecular layer
OTC	Organotypic slice culture
pA	Picoampere
PAR1	Protease-activated receptor 1
PBS	Phosphate-buffered saline
PCR	Polymerase chain reaction
PD	Parkinson’s disease
pF	Picofarad
PFA	Paraformaldehyde
PKA	Protein kinase A
PKC	Protein kinase C
PP	Perforant path
PSD	Postsynaptic density
qPCR	Quantitative PCR
RA	Retinoic acid
RALD	Retinal dehydrogenase
RARα	Retinoic acid receptor alpha
Rev	Reverse
RIP	RNA-immunoprecipitation
rMS	Repetitive magnetic stimulation

ROLD	Retinol dehydrogenase
RT	Reverse transcription
RyR	Ryanodine receptors
SA	Spine apparatus
SDS	Sodium dodecyl sulfate
SEM	Standard error of the mean
SGZ	Subgranular zone
SNAP-25	Synaptosomal-associated protein 25
SNRNP70	Small nuclear ribonucleoprotein 70 kDa
SP	Synaptopodin
Str.la-mol.	Stratum lacunosum-moleculare
Str.ori.	Stratum oriens
Str.rad.	Stratum radiatum
TACE	TNFα converting enzyme
TBS	Tris-buffered saline
TBS/T	Tris-buffered saline with Tween20
Temed	N,N,N,N-Tetramethylethylendiamin
TIRAP	TIR Domain Containing Adaptor Protein
TLR4	Toll-like receptor 4
TMS	Transcranial magnetic stimulation
TNFα	Tumor necrosis factor alpha
TRAM	Translocating chain-associated membrane protein
TRIF	TIR-domain-containing adapter-inducing interferon-β
t-SNARE	Target synaptosome-associated protein receptor
TTX	Tetrodotoxin
U1snRNA	U1 spliceosomal RNA
UTR	Untranslated region
v/w	Volume per weight
v-SNARE	Vesicle synaptosome-associated protein receptor

List of Figures

List of Boxes

List of Tables

List of Equations